ILLUMINATING THE P53 REGULATORY NETWORK

IN GENETIC MODELS

APPROVED BY SUPERVISORY COMMITTEE

John M. Abrams, Ph.D. (Mentor) _____

Helmut Kramer, Ph.D. (Chair) _____

James F. Amatruda, M.D., Ph.D. _____

Xiaodong Wang, Ph.D. _____

DEDICATION

This is dedicated to my parents.

ILLUMINATING THE P53 REGULATORY NETWORK IN GENETIC MODELS

BY

WAN-JIN LU

DISSERTATION / THESIS

Presented to the Faculty of the Graduate School of Biomedical Sciences

The University of Texas Southwestern Medical Center at Dallas

In Partial Fulfillment of the Requirements

For the Degree of

DOCTOR OF PHILOSOPHY

The University of Texas Southwestern Medical Center at Dallas

Dallas, Texas

November, 2010

ILLUMINATING THE P53 REGULATORY NETWORK

IN GENETIC MODELS

Publication No. _____

WAN-JIN LU, Ph.D.

The University of Texas Southwestern Medical Center at Dallas, 2010

Supervising Professors: John M. Abrams, Ph.D.

The tumor suppressor gene p53 is mutated in more than 50% of human cancers, and functions as a central component of stress response machinery that mediates a

wide variety of downstream responses. Interestingly, the evolutionary appearance of p53 preceded its role in tumor suppression, suggesting that there may be unappreciated functions for this protein. In order to examine physiologic functions of p53 *in vivo*, a green fluorescent protein (GFP) reporter was designed to follow the activation of this regulatory network in a genetic model, *Drosophila melanogaster*. By following the reporter during *Drosophila* development, physiological activation of the p53 regulatory network in the female germ line was discovered. It is provoked by the first enzymatic step for meiotic recombination and conserved in both flies and mice. The functional relevance of the p53 activities in the germ line was shown by the meiotic recombination frequency and genetic interactions with a meiotic effector gene, Rad54. Additionally, genotoxic stress selectively activates p53 in germ line stem cells and promotes regeneration of fertility after IR. Activation of p53 was also found in uncontrolled growth of germ cells by blocked differentiation, and surprisingly by overexpression of oncogenic protein in the germ line. Together, my thesis work indicate that the need for controlling growth by the p53 regulatory network is an evolutionary conserved feature, which may serve as a selective pressure to preserve this network. Future studies on the mechanisms of p53 actvities during meiosis and in response to oncogene activation could provide novel insights on its cancer-related functions.

ACKNOWLEDGEMENTS

I thank my mentor, Dr. John M. Abrams, for his endured guidance, encouragement and sharing enthusiasm in science. His consistent support is not limited to making a nurturing environment but also allowing me to learn through making my own mistakes, which is essential for my development to independence. All the invaluable trainings will continue to support my future endeavor.

I also thank my thesis committee members: Drs. Helmut Kramer, Xiaodong Wang, James Amatruda; previous members Mattew Porteus and Keith Wharton for providing additional outlook that broadened my sight of views. I am grateful to have joined the communicative and collaborative environment at UT Southwestern in 2003, especially the Cell Biology department, Dr. Richard Anderson, and graduate school, Dr. Melanie Cobb.

In addition, I acknowledge former and current members of the Abrams lab, who have made every working day enjoyable. With many members from Abrams lab and others at UT Southwestern, we collaborated on scientific experiments, afterhour plans and lifelong friendships – it has made my personal life transition to a new country effortless and full of excitement. These include Nikki Link, Melissa O'Neal, Su Kit Chew, Zoltan Metlagel, Naoko Sogame, Kathleen Galindo, Alex D'Brot, Aly Villasenor, Nevine Shalaby, Nancy McKinney, and Miao-Chia Lo. Special thanks to Mahesh Vaishnav for proofreading the first draft of the thesis.

Finally, I thank my family: my parents and brother for their encouragement and loving support.

TABLE OF CONTENTS

PRIOR PUBLICATIONS

1. Lu W-J, Chapo J, Roig I, Abrams JM (2010) Meiotic recombination provokes functional activation of the p53 regulatory network. ***Science*** 328: 1278-1281. [Pubmed] [News coverages including NewScientist, USA TODAY, EurekAlert!.]
2. Lu W-J, Amatruda JF, Abrams JM (2009) p53 ancestry: gazing through an evolutionary lens. ***Nature Reviews in Cancer*** 9: 758-762. [Pubmed]
3. Galindo KA, Lu WJ, Park JH, Abrams JM (2009) The Bax/Bak ortholog in Drosophila, Debcl, exerts limited control over programmed cell death. ***Development*** 136: 275-283. [Pubmed]
4. Link N, Chen P, Lu WJ, Pogue K, Chuong A, et al. (2007) A collective form of cell death requires homeodomain interacting protein kinase. ***Journal of Cell Biology*** 178: 567-574. [Pubmed]
5. Lu WJ, Abrams JM (2006) Lessons from p53 in non-mammalian models. ***Cell Death and Differentiation*** 13: 909-912. [Pubmed]
6. Chew SK, Akdemir F, Chen P, Lu WJ, Mills K, et al. (2004) The apical caspase dronc governs programmed and unprogrammed cell death in Drosophila. ***Development Cell*** 7: 897-907. [Pubmed]
7. Lu W-J, Sogame N, Abrams JM (2009) Radiation Responses in Drosophila. In: Bradshaw RA, Dennis EA, editors. ***Handbook of Cell Signaling***. 2 ed: Academic Press. pp. 261.

LIST OF FIGURES

LIST OF TABLES

LIST OF ABBREVIATIONS

ATL-1 – the C. elegans homolog of ataxia telangiectasia and Rad3-related

ATM – ataxia telangiectasia mutated

ATR – ataxia telangiectasia and Rad3 related

BH3 – Bcl-2 homology 3

Caspase – Cysteinyl aspartate-specific protease

CAT – Chloramphenicol acetyltransferase

CDK – Cyclin dependent kinase

Ced – Cell death defective

CEP-1 – C.elegans p53-like-1

ChIP– Chromatin immuno precipitation

Chk – checkpoint kinase

Dark – Drosophila apaf-1 related killer

DBD – DNA binding domain

Debcl – Drosophila executioner bcl

Dmchk2 – Drosophila melanogaster chk2

Dmp53 – Drosophila melanogaster p53

Dronc – Drosophila nedd2-like caspase

Gas1 – Growth arrest-specific 1

GFP – Green fluorescent protein

Hid – Head involution defective

HTRA – HtrA serine peptidase

IAP – Inhibitor of apoptosis protein

IR – ionizing radiation

MDM – transformed mouse 3T3 cell double minute

Mei-41 – Meiotic-41

Mre11 – Meiotic recombination-11

MSH: MutS homolog

PHG-1 – pharynx associated Gas1

RIPD – Radiation induced p53 dependent

RNAi – RNA interference

RnrL – Ribonucleoside diphosphate reductase large subunit

RnrS – Ribonucleoside diphosphate reductase small subunit

Rpr – Reaper

SAM – sterile alpha motif

Skl – Sickle

UV – ultra-vialot

XRCC – X-ray repair complementing defective repair in Chinese hamster cells

Chapter One.

Introduction

This chapter is adapted from the two following previous publications:

Lessons from p53 in non-mammalian models.

Cell Death and Differentiation 13: 909-912. (2006)

Wan-Jin Lu and John M. Abrams

p53 ancestry: gazing through an evolutionary lens.

Nature Reviews in Cancer 9: 758-762. (2009)

Wan-Jin Lu, James F. Amatruda and John M. Abrams

The tumor suppressor gene p53 is mutated in more than 50% of human cancers (Greenblatt et al 1994). The p53 protein (human TP53 gene) is a tetrameric transcription factor, functions as a central component of stress response machinery that mediates a wide variety of downstream responses. Three domains in p53, corresponding to transcriptional activation, DNA binding, and tetramerization activities, have been well characterized. The major function of p53 is a sequence-specific transcription factor, which responds to several stress signals, including DNA damage, physiological stress, and oncogenic stimulation. The activation of p53 ultimately regulates DNA repair, cell cycle progression and apoptosis (Ko & Prives 1996, Levine 1997). In human cancers, most of the mutations occur within the DNA binding domain, which is also the domain most conserved from invertebrates to mammals.

In recent years a large number of studies, predominantly focused on transformed cells, has sought to understand the function of p53 as “the guardian of the genome”. However, because majority of the studies came from tissue culture cells which provide limited information about the nonautonomous roles of p53 in living organisms (Hill et al 2005). Therefore, properties of the regulatory network of p53 that extend beyond the single cell level are not well understood. Our naivety in this area is easily exemplified by a glaring paradox: Everything we know about p53 and its role in damage response pathways predicts that transformed cells (p53-) should exhibit profound resistance to chemotherapeutic agents and radiation therapies relative to p53+ counterparts. And yet, the very fact that these anti-cancer agents actually have some efficacy in the clinic, combined with the high incidence of p53- state of human tumors, tells us just the opposite. That is, in patients, the p53- genotype of cancer tissues correlates with tumor sensitivity to genotoxic agents. These counter-intuitive observations indicate two things: one, there is still much to learn about the p53 network; two, functions of p53 deduced

from studies at the single cell level may not be adequate to predict its properties among group of cells in tissues or in tumors.

LESSONS FROM NON-MAMMALIAN MODELS

The fact that p53 genes are conserved from invertebrate to mammals affords attractive opportunities for researchers to use well-defined genetic models to examine the functions of p53 in tissues and whole animal systems. p53 orthologs have been described in clams (Barker et al 1997, Van Beneden et al 1997), squid (Ishioka et al 1995), flies (Brodsky et al 2000, Jin et al 2000, Ollmann et al 2000), frogs (Soussi et al 1987) and zebrafish (Chen et al 2005). Knowledge of p53 in different genetic research models will be summarized here. By considering this gene family from an evolutionary viewpoint and highlighting some conundrums in the field of p53 research, I hope to shed light on how potential insights from these simpler models can advance therapeutic applications in cancer.

Zebrafish

Zebrafish (*Danio rerio*) p53 shares overall 48% sequence similarity to human p53 (Cheng et al 1997). To study the *in vivo* function of p53, antisense morpholinos were injected into early embryos (Langheinrich et al 2002). In these studies, the native p53 locus remains intact but the gene product is reduced. p53 'knockdown' embryos showed normal development, but had suppressed induction of apoptosis after UV irradiation or drug treatment. Several features of zebrafish p53 regulation are similar to mammals. Firstly, like in mice and human, zebrafish MDM2 protein also negatively regulates p53. Second, the transcription level of p21 is regulated by p53 as a downstream effector. Third, p53 family members, p63 and p73 are also present in zebrafish and each evidently has separate roles depending on the context of development, tissue specificity and stress source. Recently, different splicing isoforms of human p53 mRNA transcripts

were reported (Bourdon et al 2005), although the tissue distribution and *in vivo* function of different isoforms remains unclear. In zebrafish, a truncated transcript, delta113p53 is induced by abnormal development and specifically engages in cell-cycle arrest but not in apoptosis, providing an intriguing clue into the distinct physiological roles of p53 isoforms during development. Since zebrafish strains harboring missense mutations in the DNA-binding domain of p53 showed higher susceptibility to neuronal tumors (Berghmans et al 2005), genetic screens will be useful to further understand the tumor suppressor activities of p53 in this model system.

Caenorhabditis elegans

Caenorhabditis elegans p53-like protein (CEP-1) is a 429 amino acids protein (Derry et al 2001, Schumacher et al 2001), which does not share obvious overall homology to mammalian p53 members except in the DNA binding domain. The most frequently mutated sites in DNA binding domain are well conserved in *cep-1*. Unlike zebrafish, *cep-1* is the only p53-related sequence in the genome of *C. elegans*. To understand the function of *cep-1*, a chromosomal rearrangement mutant, producing a dominant negative from of *cep-1* was studied together with RNAi knockdown experiments. Both studies documented an essential role of *cep-1* for radiation-induced apoptosis in germ cells. Although the native *cep-1* locus still remains intact, the *cep-1* phenotypes with RNAi are consistent with other animal models, where the gene is dispensable for normal development. Forced *cep-1* expression caused wide-spread caspase independent death, suggesting that the proper amount of CEP-1 is important for cell survival (Derry et al 2001). *cep-1* also mediates normal meiotic chromosome segregation and several stress-induced responses but does not engage in cell-cycle arrest after DNA damage. How does *cep-1* specify cell death? Induction of two BH-3 only proteins, EGL-1 and CED-13 in *C. elegans*, are thought to largely account for radiation-induced CEP-1 dependent cell death (Gartner et al 2000, Schumacher et al

2005b), although whether direct binding by CEP-1 occurs at these loci remains unclear. As is the case in flies (see below), regulation of p53 by MDM2 is absent in *C. elegans*, albeit other DNA damage response pathways are still preserved. For example, an ATR ortholog in *C. elegans*, *atl-1*, also triggers apoptosis via *cep-1/egl-1* pathway after radiation (Garcia-Muse & Boulton 2005). Other recently reported p53 regulators in *C. elegans* such as GLD-1 (Schumacher et al 2005a) and iASPP(Bergamaschi et al 2003), have not been examined in other systems. While the ATM/ATR mode of regulation appears well conserved here, it is not yet known whether these additional upstream regulators function similarly in other models.

Drosophila melanogaster

Drosophila p53 (dmp53) was first described as a 385 amino acid protein, with the highest homology to human p53 in the DNA binding domain (Jin et al 2000, Ollmann et al 2000), reviewed in (Nordstrom & Abrams 2000, Song 2005, Sutcliffe & Brehm 2004, Sutcliffe et al 2003). More recently, a longer 495 amino acid isoform and a shorter 110 amino acid isoform were also reported (Bourdon et al 2005). The anatomic structure of dmp53 is similar to mammalian p53. Moreover, the most frequently mutated p53 sites in human tumors are also well conserved. As in *C. elegans*, p63/73 orthologs do not occur in the *Drosophila* genome (Fortini et al 2000). The *in vivo* apoptotic activity of dmp53 was initially shown by ectopic over-expression in the eye, which induced apoptosis (Brodsky et al 2000, Ollmann et al 2000). These findings were further supported by genetic loss-of function studies, which established that dmp53 is required for transcriptional induction of *rpr* proteins (*rpr*, *hid*, *skl*) and for radiation-induced apoptosis (Brodsky et al 2000). General development was not affected in the dmp53 mutants (Lee et al 2003b, Rong et al 2002, Sogame et al 2003), but mild defects in longevity and fertility were found. Where studied, dmp53 does not engage cell cycle checkpoints and, consistent with this, the *Drosophila* ortholog of p21 is unresponsive to p53 status. As in *C. elegans*, MDM2 is absent from the fly genome, implying that alternative modes of

p53 regulation must exist. Although upstream activators in the fly p53 regulatory network are not yet defined, we do know that *Drosophila* Chk2 regulates dmp53 via direct phosphorylation (Brodsky et al 2004, Peters et al 2002) and that Chk2 and dATM are required for damage-induced apoptosis (Oikemus et al 2004, Song et al 2004). Moreover, a recent study reported that dmp53 can be activated by reduced ATP level in a cytochrome oxidase subunit mutant (Mandal et al 2005), suggesting links between energy status and dmp53 regulation. This same study implicated cyclin E, in addition to inhibitor of apoptosis (IAP) antagonists, as a possible effector of dmp53. To predict additional dmp53 target genes *in vivo*, genome-wide array experiments compared the radiation responses of normal versus dmp53 null embryos and, along with pro-apoptotic functions, genes involved in DNA synthesis and repair were also found (Akdemir et al 2007, Brodsky et al 2004).

Evolutionary lessons

p53 is structurally conserved accross different phyla, including nematoda (worms), mollusca (clams), arthropoda (insects), and chordate (vertebrates) while the p63/p73 paralogs occur in the genomes of vertebrates and mollusk, but not in insects or worms. The DNA binding domain, reflecting its activity as a transcription factor, is the most highly conserved region. Since no p53 ortholog occurs in yeast or plants, the evolution of p53 may have perhaps accompanied the appearance of metazoan animals. Attempts to reconstruct a p53 lineage infer different histories, depending on whether domain architecture (e.g. the presence or absence of SAM domain) is prioritized or whether primary sequence in the DNA binding domain is used as the primary characteristic. Applying the former criteria together with knowledge of a p73 gene in clams, we can deduce that along with a p53 gene, the most recent common ancestor of vertebrates and invertebrates probably also encoded a SAM domain-containing paralog. However if similarity scores and primary sequences in the DNA binding domain are

used, it is clear that invertebrate p53 genes share slightly more similarity to the DNA binding domains of human p63/73 (Yang et al 2002, Yang et al 2000) prompting suggestions that the ancestral origin of the p53 family were p63/73-like sequences preserved in mollusca (Figure 1-1). Despite this discrepancy, both methods deduce phyletic scenarios that include a p53-like gene (without a SAM domain) and a p63/p73-like gene (with a SAM domain) in the common ancestor of vertebrates and invertebrates.

What can we reasonably surmise about the primordial p53 gene and its regulatory network from these cross-species comparisons? Given what we know about p53 mutations in distinct models, the gene is probably non-essential, regulated by the ATM/CHK2 kinases and intimately coupled to pro-apoptotic target genes. Consistent with this, it is safe to assume that the p21-mediated checkpoint was a recent acquisition, perhaps specific to the vertebrate lineage**.** If correct, a corollary to this scenario argues that the primordial elements of the p53 death program do not require a subroutine that first impacts cell cycle checkpoints, as some have proposed. From these hypothetical considerations, perhaps the most compelling and perplexing questions relate to the adaptive pressures that presumably selected for this gene in the first place. Though radiation is commonly used as a stimulus, the p53 regulatory network is obviously not 'invented' on the chance that tissues would find themselves exposed to acute radiation doses produced by medical imaging devices or nuclear weapons. And clearly, when we impose genotoxic stress in a laboratory setting, we may be 'over-challenging' cells in a way that is analogous to 'hitting nails with a sledge hammer'. So, although it is clear that DNA strand breaks and stalled replication forks can engage the network, the proximal evolutionary pressures that shaped this network are still an enigma. One possible contender in this regard could be exogenous or endogenous reactive oxygen species, which in mammals has been intimately linked to p53 (Raha &

Robinson 2001, Sablina et al 2005) and, more recently, implicated in the *Drosophila* network through a novel 'mitochondrial checkpoint' (Mandal et al 2005).

p53 research in non-mammalian models will continue to illuminate important biological questions relevant to human health. One emerging question relates to recently discovered isoforms of p53 that arise from an internal promoter. This newly appreciated complexity embodies fundamental properties of p53 gene structure that are conserved from flies to man and are highly correlated with tumorogenesis (Bourdon et al 2005). However, since it is not understood how (or whether) these variant isoforms encode distinct activities *in vivo*, we can expect that functional lessons drawn from simpler non-mammalian should inform our knowledge of human p53. A second challenge relates to the growing appreciation for the non-autonomous properties that can impact p53 function, particularly as they relate to tumor microenvironments *in situ*. Understanding the p53 network beyond the single cell level is an essential task for describing the full dimension of tumor suppression by this oncogenic protein. This deduction follows from the notorious fact that stress-induced behaviors of cells grown in cultured dishes can differ markedly from behaviors seen for cells in their native tissues or 'niches'. Here, lessons drawn from simpler non-mammalian models should provide important insights as to how, for example, p53 action in one cell might influence the behavior of its neighbors, leading to emergent 'tissue level properties' that could otherwise not have been predicted. Finally, the simpler non-mammalian models should help us to resolve how p53 can be a fundamental determinant of so many pathogenic states— from tumor progression to neurodegeneration to aging and life span. Are these seemingly disparate pathologies intertwined through the same functional activity? Or might they result from distinct functional modalities propagated by this single factor? One way to rephrase this question at the molecular level might ask whether p53 status governs gene expression *only* in a stimulus dependent manner. A possible alternative, perhaps, is that the p53 regulatory network might also impact basal gene expression in

a way that explains these pathogenic phenotypes. We note here that recent array studies are certainly consistent with this latter possibility (Christich and Abrams, unpublished observations). Finally, considering that DNA damage response/ checkpoint genes are well conserved from yeast to humans, p53 must have been endowed with additional properties specific to metazoan organisms that should ultimately be illuminated from future studies in these non-mammalian model systems.

P53 ANCESTRY

Three members of the p53 family are found in humans: p53, p63 and p73. As shown in Figure 1-1, all include an N terminal transactivation domain, a central DNA-binding domain (DBD) and a C terminal oligomerization domain. The transactivation and oligomerization domains appear to have broadly diverged, whereas the DBD is significantly conserved (Fernandes & Atchley 2008). Notably, p63 and p73 contain a SAM (sterile-alpha-motif) domain at their extreme C terminus. This domain is likely to be involved in protein-protein interactions and, in the context of p73, has been implicated in protein turnover (Maisse et al 2003). A SAM domain is absent from p53 and, hence, based on protein architecture, p63 and p73 share a more recent common ancestor. To simplify discussion, only full-length transcripts are considered and refered collectively to p53 family members that encode a SAM domain as ‘p63/73-like’, and those lacking a SAM domain as ‘p53-like’.

New genomes uncover deeper roots

p53 family members are widespread among animals and reported from many taxa other than vertebrates, such as ascidians (sea squirt) (Dehal et al 2002), cnidarians (Pankow & Bamberger 2007, Putnam et al 2007), flatworms and other invertebrates (Figure 1-1& Table 1-1 for sequence accession numbers). Because this

gene family is absent from the yeast genome, conventional wisdom held that p53 emerged in animalia, perhaps in response to characteristic selective pressures operating on early multicellular organisms. However, the recently published choanoflagellate (*Monosiga brevicollis*) genome shatters this view (King et al 2008). Two distinct genes, one p53-like and second p63/p73-like, are both present in this unicellular protist, possibly the closest extant relative of metazoans. Likewise, a p53-like protein is also reported in another protozoan, the amoeba *Entamoeba histolytica* (Mendoza et al 2003). These discoveries significantly revise the evolutionary picture in at least two ways. First, the emergence of this gene family predated the appearance of multicellular animals. Second, both p53-like and p63/p73-like genes probably existed in the common ancestor of metazoa and protozoa.

Interestingly, p63/p73-like genes are absent from several lineages where p53-like genes are present (such as flies, nematodes and cnidarians). Furthermore, relative to p63/p73-like genes, the p53-like genes appear more extensively diversified in separate lineages of invertebrates and chordates (Nedelcu & Tan 2007). Current evidence is ambivalent regarding phylogenetic origins since the primordial history of these subfamilies could reflect acquisition of the C-terminal SAM domain by a p53-like gene, or equally likely, loss of this domain from an ancient of p63/p73 member. Compelling arguments could support either scenario. However, it is worth noting that among the sequenced genomes where this family appears, the p53-like genes are consistently present but the p63/p73-like genes are not. Similarly, it is p53, not p63 or p73, which is frequently mutated in cancer cells. Are these two facts simply a coincidence? Or do they reflect some degree of meaningful linkage? The following sections extend this theme by examining evolutionarily conserved features in p53 regulatory networks.

UPSTREAM REGULATORS

In mammals, the p53 regulatory network includes a complex array of upstream regulators and downstream effectors (Vousden & Prives 2009). The emerging picture reflects a 'hub position' whereby p53 integrates a wide spectrum of signals to promote adaptive responses to genotoxic and perhaps other types of stress. Upstream control of p53 falls into three regulatory models — stabilization, anti-repression and promoter-specific activation (Kruse & Gu 2009). The degree to which these models extend beyond mammals is not yet known. However, studies in two genetic model systems, *Drosophila melanogaster* and *Ceanorhabditis elegans,* offer some surprises and tentative conclusions.

For example, the first two mechanisms of p53 control, stabilization and anti-repression, involve Mdm2 proteins as pivotal central regulators (Figure 1-2). This notion is underscored by studies in mice and fish demonstrating that lethal Mdm2 and Mdm4 deficient phenotypes are genetically rescued by eliminating p53 (Jones et al 1995, Langheinrich et al 2002, Parant et al 2001). Yet genes encoding Mdm2 like proteins are absent from non-vertebrate lineages and, furthermore, studies in *Drosophila* suggest that genotoxic activation of p53 can occur without altering the protein level of p53 (Brodsky et al 2004). Taken together, these observations suggest that ancient circuits linking DNA damage to p53 activation existed prior to the emergence of Mdm2-mediated regulation. Thus, non-vertebrate p53 regulatory networks offer us an opportunity to understand how p53 activation may occur independently of Mdm2-mediated stabilization.

So which upstream regulatory mechanisms are conserved? In zebrafish, upstream activators include signals generated by suboptimal cell replication caused by mutations in DNA polymerase (Plaster et al 2006), oncogenic stress (Patton et al 2005, Shepard et al 2005) and genotoxic stress. While the first two conditions have yet to be fully examined in flies and *C. elegans*, it seems evident that genotoxic stress is a

commonly shared stimulus that provokes the p53 pathway in all three systems. In flies, worms (Garcia-Muse & Boulton 2005) and probably zebrafish, p53 is a downstream effector of CHK2 (Brodsky et al 2004), ATM (Oikemus et al 2004, Song et al 2004) and possibly ATR (Song 2005), all of which are activated by DNA damage (Figure 1-3). Therefore, at the minimum, these kinases constitute an ancient signaling pathway fundamental to p53 regulation in response to DNA damage. In contrast, neither flies nor worms utilize an MDM2/MDMX-associated regulatory pathway, which is present in zebrafish and in mammals. A scenario consistent with these findings proposes that MDM2/MDMX-mediated degradation of p53 appeared in the vertebrate lineage after the divergence of protosomes and deuterosomes (Figure 1-4). These regulators were perhaps de-emphasized in invertebrates, possibly in favor of alternatives such as iASPP (Apoptotic-Stimulating Proteins of p53), a shared negative regulator of p53 in nematodes (Bergamaschi et al 2003) and mammals (Figure 1-3). Another strong candidate of conserved upstream regulator is the Chk2 kinase. Like its mammalian counterparts, *Drosophila* Chk2 directly phosphorylates p53 (Hirao et al 2000, Peters et al 2002) and is required for the induction of apoptosis in response to ionizing radiation (Peters et al 2002). It is not known whether Chk2 directly regulates CEP-1, the *C. elegans* p53 orthologue, but Chk2, together with orthologs of ATM-1 and ATR/ATL-1, are necessary for cell death induced by ultraviolet radiation (MacQueen & Villeneuve 2001, Stergiou et al 2007). These cross-species similarities qualify Chk2 kinases as highly conserved p53 regulators and indicate that ancestral pathways probably include direct activation of p53 through phosphorylation and perhaps other post-translational modifications (Figure 1-2).

DOWNSTREAM EFFECTORS

Output modalities of the p53 regulatory network that contribute to growth repression have been extensively reviewed (Vousden & Prives 2009). Here we consider evidence from invertebrate models that may distinguish ancient versus derived

functions. Like their human counterparts, non-mammalian p53 proteins are intimately engaged by — and essential for — proper genotoxic stress responses that provoke apoptosis (Derry et al 2001, Lee et al 2003b, Sogame et al 2003). As illustrated in Figure 1-2, broadly conserved effectors are commonly recruited among vertebrates and invertebrates to control apoptosis, including members of the BH3-only Bcl-2 subfamily and inhibitor of apoptosis (IAP) antagonists (Figure 1-2). Likewise, common sets of targets that promote DNA repair, such as Xrcc/Ku, ribonucleotide reductase (RNR) and MutS homolog (MSH) proteins have been independently observed in mammals and in flies (Akdemir et al 2007, Brodsky et al 2004, Stergiou et al 2007). In contrast, p21-mediated cell cycle arrest appears less broadly conserved and might be restricted to vertebrates. For example, the gene encoding p21 in zebrafish is probably a p53 target (Berghmans et al 2005, Langheinrich et al 2002), but the p21 ortholog in flies is not (Akdemir et al 2007, Brodsky et al 2004). Interestingly, p53 regulates cell cycle in worms and flies through different sets of target genes. In energy deprived cells, *Drosophila* p53 can mediate G1–S cell cycle arrest independently of p21 through a mechanism that involves cyclin E (Mandal et al 2005). In worms, CEP-1 mediates UV induced arrest of germ cell proliferation through a direct target PHG-1, a human growth arrest specific 1 homolog (Derry et al 2007). Regulation of autophagy and metabolism are newly appreciated outputs from the p53 regulatory network that may turn out to be broadly conserved and quite ancient. Consistent with this view is the fact that p53 regulates autophagy in mice (Crighton et al 2006, Maiuri et al 2009) and in worms (Tavernarakis et al 2008). Other outputs from the p53 network (such as senescence) may be limited to mammalian systems and, it seems fair to assume that output processes specific to invertebrates (but yet to be identified) may also exist. Therefore, some output modalities appear to be universally represented across phyla (such as promoting apoptosis or DNA repair) while others tend toward specific representation within certain taxa.

Another interesting lesson is, although some p53 downstream outputs are highly conserved, the enabling effectors which couple p53 to a given cellular process are not necessarily shared in common and can vary across phyla (Figure 1-2). A compelling example of this principle is, perhaps, best illustrated by a conserved axis of regulation involving ribonucleotide reductase. In both mammals and in flies, this enzyme is an important p53 effector but, intriguingly, different subunits of this enzyme are the relevant target in different taxa (Akdemir et al 2007, Gatz & Wiesmüller 2006).

P53 IN DEVELOPMENT, AGING AND DISEASE

p53 activity is dispensable for normal animal development. Mice, nematodes, and fruit flies lacking p53 are all viable and, to some degree, fertile (Derry et al 2001, Donehower et al 1992, Lee et al 2003b, Sogame et al 2003). Yet, p53 is preserved in most of eukaryote lineages (Figure 1-1) and non-essential roles for p53 in development have been identified. For example, during embryogenesis, p53 contributes to neural tube closure in mice, mesoderm specification in frogs and programmed cell death in flies (Danilova et al 2008, Yamada et al 2008).

Evidence of p53 function in aging and reduced longevity came from the *Drosophila* model, where selective loss of p53 in neuronal tissue extended adult life span (Bauer et al 2005). The same genetic model was also applied in studies on mechanisms of neurodegeneration in Huntington's disease (Jackson et al 1998, Warrick et al 1998), and here p53 mediates the pathogenesis in both flies and mice (Bae et al 2005, La Spada & Morrison 2005). The developmental contributions of this gene family may also be distributed among complex isoforms of the p63 and p73 paralogs, which theoretically permit for compensation in certain knock-out strains (Bourdon et al 2005). Furthermore, in vertebrate lineages, p63/p73 genes may have acquired essential developmental roles since mice deficient for either of these genes are lethal (Mills et al

1999, Olivier et al 2009, Yang & McKeon 2000, Yang et al 1999). This seems perplexing, and perhaps counter-intuitive, since the non-essential p53-like subfamily is far more widely represented among disparate taxa (Figure 1-1). Recent studies and Chapter Three of this thesis establish that p53 family members exert important quality control functions in germ line tissue (Derry et al 2001, Ghafari et al 2009, Hu et al 2007, Suh et al 2006, Tomasini et al 2008). Therefore, one possible explanation is that activities in the germ line shaped evolutionary patterns of this gene family. Together, these observations indicate that across the animal kingdom, conserved features of the p53 regulatory network are fundamentally linked to adaptive stress responses governing aging and health.

TUMOUR SUPPRESSION – AN EVOLUTIONARY SIDESHOW?

As discussed above, in its wild type form, p53 occupies a central position in stress response networks and thereby limits oncogenesis through activities that govern adaptive responses. When cells are challenged by genotoxic agents, radiation, hypoxia or other inappropriate growth signals, p53 restrains proliferation through activities that arrest the cell cycle, promote senescence, DNA repair or apoptosis. However, unlike conventional tumor suppressors (which are typically affected by nonsense or frameshift mutations), at least 80% of p53 alterations sequenced in tumors are missense mutations (Olivier et al 2002). These encode oncogenic activities distinct from wild type and simple ‘dominant negative’ variants but, despite extensive efforts, the transforming nature of these lesions remains largely elusive. Hence, Are there special properties that impart peculiar activity to the gene and/or its product? Or is p53 simply an ordinary protein that happens to occupy a rate-limiting hub position within larger scale of regulatory networks? It seems that “The p53 gene is mutated in most human cancers” is a common axiom being routinely disseminated throughout the cancer community, but why p53 is so frequently mutated is less sharply in focus.

What selective pressures actually shaped the evolution of p53 function? Although firm conclusions are not yet possible, it is possible that protection against tumor formation was not the ancestral function of this gene or its regulatory network. Support for this idea comes from two main lines of evidence. First, the existence of family members in simple, short-lived organisms (Figure 1-1) suggests that ancestral p53 genes predated the need to suppress the deregulated growth of cells in specialized tissues. Second, until recently, human life expectancy did not exceed ~29 years of age, and it seems unlikely that typically late-onset diseases applied pivotal selective pressures at the population level (Aranda-Anzaldo & Dent 2007). Furthermore, mice and fish lacking p53 often survive longer than their feral counterparts, which usually do not die of cancers and, hence, from an evolutionary point of view, cancer was probably not a significant threat to reproductive success. Together these observations suggest that the tumor suppressive activity of p53 was probably co-opted from other more primordial functions.

One of important tumor suppressor function of p53 is mediated by oncogenic stress through ARF pathway (Martins et al 2006). The relatively late appearance of ARF gene orthologues in the vertebrate lineage (they are absent from both zebra and puffer fish genomes (Gilley & Fried 2001), Amatruda JF, unpublished) seems to suggest other corresponding proteins represent fundamental links between oncogenic stress and p53.

If the p53 family was not fixed in animal populations for cancer-related functions, then what ancestral activity was it actually selected for? Regulation of apoptotic death is a plausible candidate, as current evidence suggests that control of apoptotic death predated regulation of the cell cycle via p21 (see Figure 1-2). However, this does not explain the presence of p53 in unicellular genomes and other output modalities- such as DNA repair and metabolic regulation- are also attractive contenders as ancient outputs from this regulatory network. Fully gratifying solutions to this mystery could emerge from studies that reveal unappreciated requirements for p53 or its relatives, p63 and p73.

Here, developmental and/or physiological roles in stem cell biology (Liu et al 2009b, Meletis et al 2006a, Senoo et al 2007) and germ line tissues (Hu et al 2007, Tomasini et al 2008) seem promising. Equally mysterious, yet equally relevant, are questions related to the types of stress that primordial p53 genes might have been responding to. Here it is worth noting that most experimental stimuli for activating p53 are not encountered in the real (or primordial) world. Hence, they provide only partial clues into selective pressures exerted on the p53 family (Aranda-Anzaldo & Dent 2007). Replication repair stress is a plausible source of adaptive pressure that indeed may have been responsible for selecting or shaping p53 regulatory networks. However, empirical evidence to support this idea is scant and the actual extent of replication repair stress that occurs *in vivo* is not clear.

INSIGHTS FROM AN EVOLUTIONARY PERSPECTIVE

As it seems unlikely that these genes were originally selected to prevent cancer, can knowledge of primordial p53 functions and conserved topologies in the p53 network illuminate new insights regarding cancer-related functions? Though it may be some time before firm solutions to this question emerge, we suspect that the answers will be affirmative and might be forthcoming from models not yet contemplated. Support for optimism comes from several fronts. First, significant gaps in our understanding of p53 remain and it is likely that p53 exerts functions that are yet to be discovered. Consistent with this idea, oncogenic phenotypes associated with mutant p53 in human tumours have not yet been recapitulated by any combination of lesions in known effectors. Second, as discussed above, DNA damage pathways can engage p53 without the involvement of Mdm2 or stabilization of p53 (Langheinrich et al 2002). Hence, unappreciated upstream pathways leading to p53 activation might exist that could potentially be exploited as cancer therapies. Third, p63/p73-like genes are restricted to only certain taxa but, where tested, they are required for viability. In contrast, the p53-

like subfamily is rather ubiquitous among animal taxa and, paradoxically, these genes are not required for viability, suggesting that SAM domain-less members of the p53 family possess unique, fundamental properties. A final reason for optimism is that unanticipated (and sometimes profound) insights consistently emerge through studies that elucidate evolutionary patterns (Baker 2001, Clevers 2006, Hu et al 2007, Jiang & Hui 2008, King et al 2008, Olson 2006).

What significant lessons might be learned from a deeper knowledge of p53 evolution? One unsolved area that seems ripe for discovery relates to the nature of mutant p53 alleles in human cancers, where p53 missense mutants typically reside in trans to a deletion. This fact, together with experimental data, excludes a strict dominant negative classification for most alleles, and argues that the fully transformed state involves gain-of-function activity conferred by missense mutants (Fernald 2006) (Soussi 2007). Thirty years after the protein was described and twenty years after meaningful mutations were found, oncogenic activities conferred by most p53 variants remain mysterious. In the parlance of classical genetics, the transforming nature encoded by these alleles can be thought of as neomorphic activity. As illustrated in Figure 1-5, this category can be further subdivided. For example, some neomorphic alleles are ‘accessorized variants’ that might add functionality on top of wild type activity. Others are ‘devolved variants’ with deranged activities that might preserve only some wild type functions. And still others might produce novel activities with no resemblance to wild type functions at all. Given current evidence, most p53 missense alleles are probably not accessorized variants since hyper-expression that often occurs in human tumors is not consistently accompanied by up-regulation of known p53 target genes (Olivier et al 2009). Hence, it seems plausible that p53 mutant alleles could be either devolved variants or unrelated variants. Consequently, if oncogenic evolution produces variants of the ‘devolved’ class, then knowledge of primordial p53 functions could be important guides towards answering fundamental questions in cancer research.

DISSERTATION OBJECTIVES

The general aim of my thesis study was to understand physiological functions of the p53 regulatory network. To achieve this, I formulated specific aims that will be discussed in subsequent chapters.

1) Development of tools that enable visulization of p53 action *in vivo*

I proposed to generate tools that would allow the detection of p53 functional output in a tractable genetic model, *Drosophila melanogaster*. For this, two independent approaches were undertaken: one was to obtain an antibody to detect the native p53 protein; the second was to follow transcriptional activation by p53 using a transgenic reporter. These approaches would allow me to examine the p53 regulatory network in physiological contexts and obtain a comprehensive picture of p53 functions. Chapter Two discusses these approaches in detail.

2) Identification of physiological stimuli and functions for p53 activities

This was achieved by characterizing p53 activation status during various developmental stages as well as in response to environmental stimuli (Chapter Two). Further genetic analyses were performed to uncover a novel role of p53 during meiosis, a discovery whose validity was extended to a mammalian system (Chapter Three). I then explored the role of p53 activity in germ line stem cells and in response to oncogenic stimuli (Chapter Four).

3) Generation of a loss of function mutation in *cul-2* gene

To understand the downstream output of p53 regulatory network, a novel p53 target gene, *cul-2*, was chosen among a set of radiation induced p53 dependent genes from an array study. Chapter Five details the rationale of choosing this gene and the generation of a loss-of-function mutation in *cul-2* gene.

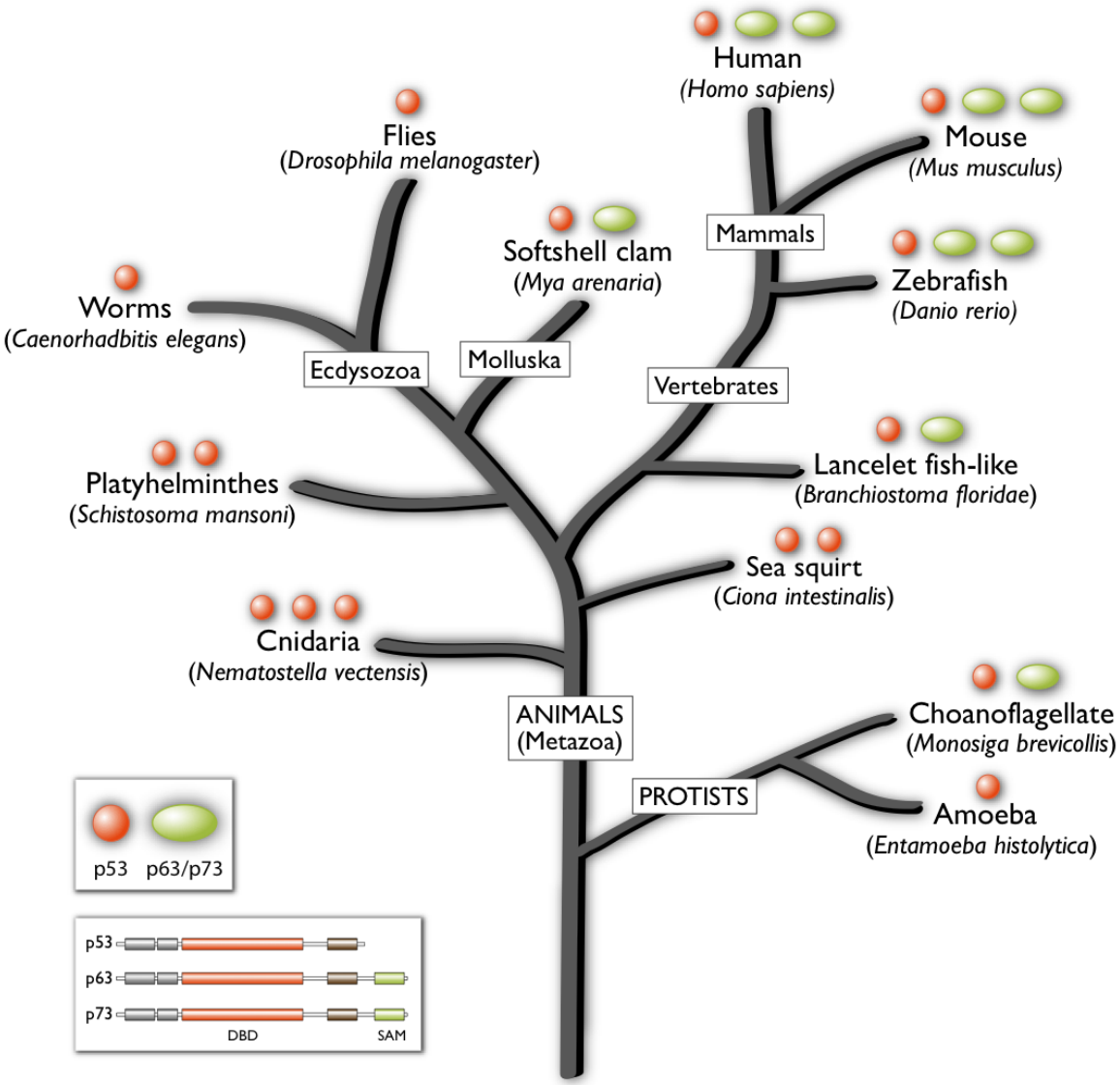

Figure 1-1. p53 homologs in evolution

All sequenced genomes with p53 family member(s) are represented in this schematized family tree. Here, subfamily classification is based solely on the C terminal SAM domain, which is present in the p63/p73-like subfamily and absent in the p53-like subfamily. p53 gene designations are based on published literature and/or predicted

annotations available from public databases but, in some organisms, are not yet functionally validated. *(Lu et al., Nat Rev in Cancer, 2009)*

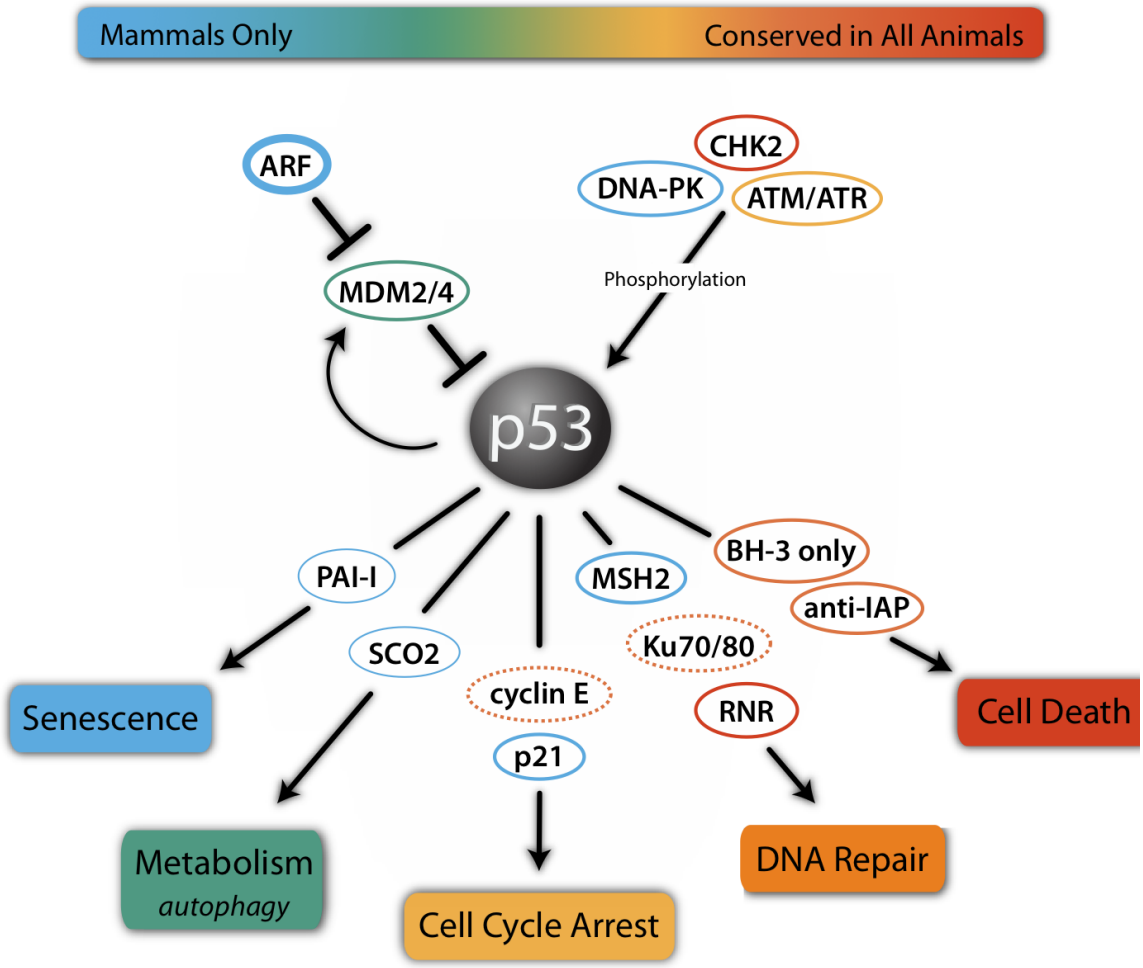

Figure 1-2. A simplified evolutionary schematic of the p53 regulatory network

Shown here are selected upstream regulators, downstream effectors (circles) and output terms (boxed) color coded to indicate conservation, based on current evidence. The color gradient illustrates the range of conservation inferred from available genomic data and functional studies in vertebrates (mouse, zebrafish) and invertebrates (*Drosophila* and *C. elegans*). Cellular processes and associated genes specific to mammals are depicted in blue (such as ARF). Broadly conserved processes and/or gene functions that span from mammals to invertebrate model systems are depicted in red. Regulators and effectors that have been empirically tested for direct links to p53 are depicted with solid lines (thickness indicates degree of confidence in the extent of conservation). Those, which are deduced or presumed, are shown with dotted lines.

Downstream targets (such as SCO2 and PAI-1) not tested beyond mammalian systems are depicted with thin lines.
(Lu et al., Nat Rev in Cancer, 2009)

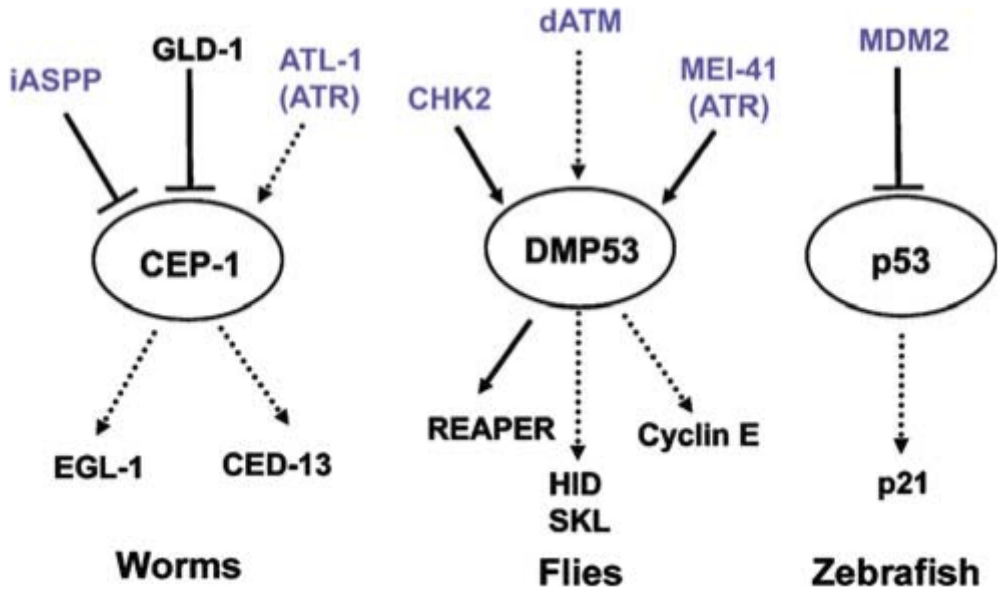

Figure 1-3. Upstream and downstream regulators of p53 in non-mammals

Known components of the p53 regulatory network in non-mammalian models. Components in blue share conserved regulatory functions with mammalian counterparts. Regulators and effectors that have been empirically tested for direct links to p53 in the specific organisms are depicted with solid lines. Those, which are deduced from genetic evidence, are shown with dotted lines.
(Lu et al., Cell Death and Differentiation, 2006)

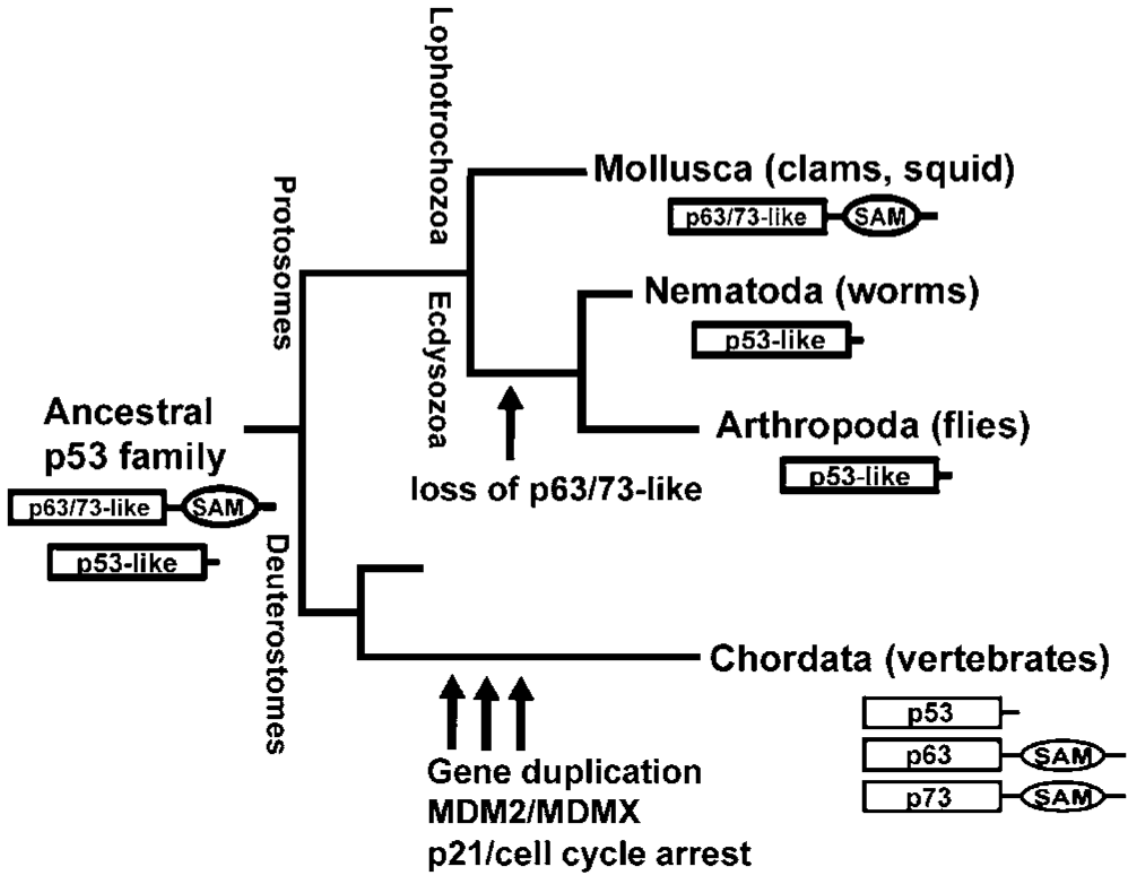

Figure 1-4. Hypothetical p53 ancestry

A parsimonious phyletic tree of the p53 gene family. The common ancestor of vertebrates and invertebrates is proposed to encode an ancient p53- like sequence together with a p63/p73-like paralog containing a SAM domain. This presumed paralog was lost in the ancestor shared by nematodes and flies but retained in molluscs. *(Lu et al., Cell Death and Differentiation, 2006)*

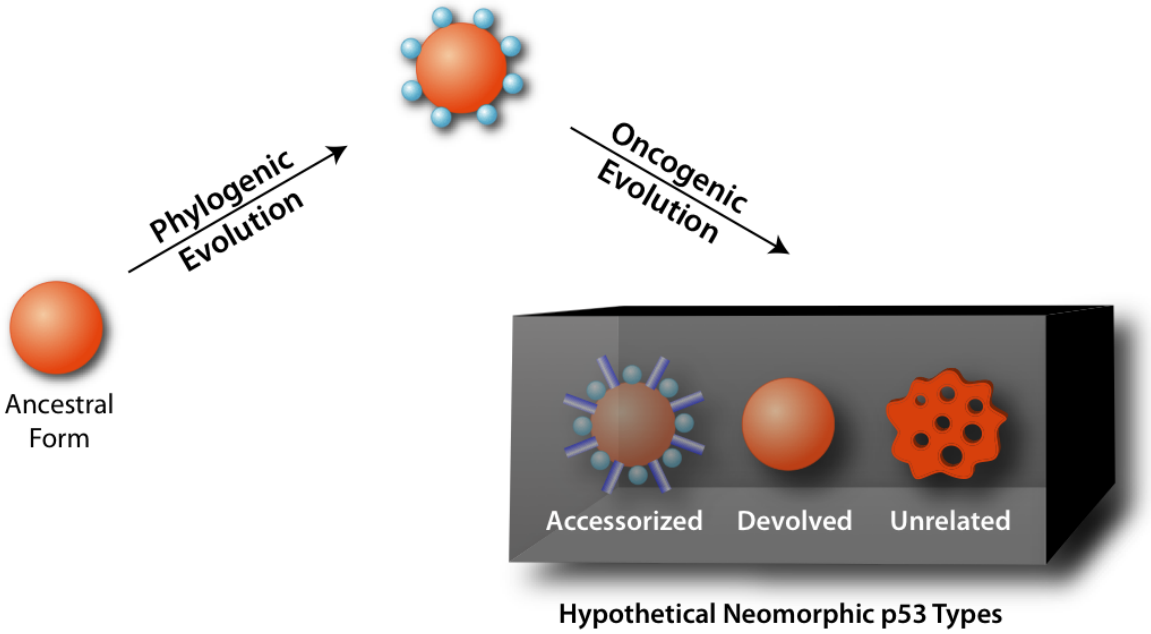

Figure 1-5. A black box of oncogenic evolution of p53

Hypothetical changes during phylogenic and oncogenic evolution of p53 are compared. Possible neomorphic products are shown within the black box. Relative to wild type, these alleles could encode accessorized, devolved or entirely unrelated functions. Note that some functions acquired during phylogenic evolution of p53 appear to be lost during oncogenic evolution (such as p21 regulation). Therefore, missense p53 mutations could produce either 'devolved' or 'unrelated' variants.
(Lu et al., Nat Rev in Cancer, 2009)

Organism	Gene	NCBI accession number	other ID number/database	encoded protein a.a.	Expression or functional evidence
Human					
Homo sapiens	p53	NM_000546.4		393	Y
	p63	NM_003722.4		680	Y
	p73	NM_005427.2		636	Y
Mouse					
Mus musculus	p53	NM_011640.3		390	Y
	p63	NM_001127259.1		680	Y
	p73	NM_001126330.1		638	Y
Zebrafish					
Danio rerio	p53	NM_131327.1		373	Y
	p63	NM_152248.1		576	Y
	p73	NM_183340.1		640	Y
Lancelet fish-like					
Branchiostoma floridae	p53-like	XM_002212112	BRAFLDRAFT_74551(GeneID: 7230376)	416	
	p63/p73-like	XM_002204858	BRAFLDRAFT_67483(GeneID: 7222337)	649	
Flies					
Drosophila melanogaster	p53-like	NM_206544	CG33336	495	Y
Worms					
Caenorhadbitis elegans	p53-like	AF440800	Cel.18659	644	Y
Softshell clam					
Mya arenaria	p53-like	AF253323		443	Kelley et al. Oncogene 20, 748--58 (2001)
	p63/p73-like	AF253324		621	Holbrook et al. Gene 433, 81--87 (2009)
Platyhelminthes					
Schistosoma mansoni	p53-like	Sm_139530	http://www.genedb.org/genedb/smansoni/	696	
	p53-like	Sm_136160.2		410	
Sea squirt					
Ciona intestinalis	p53-like	AB210621	GeneID:100169917	489	
	p53-like	AB210624	GeneID: 778724	419	
Cnidaria					Pankow et al. PLoS ONE 2, e782 (2007)
Nematostella vectensis	p53-like	DQ632751	GENE ID: 5513273 NEMVEDRAFT_v1g104131	492	
	p53-like	EF424411	GENE ID: 5514421 NEMVEDRAFT_v1g100372	203	
	p53-like	EF424412	GENE ID: 5509008 NEMVEDRAFT_v1g211521	369	
Choanoflagellate					
Monosiga brevicollis	p53-like	XM_001747604	ProteinID.27210	571	
	p63/p73-like	XM_001745968	ProteinID.25618	523	
Amoeba					Mendoza et al. Microbiology 149, 885--893 (2003)
Entamoeba histolytica	p53-like	AJ489250		430	

Table 1-1. Accession number of p53 homolog genes

(Lu et al., Nat Rev in Cancer, 2009)

Chapter Two.

p53 network activation in *Drosophila melanogaster*

Materials of this chapter were originally published in:

Meiotic recombination provokes functional activation of the p53 regulatory network

Science 328: 1278-1281. (2010)

Wan-Jin Lu, Joseph Chapo, Ignasi Roig and John M. Abrams

SUMMARY

Two independent approaches were undertaken to follow p53 activity *in vivo* in *Drosophila*. The first approach was to generate an antibody to detect native p53 protein. A new rabbit antiserum against dmp53 was obtained, and over-expressed protein from transfected cells and from larval tissue can be detected by this antiserum. However, this antibody did not reproducibly detect native dmp53 from normal or radiation challenged animals. The second approach was to generate transgenic reporter strains (p53R-GFPnls and p53R-GFPcyt) to detect the transcription activation status of p53. Validation of reporter activities established these strains as useful tools to follow functional output of the p53 regulatory network in real time, in live animals.

INTRODUCTION

Apoptosis

Apoptosis, also regarded as programmed cell death (PCD), is a crucial event that regulates development, homeostasis, and damage responses by engaging caspase activation in metazoans. It is morphologically distinguished by cell shrinkage, blebbing of the plasma membrane, disruption of organelle integrity, condensation and fragmentation of DNA, followed by ordered removal through phagocytosis (Kerr et al 1972).

The core machinery of apoptosis execution is conserved in worms, flies and vertebrates. It consists of a family of cysteine proteases, known as caspases, which are activated by various death signals. Distinct control points have evolved among different species. In *C. elegans*, the decision of cell death is made at EGL-1, which binds to CED-9 and thereby allows CED-4 / CED-3 to activate cell death (Ellis & Horvitz 1986). In mammals, extrinsic signals activate initiator caspases and lead to apoptosome activation. Upstream or parallel to caspase activation are inhibitors of apoptosis (IAPs) that act to prevent cell death by protein-protein interactions and proteolytic degradation (Clem et al 1991, Liston et al 2003). In *Drosophila melanogaster*, important cell death regulation occurs through the induction of pro-apoptotic proteins such as RPR (*reaper*), HID (*head involution defective*), GRIM, SKL (*sickle*) and JAFRAC2 (Christich et al 2002, Tenev et al 2002, White et al 1994). These proteins disrupt IAP-caspase interactions and unleash a cascade of apoptosis-inducing caspase activities to promote cell death (Hays et al 2002, Holley et al 2002, Ryoo et al 2002, Wang et al 1999, Wilson et al 2002, Yoo et al 2002).

Regulation of reaper

Reaper (*rpr*) was first identified in the H99 deficiency mutants, where nearly all apoptosis was blocked during embryogenesis. The chromosomal deletions of *reaper, hid* and *grim* (RHG) genes caused embryonic lethality and resistance to various apoptotic stimuli (White et al 1994). Two mammalian factors, Smac/Diablo and Omi/HtrA2, have been identified as functional homologs of the RHG genes (Du et al 2000, Srinivasula et al 2000). Knockout studies on Smac/Diablo and Omi/HtrA2 in mice model suggested that they are more likely involved in protection against cellular stress (Martins et al 2002, Okada et al 2002). In fly model, the transcriptional control of *rpr* expression appears to be the one of the primary outputs that is regulated by both DNA damage and aberrant development.

Control of cell death by p53

The p53 tumor suppressor protein has a crucial and complex function in the regulation of cell division and cell death. The fundamental role of p53 in apoptosis is emphasized by the evolutionary conservation in both *Drosophila* and *C. elegans*, where the pro-apoptotic role of p53 is suggested to be its ancient function (Ollmann et al 2000, Schumacher et al 2001). The transcriptional control of *rpr* expression by dmp53 appears to be the primary response to both genotoxic damage and aberrant development (Brodsky et al 2000, Nordstrom et al 1996). Within the upstream regulatory region of *rpr* locus, a 150bp enhancer is responsible for gamma-radiation induced transcription activity, and contains a 20bp consensus p53 binding site (Brodsky et al 2000, Nordstrom et al 1996). This 20bp p53 responsive element (p53RE) is unresponsive to signal that induces excessive apoptosis during abnormal development, suggesting distinct regulatory regions are used to sense different apoptotic stimuli. In addition, *dmp53* null embryos lose this stress-induced transcriptional activity upon ionizing

radiation, suggesting that this enhancer region is an important effector of p53-induced apoptosis in response to radiation (Sogame et al 2003).

MATERIALS AND METHODS

Transfection of *Drosophila* S2 cells

Drosophila S2 cells were cultured in SF900-II with Pen/Strep antibiotics at 25°C. After transfected with 2µg of plasmid DNA, pMTAL-p53-EGFP (CellFECTIN, Invitrogen), protein expression was induced with copper sulfate and cell lysate was harvested 5hr after induction.

Preparation of tissue extracts from embryo:

Embryos were collected and dechorionated in 50% bleach. After washes, embryos were first snap-frozen in liquid nitrogen then homogenized in glass pestle containing lysis buffer. Lysis buffer includes Buffer A, Triton X-100 and Protease inhibitor (Roche). Buffer A: 20mM HEPES, 10mM KCl, 1.5mM MgCl2, 1mM EDTA, 1mM EGTA, 250mM sucrose. 0.5% Triton-X100 was added to Buffer A before use. 1 mini-tablet of protease inhibitor cocktail (Roche) was used in 7ml of lysis buffer. After repeated centrifugation for 30min 13,000rpm at 4°C to clean up tissue debris, concentration of extracts was measured by standard Bradford protein assay. Clear extracts were transferred to new eppendorfs and snap-frozen in liquid nitrogen before storing at -80°C.

Affinity purification of dmp53 antiserum

10mg of peptide (1:1 mix of the two synthesized peptides) was reduced and coupled to a gravity-flow column for antiserum purification. The purification steps were performed with SulfoLink (PIERCE). 100mM of glycine, pH3.0 was used for elution and neutralized with 1M Tris, pH 7.5. Absorbance at 280nm was used to identify fractions containing protein and pooled for an additional concentrating step using cetricon filter (Millipore).

Immunoblot analysis:

6µg of tissue extracts were subjected to 10% SDS-PAGE (NuPAGE, Invitrogen), after which the proteins were transferred to PVDF membrane. The immunoblots were performed at 4°C overnight using the following primary antibodies: 1:5000 anti-tubulin (E7, Developmental Studies Hybridoma Bank, University of Iowa), 10 *µ*g of affinity purified rabbit polyclonal antibody against dmp53 (627A) in 1% skim milk/ 0.2% Tween-20/TBS. Bound antibodies were visualized by chemiluminescence ECL Plus kit (Amersham Biosciences/GE Healthcare) using a 1:5000 dilution of anti-mouse IgG (Jackson ImmunoResearch Laboratories, Inc.) or a 1:5000 dilution of anti-rabbit conjugated to horseradish peroxidase (Amersham Biosciences). The filters were exposed to Kodak X-Omat Blue XB-1 film at room temperature.

Radiation induced apoptotic cell detection by acridine orange staining:

Third instar wandering larvae were hand-picked and exposed to 40Gy of IR. After 4hr of recovery at 25°C (cell death became first apparent 3 hr after irradiation), wing imaginal discs were dissected from larvae in PBS or Ringer's and stained for 8 min in 1 *µ*g/ml acridine orange in PBS (AO stock solution: 5 *µ*g/ml). Dissected tissue were protected from light during staining. After washing with PBS-Triton (0.1%), discs were transferred to glass slide using the pippet tip with the sharp end trimmed off. The glass slides were pre-coated with halocarbon oil in a circle and tissues were placed in the center of oil then mounted with coverslip. To avoid photo-bleaching, discs were imaged within 10min with decreased arc lamp intensity to 35~40%. The discs were examined in the fluorescein (FITC) or Rhodamine channel and the total number of stained nuclei was determined for each disc by manual counting.

Radiation induced apoptotic cell detection by immunohistochemistry

Third instar wandering larvae were treated as described in acridine orange staining, except the tissues were fixed in 4% formaldehyde/ PBS and heptane (1:1) with

rotation for 30min. After removing fixative, tissues were washed with PBS-0.1% Tween-20 (PBT) twice for 5 min each. After Blocking with PBT-1.5% bovine serum albumin (BSA) and 5% normal goat serum (NGS), discs were incubated with primary antibody, anti-GFP (1:1000) or preadsorbed antiserum 627A (1:250). For antiserum pre-absorption, 4µg of purified 627A was incubated with 1.3mg of *p53*^{ns} embryo extracts (1:3 ratio) and rotated overnight at 4°C. After washes, FITC or Texas-Red conjugated ant-rabbit secondary antibodies were used for visualization.

p53Rps transgenic transformation constructs:

Plasmid Constructions – The transfomation vectors, pH-Stinger and pGreeen-H-Pelican (Barolo et al 2004), were obtained from Drosophila Genomics Resource Center (Bloomington, IN, USA). Two primers of 98 base pairs in length: CTA GAA TTC CGT CCG CTC GAC TTG TTC AAA CAT GTC AGG TTG GTT CTT CCA CTT TTA TTT GAG TAA TTT TCG CCC TTT TTC CAT AGA TTT TCA TAG AT, and AGA GGA TCC CTC GAA CAC GTC GAT GCA CGC TGA GTG AAG AAA TCT GAA AAC CCA TTC CGA AAA TTC GTT ATC TAT GAA AAT CTA TGG AAA AAG GGC GA, were synthesized and allowed to hybridize via 29bp overlapping sequence, and were then filled with Klenow and dNTPs. The fragment was placed between EcoRI and BamHI sites. After amplification, plasmids were injected into fly embryos.

Transgenic animals – After standard transformation, the transgenic lines that were obtained were named “GHP150/ p53R-GFPcyt” and “STI150/ p53R-GFPnls”. The insertion sites in each transgenic line, STI150 at 2R:52C and GHP150 at 3R:100C, were mapped using standard inverse PCR. Both transgenic lines were homozygous viable stocks.

Fly stocks and genetics:

All fly stocks were maintained at 22-25°C on standard food media. We obtained *chk2* mutant (*mnk*^{p6}) from T. Schupbach (Princeton University, Princeton, NJ, USA). All

other stocks were from Bloomington Stock Center (Indiana University, Bloomington, IN, USA). STI150 line and *chk2* allele, *mnk*^{p6} were both located on the second chromosome and standard meiotic recombination method was carried out to obtain recombinants, which were then verified by genomic PCR. Primers specific for STI150 construct, 150-Fwd (TCC GTC CGC TCG ACT TGT TCA AA) and eGFP-Rev1" (TGT GGC GGA TCT TGA AGT TCA CCT) were used together with primers specific to *mnk*^{p6} locus, mnk-F1 (AGA AAT TGT AGT CCC TCG CGC AGT) and lacW-R1 (TGT AAC TCG CCT TGA TCG TTG GGA). Multiple *p53* null alleles, ns, 1 and 2 (Rong et al 2002, Sogame et al 2003), were used in single allele state or in trans-combination to reduce background genetic influences.

Radiation response assay and microscopy:

Staged embryos (4.5-7h AEL for early stage, or 9-12h AEL for late stage) were exposed to 40Gy of ionizing radiation using a Cs-137 Mark 1-68A irradiator (J.L. Shepherd & Associates, San Ferando, CA, USA). To examine GFP expression, embryos were dechorionated in 50% bleach 120-150 min after IR, and immersed in halocarbon oil 700 (Sigma-Aldrich) for imaging. Time-lapse images were acquired on TCSSP Spectral Confocal Microscope (Leica Microsystems). Z-stacks of images from each time point were projected using Image J software (NIH, Bethesda, MD, USA). Epifluorescence images were acquired on Axioplan 2E microscope (Carl Zeiss) attached with Hamamatsu monochrome digital camera. Figures were prepared using Adobe photoshop and Illustrator CS2 (Adobe Systems).

RESULTS

Generation of a polyclonal antibody against dmp53

Two peptides were designed according to the protein structure of dmp53 (Figure 2-1) and equal mixture of the two peptides was used to immunize rabbits by Core facility in UTSW. After the antiserum was obtained, peptide affinity purification was carried out due to the high background of non-specific bands on immunoblots (data not shown). Using transfected EGFP-fusion dmp53 protein in S2 cells as positive controls, purified 627A (p627A) detected overexpressed dmp53 protein (Figure 2-2). However, purified 627A serum failed to detect specific signals of native p53 protein from irradiated embryo or adult extracts.

I next tested whether purified dmp53 antiserum could detect native or overexpressed dmp53 protein in animal tissues. First I over-expressed dmp53 using engrailed-Gal4 driver and UAS-dmp53 in larval wing discs. Using co-expressed EGFP to label active Gal4 drivers, co-localized dmp53 protein was detected at low intensity by pre-adsorbed p627A (See Material and methods) (Figure 2-3). For the detection of endogenous dmp53, I irradiated *wild type* and *p53*$^{-/-}$ larvae with 40Gy of IR, and immunostained their wing discs, with p627A. However, p627A failed to detect endogenous dmp53 (Figure 2-4).

The purpose of generating an antibody to dmp53 was to detect endogenous protein, but p627A did not meet our expectation and was not used for later studies. Two other monoclonal antibodies (c7a4 and H2) were able to detect endougeneous dmp53 in germ line tissue, which will be described in Chapter Four.

Construction of genetic reporters for p53 regulatory network

I placed green fluorescent protein (GFP) under the control of an enhancer taken from sequences upstream of the *Drosophila reaper* (*rpr*) locus, which included a p53 consensus binding site (Figure 2-5). The 150bp fragment was inserted into two separate plasmids, pH-Stinger and pGreen H-Pelican (Barolo et al 2004). The STI150 strain produced nuclear localized GFP (p53R-GFPnls) and the GHP150 did not (p53R-GFPcyt). p53Rps (p53 Reporters) is used hereafter to refer both strains. The genomic insertion site of each transgenic line was mapped by inverse PCR. Both strains were homozygous viable and showed fertility comparable to *wild type* flies.

Radiation induced p53Rps activation in Drosophila

To establish whether p53Rps recapitulate DNA damage-induced p53 activation *in vivo*, p53Rps transgenic embryos were exposed to 40Gys of IR and GFP expression was examined by time-lapse live imaging. GFP expression was observed as early as 70min after exposure, and was prominent at 180min in virtually all embryos (supplemental movie 1 and Figure 2-5). Both transgenic strains showed a similar pattern of GFP expression kinetics after IR (Figure 2-6). The nuclear localized GFP was punctate and facilitated studies in the embryo.

Validation of reporters

In order to validate that radiation-induced GFP expression was due to activation of p53 signaling, I tested if *p53* and its upstream kinase, *chk2* (Peters et al 2002) were genetically required for p53R-GFP activation. GFP expression was not observed in irradiated embryos lacking *p53* or *chk2* (Figure 2-7), showing that p53 signaling pathway was required for p53Rps activity. Thus, the p53Rps was validated as an authentic proxy to monitor p53 activation *in vivo*.

p53 activation in response to other stimuli

One of the major consequences of IR exposure is to create DNA double-stranded breaks (DSBs). To address whether DNA break ends were sufficient to activate p53, p53Rps embryos were injected with restriction enzyme digested phage DNA. GFP expression was observed in DNA injected embryos, but not in buffer injected controls (Figure 2-8, A and B). I also tested whether other forms of DNA damage could activate p53. After treating p53R-GFPnls embryos with UV radiation, the induction of GFP was observed (Figure 2-8, C and D), although at lower penetrance when compared to IR. Thus I found that UV mediated *reaper* induction was due to p53 activation. In summary, these results showed the p53 regulatory network could be activated by multiple sources of DNA damage including IR, UV, and injected DNA fragments.

Tissue and developmental constrains of p53 activation

It has been suggested that the p53 network operates in a tissue-specific context since p53 knock-out mice develop tumor only in certain tissues. This raised the question: how does a cell determine its fate (survival or death) after DNA damage in relation to p53 activation? p53Rps offered a new opportunity answer this question, in particular whether this decision would be made upstream or downstream of p53 activation.

I tested whether p53R-GFP expression was induced in all cells. Interestingly, despite the ubiquitous presence of p53 RNA (Jin et al 2000), GFP expression was virtually absent in mesodermal tissue after IR (Figure 2-9). Additionally, aged embryos showed attenuated radiation-induced p53 activation, and became non-responsive at 9hAEL/stage 13 (supplemental movie 2 and Figure 2-10). The results showed the p53 activation was under the influence of tissue type and developmental stages, suggesting the decision of radio-sensitivity was made at/or upstream of p53 action, but certainly not downstream.

Assessments of genetic screens

In order to identify novel upstream components of p53 activation in response to genotoxic stress, three possible genetic screening strategies were taken into consideration:

1) Embryo sorter

With the advantage of having GFP as a quantifiable readout, an automated embryo-sorting instrument could be used for high-throughput genetic screening. However, the design of the machine requires amounts of embryos incompatible with high throughput tests of genotypes.

2) Classical screen

I also considered using collections of deficiency kit or P element insertion lines. However, two generation of genetic crosses were needed to obtain homozygous mutant adult with p53R-GFP transgene for embryo collection. In addition, of the lethal mutations to be examined, embryos could be only collected from heterozygous parents and phenotypes were expected in 25% of the embryos. Due to the common challenges such as aberrant embryogenesis, and rescue effect from transcript that were maternally loaded during oogenesis, this type of genetic screen was generally discouraged.

3) Double-strand RNA (dsRNA) screen

Genome-wide knock-down using dsRNA was comparably more attractive method than the previous two, for two reasons. First was the availability of dsRNA library, which was constructed by several collaborative efforts by *Drosophila* research community. Secondly, there were several precedents for this screen method, and the materials were not limited because the number of embryos needed for microinjection could be easily collected in large quantity from homozygous p53Rps strains. There was the possibility of carrying a genetic screen using microinjection methods, which I pursued further. I started by testing “proof of concept” dsRNA that knocked down GFP and p53 along with

a non-relevent knock down control, luciferase gene (Figure 2-11). I was able to show that the IR induced p53R-GFP response can be reduced about 50% (p53 or GFP, see panel C in Figure 2-11). Although dsRNA knock-down strategy seemed to be effective, I decided not to pursue further (see discussion).

Survey of stimuli for p53 activation

To identify physiological stimuli that might activate p53 during fly development, I characterized the reporter behavior at various stages. In larval tissues such as brain, midgut, hemolymph, imaginal discs, etc., p53Rps were not responsive to IR (summarized in Table 2-1). One particular exception was seen in larval salivary glands where reporters were on in unirradiated larvae and was modulated by p53 status (Figure 2-12). Another form of programmed cell death (PCD) happens in wing epithelial cells after eclosion (Link et al 2007). In order to test whether p53 activation occurs during this process, wings from p53R-GFP transgenic animals were imaged within 40min after eclosion, and GFP expression was not found (data not shown). This result suggested that p53 is not required for post-eclosion wing PCD, and is consistent with the observation that p53 mutant does not develop wing blemish spontaneously (see discussion).

Taken together, these results showed that the p53 regulatory network varied in different cell types and developmental stages. The only tissue type in which I found p53R-GFP activation during normal development was female ovary. Activation of p53 and its functional relevance in germ line tissue will be further discussed in Chapters Three and Four.

DISCUSSION

A large body of knowledge on how p53 responds to stress and engage its downstream functions was based on transformed human cancer cell lines in tissue culture, and stimulated with non-physiological level of genotoxic stress. These type of studies provided only limited information about the nonautonomous roles of p53 in whole organisms and mystery remain regarding what physiological stimuli the p53 network responds to. Three types of reporters were previously constructed in mice. First one was a p53 promoter-CAT transgenic mice by Rotter lab (Almon et al 1993); second one was a p53 responsive element-lacZ reporter mice independently generated by Gudkov lab and Oren lab (Gottlieb et al 1997, Komarova et al 1997); the third type was a luciferase-based reporter by Vassaux lab (Briat & Vassaux 2008). However, during early development and adults, it is difficult or not possible to visulize robust signals in live animals. In contrast, GFP-based reporters described here permit the possibility of monitoring p53 transcriptional activities by live-imaging in real-time.

Very little p53 activity occurred throughout *Drosophila* embryonic development. This observation was consistent with previous studies in mice (Gottlieb et al 1997, Komarova et al 1997). However, when DNA damage-induced p53 activation occurred in developing embryos, it was a fast and robust process (within 70min in virtually all embryos) during which germband retraction was able to proceed (supplemental movie 1 and Figure 2-5). The reporter system also indicated that the p53 regulatory network in developing embryos was a potent sensor for DNA double-strand breaks (DSBs) generated by IR, UV or injected DNA. The GFP intensity and penetrance was lower in UV (Figure 2-8) raised the question whether amount of DNA damage corelates to reporter activities. This hypothesis would require a degradable-GFP construct allowing protein turnover rate to be quantified in the future.

In aged embryos, the radiation-induced p53R-GFP activation was completely abolished (Figure 2-10). This developmental "switch" phenomenon was also reported in several other radio-responsive genes including *reaper*, and it was proposed that this sensitive-to-resistant transition was due to the blocking of the enhancer region by large-scale chromatin factors (Zhang et al 2008). However, the 150bp element that I constructed still observed this constraint, suggesting the transition was captured by this fragement and can be position independent.

When p53Rpr behavior was examined in different developmental stages, larval salivary gland was one of the tissues of particular interest due to its polyploidy chromosome. In contrast to most of other tissue the lacked p53R-GFP activity, GFP expression was constitutively active in salivary gland starting from the transition from L3 to late L3. In this context, reporter appeared to be either p53 suppressed or independent of p53 (Figure 2-12). This suggested that other active enhancer elements within the 150bp sequence could be negatively regulated by p53 before/during the onset of metamorphosis.

p53 was dispensable for most of the developmental processes, including communal post-eclosion PCD. This notion was confirmed by the absence of p53R-GFP activity in wing epithelial cells after eclosion (data not shown), despite that p53 function is required for damage induced cell death in larval wing discs (Sogame et al 2003). Interestingly, in hypomorphic allele of $dark^{CD4}$ mutants, absence of p53 induced severe wing blemishes, revealing a genetic interaction between p53 with *Drosophila* Apaf-1 homolog (Sogame PhD thesis, 2005). Therefore, p53 may not be required for most of the PCD but could operate functions under certain "stressed" circumstances.

To search for new components in DNA damage response of p53, I considered three possible strategies to perform genetic screens using p53Rps. Although the dsRNA knock-down strategy was effective (Figure 2-11), there were several limitations: first the phenotype scoring was largely relying on the consistency on embryo survivals after microinjection. Second, the intensity of GFP output was highly variable and scoring was

subjected to human bias. Therefore, I did not perform genetic screens using dsRNA microinjection in the embryo.

On the other hand, I discovered germ line specific p53 activations under both physiological and stressed conditions, which offered intriguing opportunities to investigate the ancestral functions of p53. Germ line related studies will be discussed in detail in Chapters Three and Four.

Figure 2-1. Dmp53 protein structure and the peptides for antibody production

Transactivation domain (Tx), DNA binding domain, and tetramerization domain (Tet) of dmp53 are illustrated. Positions of the two peptides used for immunization are depicted in blue (1 and 2), the design of peptide 2 spands the Tet domain was based on the protein structure. Distance is not to scale.

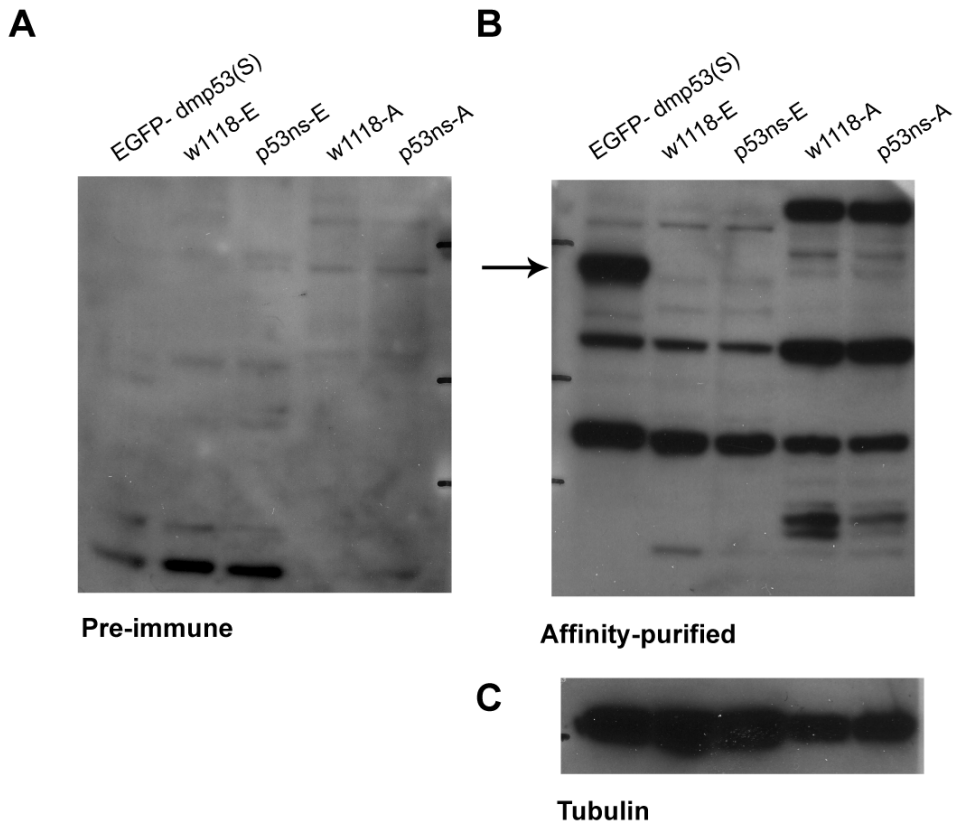

Figure 2-2. Immunoblot of endogenous and overexpressed dmp53

Western blots showing **(A)** Pre-immuned anti-dmp53 serum and **(B)** purified 627A serum was used to detect overexpressed dmp53 from S2 cells or endogenous dmp53 from wild type and p53 mutants. **(C)** gamma-tubulin showing loading control. S2 cells were transfected with short-form of dmp53 fused with EGFP. Extracts from w^{1118} embryo (E) or adult (A) was used as *wild type*; $p53^{ns}$ lacked native dmp53. Arrow indicates the specific signal from overexpressed dmp53-EGFP.

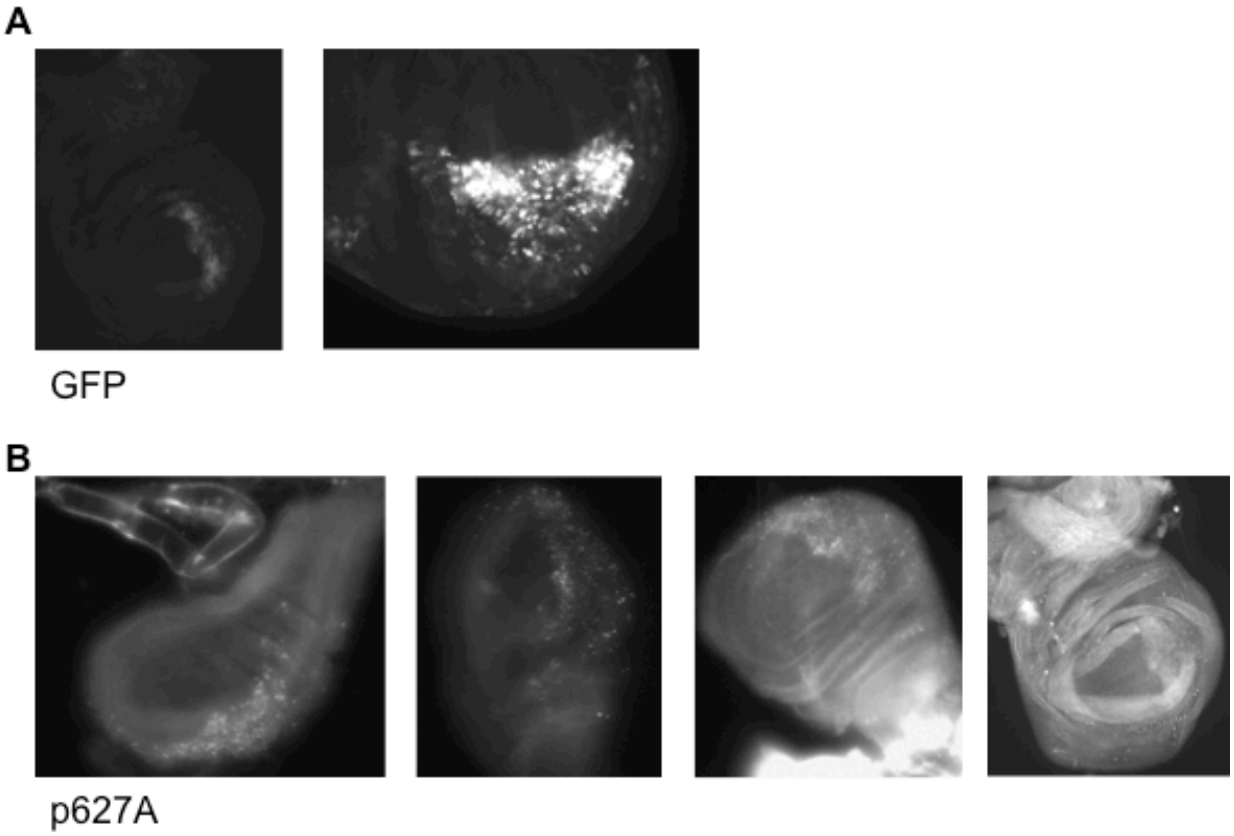

Figure 2-3. Over-expressed dmp53 in wing disc

Immunostaining for **(A)** GFP and **(B)** dmp53 using anti-GFP and p627A antibodies in larval wing discs dissected from animals that over-expressed EGFP and dmp53. Engrailed-Gal4 driver was used. Multiple examples are shown from each antibody. Non-specific fluorescence background was high with p627A.

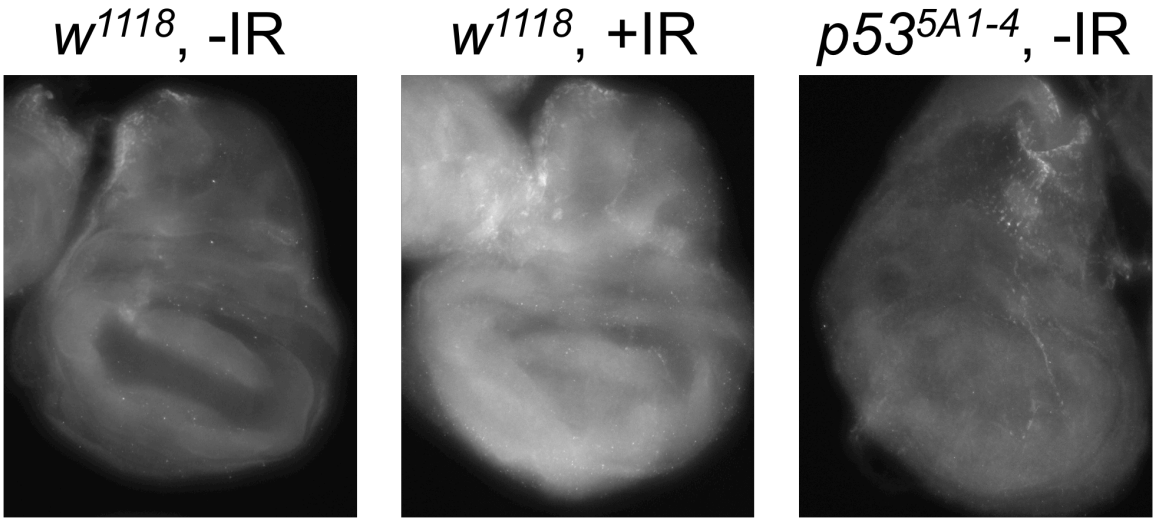

Figure 2-4. Antiserum fails to detect endogenous dmp53

Immunostaining of dmp53 in larval wing discs dissected from *wild type* or $p53^{-/-}$ animals with or without IR. No specific signal was observed.

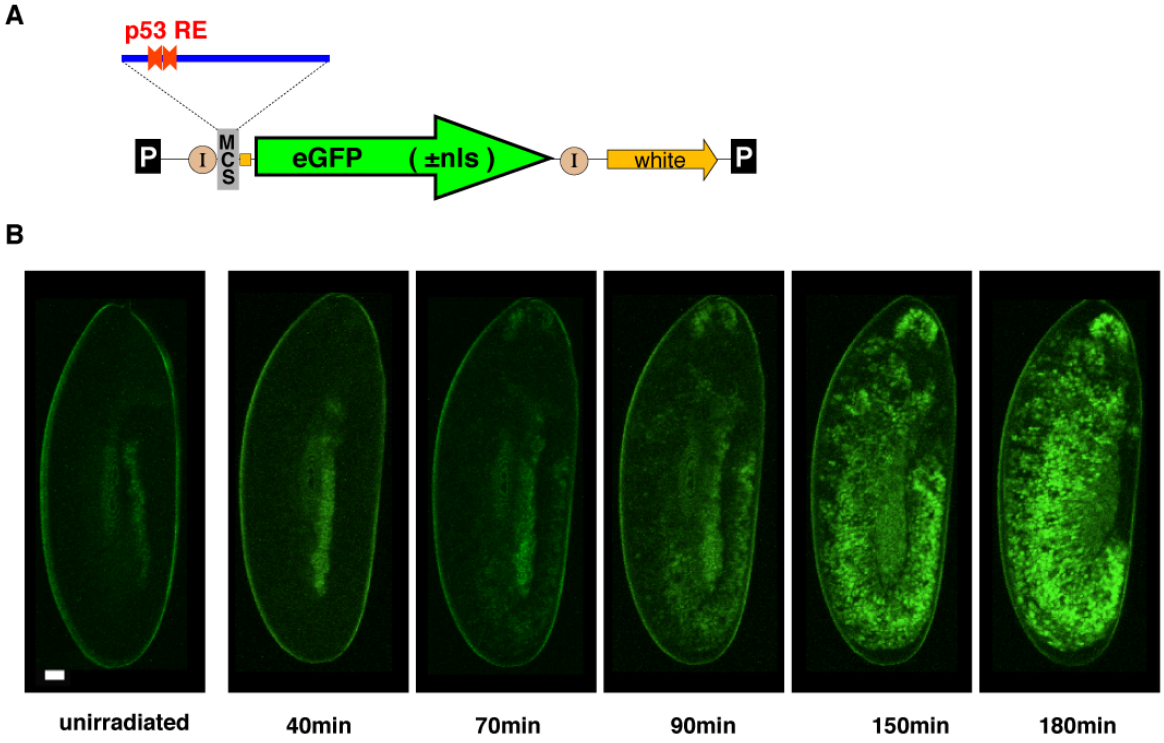

Figure 2-5. p53Rps construct and its activation in *Drosophila* embryos

(A) Illustration of p53Rps transgenes. A 150bp enhancer (blue) containing a consensus p53 binding site (p53RE, red arrows) drives two different eGFP constructs. One bears a nuclear localization signal (p53R-GFPnls) and one does not (p53R-GFPcyt). Distances are not to scale. P, P element sequence; MCS, multiple cloning site; I, insulator; white, eye color for transformant selection; nls, nuclear localization signal; distances are not to scale. **(B)** Confocal images of p53R-GFPnls activation in *Drosophila* embryos at various time points after exposure to ionizing radiation followed by time-lapse live imaging. Scale bar, 10 microns.

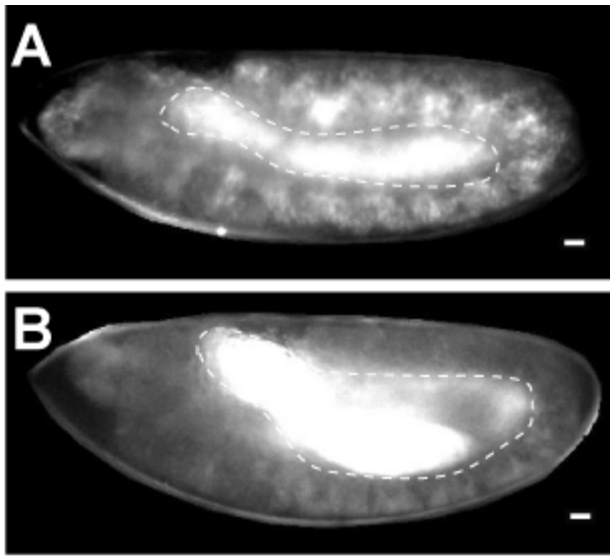

Figure 2-6. Activation of the p53Rps by IR in two independent transgenic strains

Epifluorescent images of irradiated *wild type* embryos. **(A)** Transgenic nuclear-localized GFP strain, p53R-GFPnls and **(B)** cytoplasmic-localized strain, p53R-GFPcyt are shown. Autofluorescence from the yolk is marked with dotted lines. Scale bar, 10 microns.

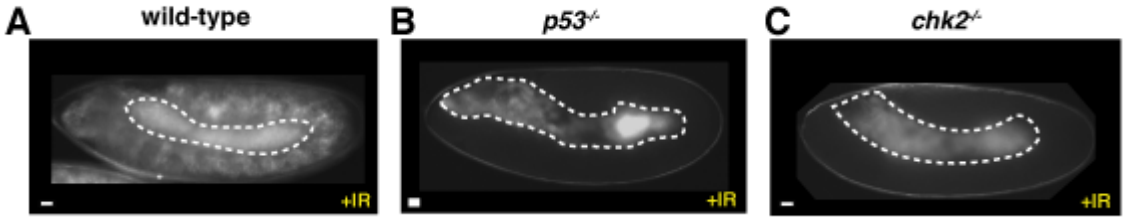

Figure 2-7. p53 and chk2 dependent p53Rpr activation by IR

(**A**) Stimulus induced p53R-GFP expression seen in *wild type*, is not seen in **(B)** $p53^{-/-}$ or **(C)** $chk2^{-/-}$ animals. Autofluorescence from the yolk is marked with dotted lines; scale bar, 10µm.

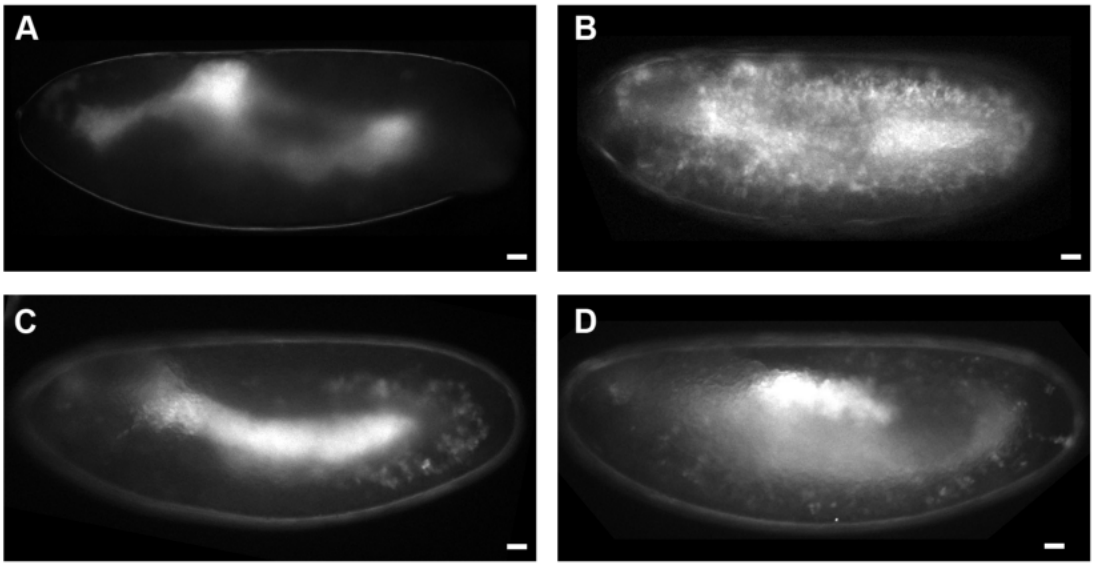

Figure 2-8. Activation of the p53Rps by injected double-strand DNA and UV in *Drosophila* embryos

Epifluorescent images of p53R-GFPnls embryos. **(A)** Buffer-injected control embryos. **(B)** Embryos injected with ΦX174 HaeIII digested DNA fragments (0.5µg/µl). 0-30min after egg laying (AEL) embryos were collected, dechorionated and injected. After recovery at 25°C, embryos at 8-9hr AEL of age were imaged. **(C)** Embryos irradiated with 100J/m^2 of UVB. **(D)** Embryos irradiated with 500J/m^2 of UVB. In these studies, both expressivity and penetrance of these responses were incomplete and appeared less robust than IR. Responses were not intended for quantitative comparison and were not kinetically measured. Scale bar, 10 microns.

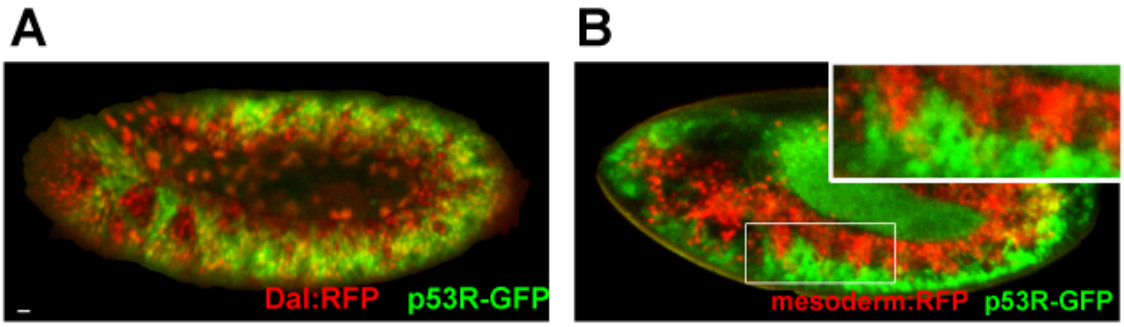

Figure 2-9. Tissue specificity of Rpr150-GFP IR response

(A) DsRed is ubiquitouly expressed by doughterless-Gal4 driver (red) **(B)** DsRed were expressed under the control of P{GawB}how24B in embryonic mesoderm (red). In (A) and (B), p53Rps-nls responsive cells are illustrated in green. Magnified inset in (B) shows little overlap of p53 activation with mesodermal cells (red).

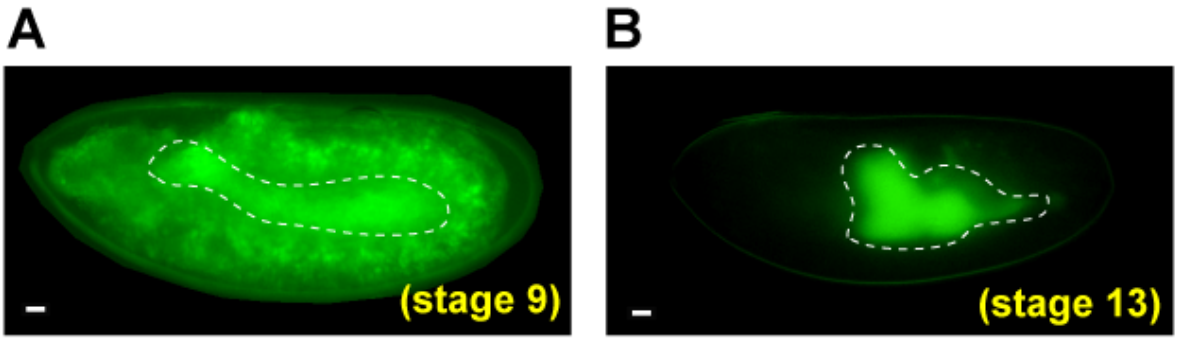

Figure 2-10. Age-dependent radiation induced p53Rps response

(**A)** Epifluorescent images of live embryos that were irradiated at stage 9 then recovered for 2hr. **(B)** irradiated at stage 13 with the same recovery time. Autofluorescence from the yolk is marked with dotted lines. Scale bar, 10 microns.

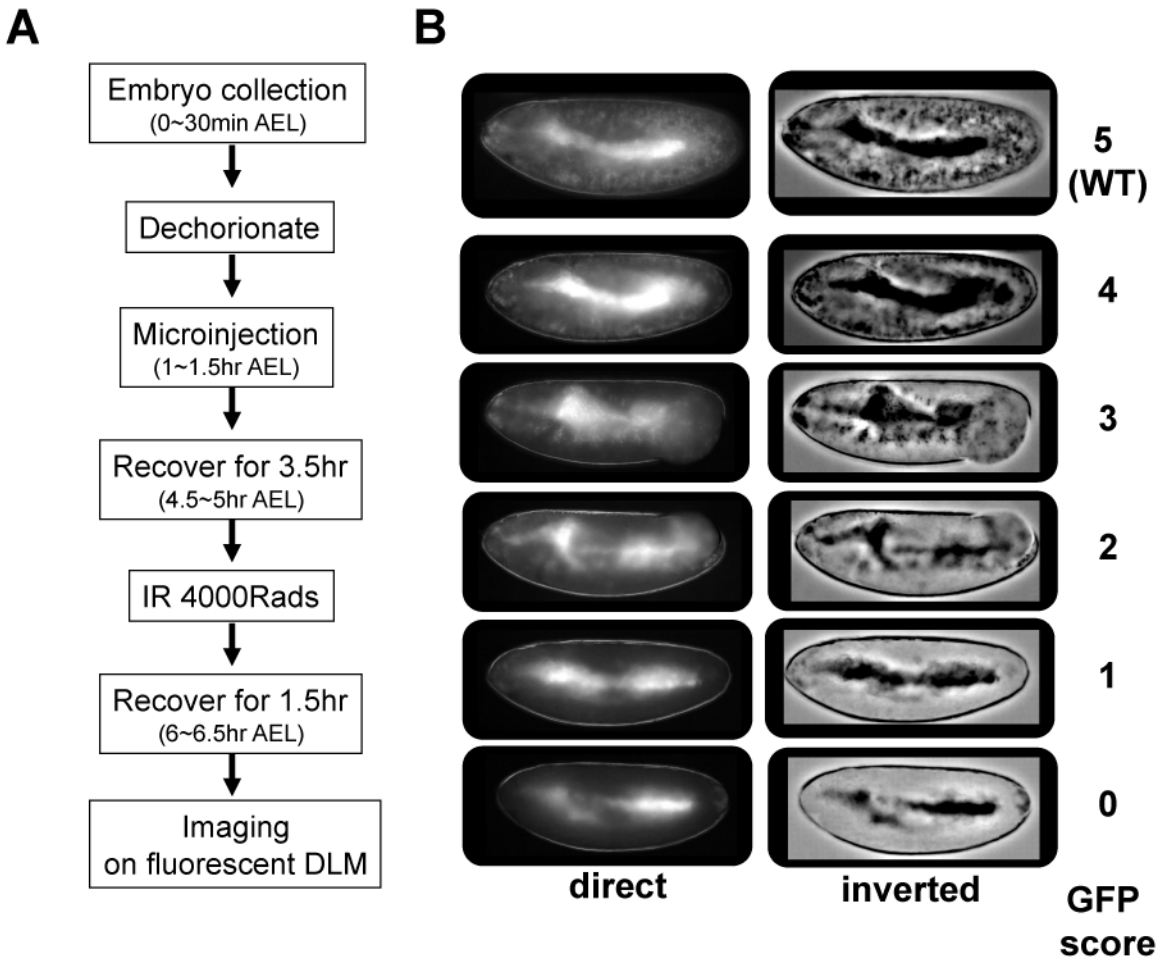

C

	p53		rluc		GFP			
trial date	dsRNA_1		dsRNA_2		dsRNA_3		uninjected	
	n	IR score	n	IR score	n	IR score	n	IR score
20060908	20	1.5	19	4	20	0.7	4	3.5
20060913	14	1.8	21	3.4	29	2.2	7	5
20060920	27	1.9			55	0.9	32	4.3
Total	**61**	**1.7333**	**40**	**3.7**	**104**	**1.2667**	**43**	**4.2667**

Figure 2-11. Knock-down of p53 or GFP transcript for radiation induced p53Rps response

(A) Flow chart scheme showing the protocols used for microinjection of dsRNA then assayed for IR induced p53R-GFP response. DLM, digital light microscope. **(B)** Direct

epifluorescent or FFT-bandpass filter inverted images showing the number of GFP expressing cells. Due to the variability of knock-down, arbitrary score from 5 (comparable to *wild type*) to 0 was used and examples for each score are shown here. **(C)** Scoring results of the three dsRNA: p53, GFP or rluc (luciferase, for negative control) to determine the feasibility of the method.

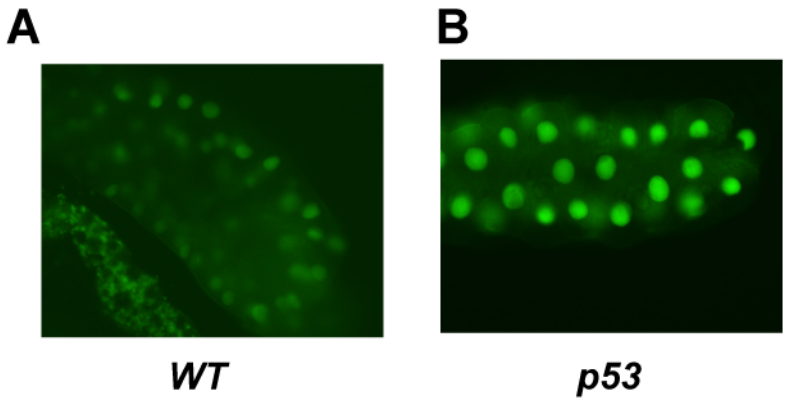

Figure 2-12. p53R-GFP expression in larval salivary gland

Live GFP fluorescent image of p53R-GFPnls in **(A)** *wild type* and **(B)** $p53^{ns}$ animals. Note that reporter in this instance appeared to be either p53 suppressed or independent of p53.

Development Stage & Tissue		- IR	+IR	p53 Required?
Embryonic	0~4hr AEL	-	-	-
	5~8hr AEL	-	+	Yes
	12~16hr AEL	-	-	-
Larval	L1 & L2	-	-	-
	Hemolymph	-	-	-
	Imaginal discs	-	-	-
	Brain lobe	-	-	-
	Salivary gland	+	+	Modulated
Adult	Testes	+/-	+/-	No
	Ovary	+	+	Yes

Table 2-1. Survey of p53Rps activation during *Drosophila* development and stress response

Special thanks to Joe Chapo for building p53Rps contructs and UTSW Core Facilities for synthesizing peptides and generating dmp53 polyclonal antibody.

Chapter Three.

Meiotic recombination instigates functional activations of the p53 regulatory network

Part of this chapter is based upon:

Meiotic recombination provokes functional activation of the p53 regulatory network

Science 328: 1278-1281. (2010)

Wan-Jin Lu, Joseph Chapo, Ignasi Roig and John M. Abrams

SUMMARY

Multiple lines of evidence indicate that the evolutionary appearance of p53 preceded tumor suppression, suggesting unappreciated functions for this regulatory network. By following genetic reporters in the *Drosophila* model, I found a transient activation of p53 during germ line development, which was instigated by an ancient physiological process, meiotic recombination. Specifically, the first enzymatic step by SPO11 for generating meiotic DSBs provoked this transient p53 activity. The p53 activity was substantially prolonged in cells defective for meiotic repair and retrotransposon silencing. Likewise, p53 in the germline controlled recombination frequency and specified proper gametogenesis when meiotic effectors failed. The initiation of meiotic crossover events as an intrinsic stimulus for the p53 regulatory network is highly conserved, because Spo11-dependent activation of p53 also occurred in mice.

In this part of the thesis, I established a physiological role for p53 in meiosis and the results suggested that tumor suppressive functions may have been co-opted from primordial activities during meiotic recombination.

INTRODUCTION

Drosophila female germ line

General morphology

The *Drosophila* ovary consists of 10-18 ovarioles, which are individually surrounded by a layer of muscle sheath (Figure 3-1, A). Within each ovariole, oocytes develop in a sequential fashion, starting from the anterior tip within a structure called germarium, then into a series of four to six egg chambers at stages in developmental progression (stages 1-14), see panel B of Figure 3-1. The production of eggs (oogenesis) starts from the germarium, which can be further divided into three regions (Figure 3-1, C). In region 1, two to three stem cells known as germ line stem cells (GSCs) divide asymmetrically and give rise to immediate daughter cells, cystoblasts (CBs). CBs then undergo four rounds of mitosis without completion of cytokinesis, forming clusters of cystocytes and travel into region 2a. New cysts of sixteen interconnected germ cells are enveloped by follicle cells in region 2b and enter region 3, bud off from the germarium to enter stage 2. Every successive step in oogenesis occurs in a sequential, assembly line fashion and individual egg chamber remains connected by short stalks of specialized follicle cells. Transplantation experiments showed that a germarium can reconstitute nearly all aspects of development; the rate of development was estimated at ~2.4 egg chamber per day, and roughly 96hr (four days) from stage 1 to 14 (Lin & Spradling 1993). For detailed oogenesis review, see (Spradling 1993).

Oocyte specification and meiosis

Within the interconnected cyst, two of the sixteen cells will enter meiotic prophase to become pro-oocytes (marked by chromosome condensation and formation of synaptonemal complexes), however, only one is selected to differentiate into a mature oocyte. This cell remains in meiosis and condenses its chromatin into karyosome seen

in egg chamber when visualized with DNA staining; the other fifteen cells start to endoreplicate DNA and become polyploid nurse cells. During meiotic prophase, DNA double-strand breaks (DSBs) are created by a TOPO II-like isomerase, SPO11, to initiate recombination and crossing over through mechanisms that are conserved from yeast to mammals (Baudat et al 2000, McKim & Hayashi-Hagihara 1998). Due to the high number of breakage events and controlled resolution into either crossovers or gene conversions, checkpoint signaling has been proposed during this process. In mutants of defective meiotic DNA repair, such as *rad54/okra*, *spindle-B*, (homologs of RAD51 and DMC1), *brca2*; persisting breaks in the oocyte activate checkpoint in mid stage of egg chambers and lead to eggshell patterning defects (Ghabrial et al 1998). This patterning checkpoint affects the translation control of *gurken* mRNA, and requires *chk2* and *ATR/mei-41* signaling. Interestingly, *p53* and ATR-IP homolog, *mus304* are not involved in the patterning defects (Abdu et al 2002).

MATERIALS AND METHODS

Fly stocks and genetics

All fly stocks were maintained at 22-25°C on standard food media. We obtained *okr^{RU}, okr^{AA}* from T. Schupbach (Princeton University, Princeton, NJ, USA). All other stocks were from Bloomington Stock Center (Indiana University, Bloomington, IN, USA). In meiotic recombination and *rad54* interaction studies, three *p53* null alleles, ns, 1 and 2 (Rong et al 2002, Sogame et al 2003), were used in trans-combination to reduce genetic background influences in each individual stock. To generate *rad54* mutant flies, okr$^{AA/RU}$ (RU, 391 Q to amber; AA, 9 Q to ochre) alleles were used due to poor viability in either allele.

Determination of fertilization rate by sperm tail entry

Wild type and *p53* females were mated to Canton S males for three days, and embryos were collected. After two pre-collections, embryos at 0-2hr AEL were dechorionated in 50% bleach for 2min and fixed in PBT/heptane (1:3) for 20min then devitellinized in methanol with vigorous shaking, and washed two times with fresh methanol. After rehydration with serious dilutions of methanol/PBT, embryos were blocked in PBT-1.5% BSA for 1hr and incubated in sperm-tail antibody (DROP 1.1, (Karr 1991)) at 1:500 dilution in PBTA overnight at 4°C. Mouse-FITC (1:250) was used for fluorescent detection. DAPI staining was performed during the three times of wish in PBT. Embryos were mounted in 25% glycerol/PBS and imaged. Fertilization rate was calculated from the percentage of embryos with complete entry of sperm tail.

X-linked lethality and X chromosome non-disjunction assay

X-linked lethality was measured by crossing *wild type* or *p53* null females to FM7a males (B^{1} sc^{8} v^{Of} w^{a} y^{31d}) and F1 females were individually crossed to yw males. Lethality linked to X chromosome produced by F0 females can be scored by absence of

wild-typed eye in F2 males. For radiation induced X-linked recessive lethality, F0 females were irradiated at 750 Rads. X-nondisjunction was measured by crossing *wild type* or *p53* null females to FM7a males (B^1 sc^8 v^{Of} w^a y^{31d}) and progenies were scored for incidence of nullo-X (bar-eye) males and attached X (wild-typed eye) females.

Measurement of meiotic recombination frequency

Meiotic recombination frequency was measured by crossing *wild type* (Canton S and yw) or *p53* (*$p53^{ns/1}$, $p53^{ns/2}$, $p53^{1/2}$*) females that were heterozygous for al^1 dp^{ov1} b^1 pr^1 Bl^1 cn^1 c^1 px^1 sp^1, to al^1 dp^{ov1} b^1 pr^1 c^1 px^1 sp^1 homozygous males. Segregations of three markers (c, px, sp) were scored from each progeny and the percentage of progeny with crossover events was plotted. Statistics analysis: Fraction was calculated using one haploid chromosome to determine the total number of crossover products and applied with the following formula: (2x number of progenies with observed crossovers)/ 2x(number of non-crossover + crossover). Symmetrical confidence interval at 95% CI was calculated using modified Wald method (http://graphpad.com/quickcalcs/ ConfInterval1.cfm). Average of the two wild-typed strains was used as a baseline to calculate decreased recombination frequency in p53 strains. Probability (p value) was calculated using CHITEST in Microsoft Excel 2008 for Mac Version 12.1.0. Chi squared equals with 1 degree of freedom. Significance degrees were denoted with ***, $p<0.001$; **, $p=0.001$ to 0.01; *, $p=0.01$ to 0.05; ns, $p>0.05$.

Quantification of nurse cell nuclei number and egg length:

Dissected egg chambers were stained with 0.1µg/ml of DAPI and imaged on Leica TCS SP5 confocal microscope. To facilitate visual counting, z stacks of each genotype were processed with the same scripts using Image J as follows: “Despeckle, Subtract Background, Gaussian Blur (sigma=2), 3D Project (projection=[Brightest Point] axis=Y-Axis slice=’thickness of z-stack’ initial=-30 total=180 rotation=15 lower=1 upper=255 opacity=0 surface=100 interior=50 interpolate), Make Montage (columns=5

rows=1 scale=1 first=1 last=5 in crement=1 border=2)". Sample sizes, n= 141 (*spo11*$^{-/-}$, *p53*$^{ns/1}$, *rad54*$^{AA/RU}$), 44 (*p53*$^{ns/1}$, $^{AA/RU}$), 25 (*p53*$^{-/-}$), 24 (*rad54*$^{AA/RU}$), 21 (*wild type*). For egg length measurements, eggs were collected on standard juice agar plates and manually orientated horizontally for imaging. Images were taken on the Zeiss SteREO Discovery V.12 and processed with Image J using the following script: "Enhance Contrast (saturated=0.5), RGB Color, Set Scale (distance=0 known=1 pixel=1 unit=pixel)". Pixel unit was further converted to microns according to the scale of magnifications. Sample sizes, n= 936 (*spo11*$^{-/-}$, *p53*$^{ns/1}$, *rad54*$^{AA/RU}$), 1468 (*p53*$^{ns/1}$, *rad54*$^{AA/RU}$), 893 (*p53*$^{ns/2}$, *rad54*$^{AA/RU}$), 540 (*p53*$^{-/-}$), 908 (*rad54*$^{AA/RU}$), 1070 (*wild type*). Prism 5 software (GraphPad) was used to perform statistics.

Immunostaining of fly ovaries:

3-5 days old well-fed females were dissected in PBS and fixed in 4% EM-grade formaldehyde (Polysciences) diluted in PBS-0.1% tween-20, with three times volume of heptane. After washing, tissues were blocked in 1.5% BSA, then incubated with primary antibodies at 4°C overnight. The following concentrations of primary antibodies were used: rabbit α-GFP, 1:1000 (Invitrogen), mouse α-HTS clone 1B1, 1:500 (obtained from D. McKearin). Alex-488, 568, 1:250-500 (Invitrogen) were used for fluorescence visualization. 0.1µg/ml of DAPI (Invitrogen) was used for DNA staining. Ovaries were further hand dissected and mounted in VECTASHIELD (Vector Laboratories) for microscopy imaging.

Immunohistochemistry of mouse testes:

10 week age *wild type* male mice were initially fixed via whole-body transcardial perfusion with freshly-prepared, cold 4% PFA prior to organ dissection and further drop fixation. Sections were de-waxed in xylene and rehydrated in graded concentrations of alcohol. After rinsed in distilled water, antigen retrieval was performed in a modified citrate buffer, pH 6.1 (Target Retrieval Solution, S1700, DAKO) for 30min using a 95–

99°C waterbath. After peroxidase block, slides were incubated with mouse anti-phospho-Ser15-p53 (Cell Signaling), 1:25 dilution in Antibody diluent (DAKO) in a humidified chamber at 4°C overnight. For negative controls, primary antibodies were omitted. To detect signals, EnVision HRP-polymer with DAB (DAKO) systems were used. Slides were counterstained with hematoxylin and bluing agent (0.037 mol/L ammonia, Sigma) before standard dehydration and mounting procedures. Several modifications were made for Spo11-knockout and littermate controls: Testes from 3.5 month-age males were drop fixed in freshly prepared, cold 4% paraformaldehyde overnight with agitation, followed by standard paraffin embedding. Antigen retrieval was performed in Retriever 2100 (PickCell). For signal amplification and detection, combinations of EnVision HRP-polymer (DAKO) with TSA (Perkin Elmer) systems were used. Slides with fluorescent detection were extensively washed and mounted in mounting medium (DAKO) containing 0.1mg/ml of Hoechst 33342 (Invitrogen). Criteria used for staging of seminiferous tubules were based on nuclear morphology described here (Ahmed & de Rooij 2009).

RESULTS

p53 activation during meiosis in female germline

We surveyed reporter activity throughout development (Table 2-1). Surprisingly, transient p53Rps expression was observed in germ line precursors of all female ovaries, specifically in region 2a and 2b of germaria (Figure 3-2). Activity was localized in region 2a and 2b of virtually all germaria and was notably absent beyond region 3. Furthermore, p53Rps activity was also absent in the germaria from *p53*$^{-/-}$ or *chk2*$^{-/-}$ animals (Figure 3-2), confirming that, as in somatic tissues, these reporters were genuine surrogates for p53 network activity.

p53 activation by meiotic recombination

Meiotic recombination is initiated in region 2a and 2b by Spo11 (also known as *mei-W68*), a topoisomerase that generates DNA double strand breaks (DSBs) needed for strand exchange (Jang et al 2003). Therefore, we tested if meiotic DSBs were required for p53Rps activity. In germaria lacking Spo11, activation of p53 in regions 2a and 2b was absent (Figure 3-3). Consistent with the fact that meiotic recombination does not occur during *Drosophila* spermatogenesis, p53R-GFPnls expression was random with incomplete penetrance, and independent of p53 status in male testes (Figure 3-4). In order to test if the genetic requirement for *spo11* was due to its enzymatic activities for generating DNA breaks; I used IR to generate ectopic DSBs in the absence of *spo11*, and found that p53Rps activity in regions 2a and 2b was restored in irradiated *spo11*$^{-/-}$ germaria (Figure 3-3). Thus, the above results showed that DSBs used for initiating meiotic recombination were required and sufficient for a short pulse of p53 activation in *Drosophila* female germ line.

ATM and ATR signaling pathways were not rate limiting for meiotic activation of p53

In somatic tissue, DNA damage signals are detected by various components such as the MRN complex (Mre11, Rad50 and Nbs1) and transduced to ATM, ATR and CHK2 kinases for p53 activation. In order to test if the same pathways were utilized by meiotic DSBs in germ line tissue, mutations in Mre11, Rad50, ATM or ATR were examined for p53 activation in region 2a and 2b (Bi et al 2005a, Bi et al 2005b, Ciapponi et al 2004, Laurencon et al 2003). However, mutations in Mre11 did not give rise to viable adults (data not shown); *dATM* and *Rad50* mutant flies had escapers that survived to adult stage and most animals showed impaired oogenesis. However, $dATM^{stg/wk}$ and $rad50^{ep1/d5.1}$ females occasionally produced intact germarium, based on the fusome morphology and in these germaria, p53R-GFP activity was detected in region 2a (Figure 4-6). Strong allele of ATR, D3, was viable and females showed normal oogenesis. In ATR^{D3} mutants, p53R-GFP expression at region 2a and 2b was also observed (Figure 3-5). These results together indicate ATM/ATR signaling are not rate limiting steps for p53 activation during meiotic recombination.

Characterization of mutator phenotypes in p53 mutants

In somatic cells, p53 played “the guardian of the genome” roles to promote genomic stability. It was shown that p53 promotes genome stability after IR during development in somatic cells (Sogame et al 2003), however the extent to which p53 contributes to genomic stability in the germ line tissue remained unclear.

In order to test if *p53* could promote the germ line genome stability, mutations that occur spontaneously during oogenesis in $p53^{-/-}$ females can be examined by their association with dominant or recessive lethality in the offsprings. For dominant lethality, hatch rate of embryos were scored to indicate successful embryogenesis. As shown in Table 3-1, panel B, $p53^{-/-}$ females produced eggs that showed higher percentage of

unhatched embryos, suggesting higher rate of dominant lethality. To rule out the cause of fertilization defects, sperm tail entry rate was used as an indication for successful fertilization, and non-fertilized eggs were subtracted from the un-hatched embryos (Table 3-1, panel A). The results showed the inferred "abortion rate" increased from 5% in *wild type* to average of 10% in all *p53*$^{-/-}$ mutants, suggesting that the maternal contribution of *p53* was necessary to promote robust embryogenesis in the next generation. In order to detect spontaneous recessive mutations, *wild type* and three trans-allelic combinations of *p53*$^{-/-}$ females were assayed using a classic X-linked lethality assay. No difference was found from well fed, 3-7 day old females among genotypes (data not shown). Then I tested if addictive effect can be induced by radiation. After 750 Rads of IR exposrue, all genotypes equally doubled the lethality (data not shown). Therefore I did not find a significant maternal contribution of p53 in suppressing spontaneous or IR induced X-linked lethality.

Characterization of meiotic phenotypes in p53 mutants

p53$^{-/-}$ flies were viable and fertile (Lee et al 2003b, Rong et al , Sogame et al); therefore, the gene did not exert essential functions needed for either development or gametogenesis. To test if the fertility of *p53* mutants was partially impaired, I measured fertility in individually mated *wild type* and *p53*$^{-/-}$ females and found all *p53*$^{-/-}$ animals were nearly 100% fertile (data not shown). I also tested if p53 was necessary for chromosome segregation during meiosis, but *p53*$^{-/-}$ females did not show abnormal rate of X chromosome non-disjunction (Table 3-3).

Because p53 activation was provoked by the initiating step of meiotic recombination (Figure 3-3), I tested if p53 could regulate the outcome of meiotic crossovers. For this hypothesis, three distinct *p53* alleles in trans-allelic combinations were assayed for meiotic exchange frequencies using visible markers on the second chromosome, and 21-54% reductions in crossover rates were observed (Figure 3-6 and

statistically analysis in Table 3-2). Similar results were also obtained from different markers on X chromosome (data not shown).

Persisting p53 activation under meiotic DNA repair defects

To understand the function of p53 during meiotic recombination, we tested p53Rps strains in mutants defective for proper meiotic repair. *Rad54* was required to properly resolve DNA crossovers and in the germaria of $rad54^{AA/RU}$ (okra) mutants, unrepaired DNA breaks were known to abnormally persist in (Kooistra et al 1997). I found that a substantial increase in the percentage of p53R-GFP expression was detected beyond region 2a/2b of $rad54^{AA/RU}$ mutants, indicating persisting activation of p53 occurred in this background (Figure 3-7). The results showed that failure to properly resolve DNA breaks leads to sustained p53 activity during meiosis.

Genetic interaction of p53 with meiotic DSB repair gene, rad54

To test whether persisting p53 activation in *Rad54* mutant background was functionally relevant, we examined animals doubly mutated for *p53* and *rad54*. Interestingly, $p53^{ns/1}rad54^{AA/RU}$ females were completely sterile despite the fact that corresponding trans-allelic combinations of the single-gene mutants were fertile (see materials and methods for allele descriptions). Furthermore, oogenesis defects were evident in $p53^{ns/1}rad54^{AA/RU}$ mutants, including abnormal numbers of nurse cell nuclei (Figure 3-8) and shortened eggs (Figure 3-9). To test whether genetic interactions between *p53* and *rad54* were downstream of meiotic DSBs, genetic epistasis with *spo11* was examined. In these triply mutated $spo11^{-/-}p53^{-/-}$ $rad54^{AA/RU}$ animals, fertility, defects in nurse cell numbers and egg lengths were completely suppressed (Figure 3-8, Figure 3-9, Figure 3-10), showing spo11 was upstream of their interactions. Together, these results indicated that p53 activity in response to unresolved meiotic DNA breaks is functionally required for successful gametogenesis.

p53 activation in mouse spermatogenesis

To determine whether activation of p53 by meiotic recombination was a conserved feature in mammals, mouse testes were examined for an active-form of p53 using antibodies that detect phosphorylated Ser15-p53 (Shieh et al 1997). In seminiferous tubules from *wild-typed* animals, I detected a transient expression of the activated p53 in early spermatocytes (Figure 3-11). Based on the nuclei morphology (expertise kindly offered by Dr. Kent Hamra), the stages of spermatocytes with active p53 signals were mapped between leptotene/ zygotene at the highest level, and disappeared after early pachytene stage. This expression pattern also matched the stages where meiotic recombination occurs in primary spermatocytes. Remarkably, the staining for phospho-p53 (Ser15) became absent in Spo11-deficient mice (Figure 3-11), showing that SPO11-dependent activation of p53 occurred in both flies and mice. These data suggest that meiotic recombination may be a conserved stimulus for p53 activation.

DISCUSSION

Using genetic reporters to observe the functional output of the p53 regulatory network in live animals, I discovered that p53 is functionally activated during meiosis. The source of p53 activation came from “programmed” DSBs that were essential for meiotic recombination, distinct from the stochastic DSBs created by conventional genotoxic stress. The difference of stimuli raised a question whether the DNA break signal were processed differently. How were the programmed DSBs being detected in germ cells? In somatic cells, DNA damage created by genotoxic stress is first detected by MRN complex, and signals are transduced to ATM/ATR kinases for p53 activation. Interestingly, I found that p53R-GFP was still active in the surviving cyst in rad50, ATM and ATR mutants (Figure 3-5, Figure 4-6). The results suggest that some other unidentified machinery is used for p53 activation in meiotic context.

The function of *Drosophila* p53 activation in meiotic context is distinct from previously characterized role to promote apoptosis within somatic cells. The high penetrance of activation ruled out the possibility to promote apoptosis in every oocyte precursor. Several genetic assays were used to identify mutator and meiosis related phenotypes in p53 mutants. However, few defects were found except reduction in meiotic recombination frequency and a modest increase of dominant lethality (Figure 3-6, Table 3-1). This raised the possibility that p53 exhibited an “alarm” mechanism related to quality control, rather than directly participated in meiotic process. This hypothesis was further supported by the persistent p53 activation seen in meiotic DNA repair mutants, as well as their genetic interactions, revealed by defects in nurse cell nuclei number, shortened egg lengths, and loss of fertility (Figure 3-8, Figure 3-9). The genetic interactions were downstream of p53 activation seen in region 2a and 2b, because the absence of meiotic DSBs completely suppressed the defects and restored animal fertility (Figure 3-10).

Despite the genetic evidence indicating that activation of p53 is functionally relevant, specific mechanisms of meiotic p53 actions still remain unclear. One attractive hypothesis is that p53 coordinates the choice of DNA repair pathway. Normally DNA breaks were repaired by one of the two pathways, homologous recombination (HR) or non-homologous end joining (NHEJ). Meiotic recombination predominantly utilizes the HR pathway, and NHEJ is probably suppressed during meiosis due to its error-prone nature. Engels et al. designed a reporter system that allowed measurement of DSB repair pathways from male germ line (Preston et al 2006a, Preston et al 2006b) and future studies using this reporter system would determine if p53 is a determinant that diverts decisions on DNA repair pathways.

Using the mouse spermatogenesis as a model to examine whether meiotic activation of p53 could occur in mammals, I found that an active form of p53 (phospho-specific on Ser15) was present in primary spermatocytes. Supporting evidence came from a previously reported p53 promoter driven-chloramphenicol acetyltransferase (CAT) transgenes that showed similar activities (Almon et al 1993), and the localization of meiotic DSBs in this tissue (Mahadevaiah et al 2001). As in flies, the active form of p53 in primary spermatocytes genetically required Spo11 (Figure 3-11). The responses to the absence of meiotic crossovers differs among species, because SPO11-deficient spermatocytes underwent apoptosis and caused male sterility in mice, while *spo11*$^{-/-}$ flies were still fertile with high nondisjunction defects (McKim & Hayashi-Hagihara 1998). Since loss of cells in Spo11$^{-/-}$ testes occurred mostly after spermatocytes arrested in the pachytene stage (Baudat et al 2000, Mahadevaiah et al), the absence of Ser15-p53 staining was not due to cell lethality. Therefore, p53 activation by meiotic recombination is an evolutionarily conserved feature and its functions related to this activity may constitute the selective pressure for the p53 family during evolution.

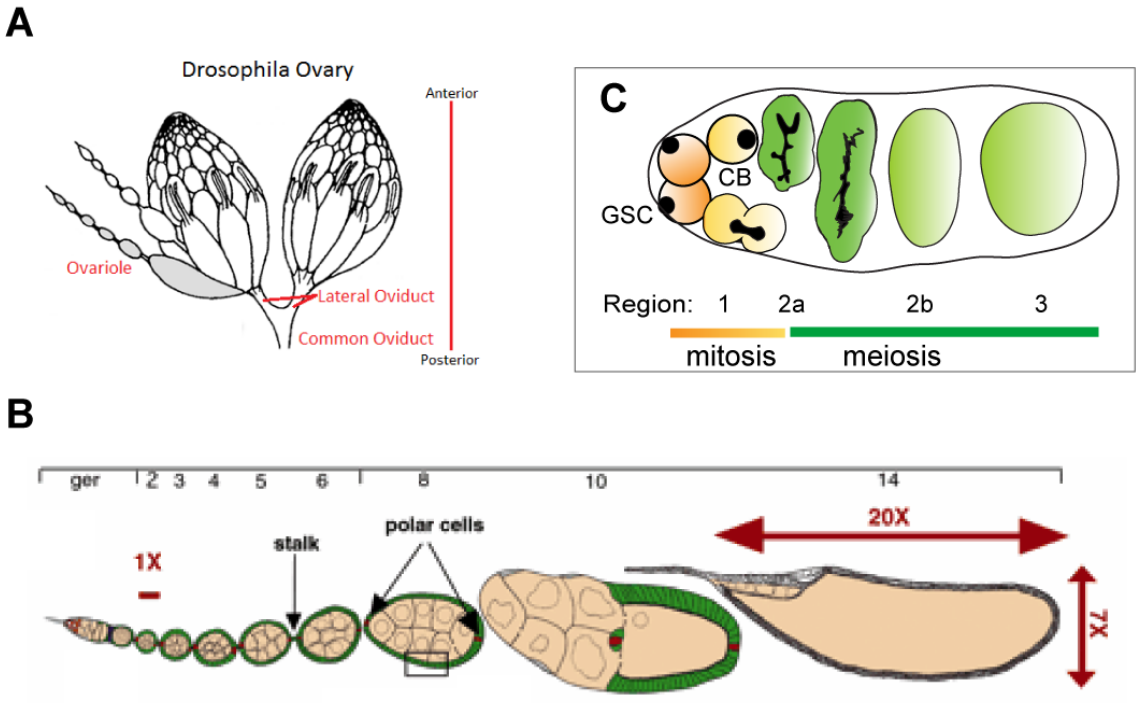

Figure 3-1. Introduction of *Drosophila* female germ line

(A) A drawing of *Drosophila* ovaries. Each ovary contains 10-20 ovarioles. **(B)** Individual ovariole can be divided into 14 stages. Most anterior tip of the ovariole located germarium (ger) where germline stem cell (GSC) divide and give rise to all subsequent stages of egg chamgers that develop progressively to the posterior direction, adapted from (Drummond-Barbosa & Spradling 2001, Spradling 1993). **(C)** Schematic illustration of female germarium. Region 1 contains GSCs and their daughter cells, cystoblasts (CB). Cysts in region 2a/2b initiate meiosis and further develop into egg chamber in region 3. The transition of mitosis to meiosis occurs in region 2a.

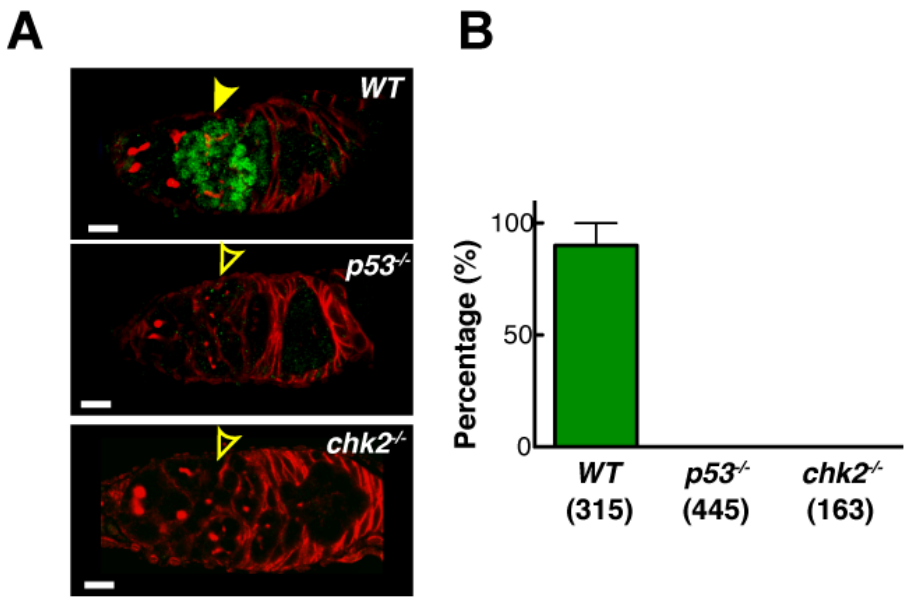

Figure 3-2. Activation of p53 in the *Drosophila* female germ line

(A) Immunostainings for GFP (green) and HTS (red) in p53R-GFPnls animals that were either *wild type* (*WT*), $p53^{-/-}$ or $chk2^{-/-}$. Stereotyped GFP activation in region 2a and 2b (noted by a solid arrow) occurred, and was absent in $p53^{-/-}$ and $chk2^{-/-}$ germaria, (noted by a open arrow). **(B)** Percentage of germarium with p53R-GFPnls expression in regions 2a and 2b. Means of at least three independent trials ± standard deviation were plotted and sample size is denoted within parenthesis. Scale bar, 10 microns.

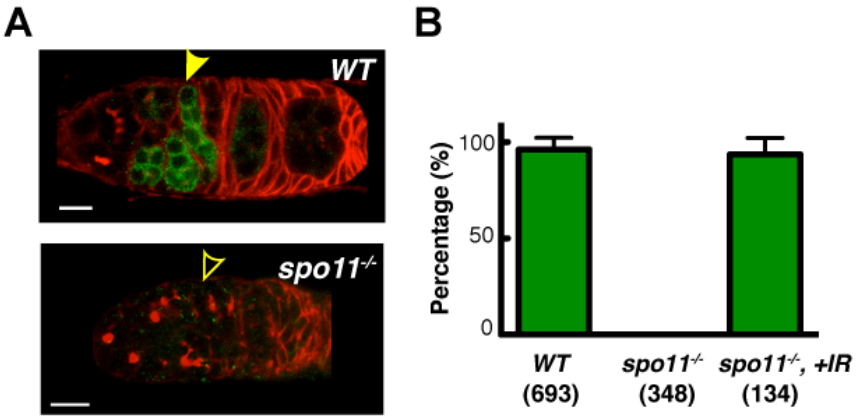

Figure 3-3. Meiotic recombination instigates programmed activation of p53

(A) Immunostainings for GFP (green) and HTS (red) in p53R-GFPcyt transgenic animals that were *wild type* (*WT*) or *spo11*$^{-/-}$. **(B)** Percentage of germarium with p53R-GFPcyt expression in region 2a and 2b in *wild type* (*WT*), *spo11*$^{-/-}$, and irradiated *spo11*$^{-/-}$. Note that after IR, the expression of p53R-GFPcyt was restored in *spo11*$^{-/-}$ germaria. Means of at least three independent trials ± standard deviation were plotted and sample size denoted within parenthesis. Scale bar, 10 microns.

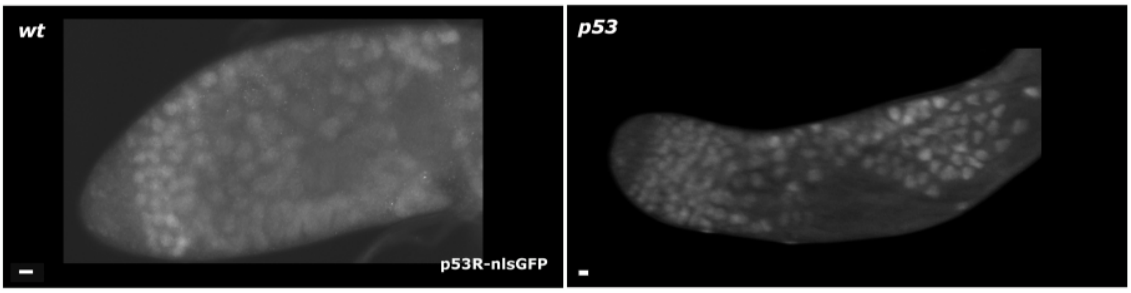

Figure 3-4. Absence of p53 dependent reporter activities in male testes

Immunostainings for GFP in *wild type* and *p53*$^{-/-}$ male testes. Note that the penetrance of GFPnls expression was incomplete and appeared to be independent of *p53* status in this tissue. Scale bar, 10 microns.

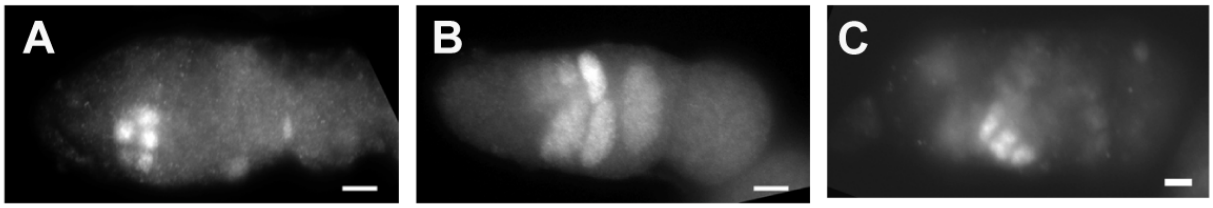

Figure 3-5. Activation of the p53Rps in ATM and ATR mutants

Immunostaining for GFP from animals genotyped as **(A)** *ATM*$^{stg/wk}$ with p53R-GFPnls, **(B) (C)** *ATR*^{D3} with p53R-GFPcyt (B) or p53R-GFPnls (C). Note that stereotyped activations of p53Rps in regions 2a and 2b were unaffected in the intact germaria of those mutants. Scale bar, 10 microns.

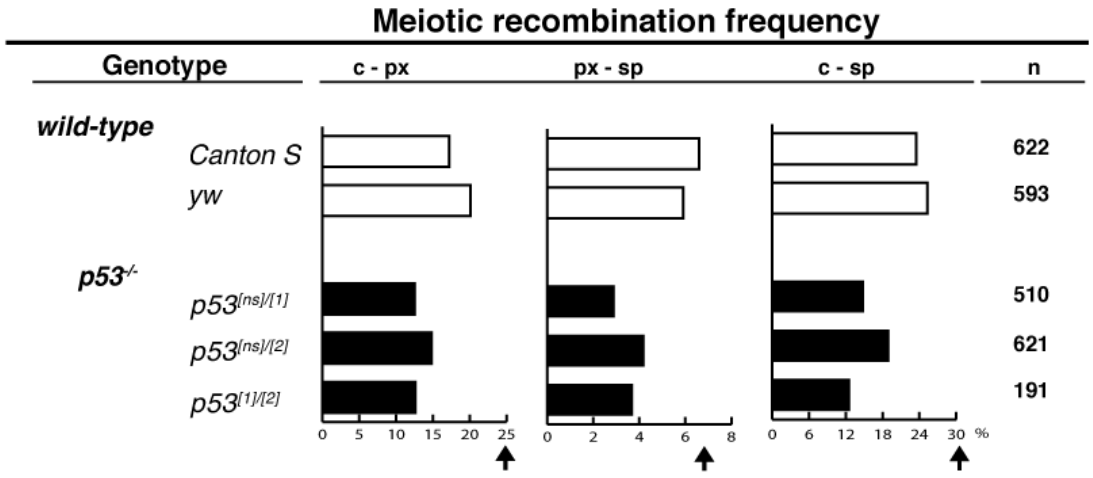

Figure 3-6. Reduced meiotic crossover frequency in *p53* mutants

Meiotic recombination frequencies in *wild type* and *p53*$^{-/-}$ flies measured at three different intervals. Crossover frequencies were reduced in all *p53* trans-allelic combinations when compared to *wild type* (*Canton S* and *yw*) at all intervals. Arrows depicted expected frequencies (FlyBase).

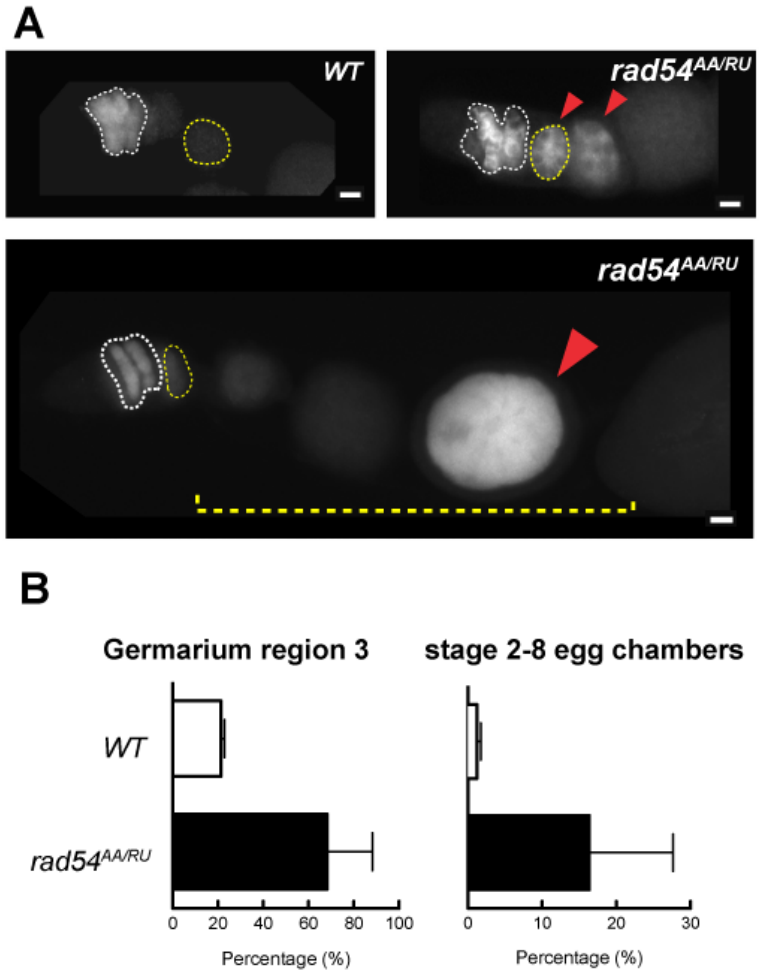

Figure 3-7. Persisting p53 activation in DNA repair defective mutants, *rad54*

(A) Immunostainings for GFP in p53R-GFPcyt transgenic animals that were *wild-type* (*WT*) or *rad54* mutants. Persisting GFP expression beyond region 2a/2b (white dotted circle) was observed in *rad54*$^{AA/RU}$ mutants (noted by red arrows). **(B)** The incidence of p53Rps expression was quantified in region 3 (noted by yellow dotted circle) and in stage 2-8 egg chambers (yellow dotted line) as indicated. Scale bar, 10 microns.

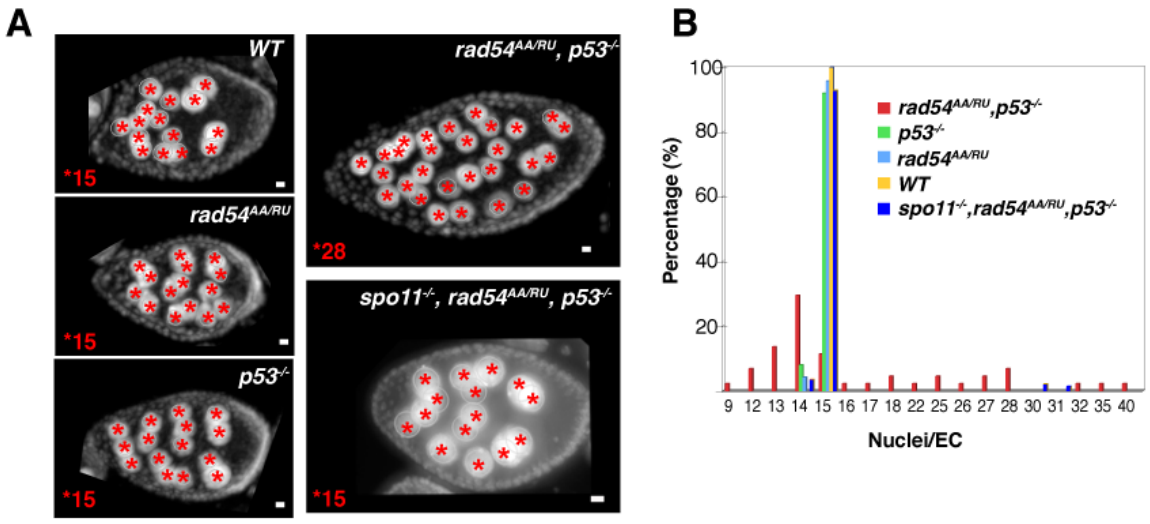

Figure 3-8. Genetic interaction of *p53* and *rad54* downstream of *spo11*

(A) Images of egg chambers stained with DAPI from indicated genotypes. Abnormal nurse cell nuclei numbers, seen in *rad*54$^{AA/RU}$*p*53$^{-/-}$ egg chambers, were not seen under the absence of meiotic DSB formation in *spo*11$^{-/-}$*rad*54$^{AA/RU}$*p*53$^{-/-}$ animals. **(B)** Showed the distribution of nurse cell nuclei number per egg chamber (nuclei/EC). Single gene mutants showed 15 nuclei/EC, but *rad*54$^{AA/RU}$*p*53$^{-/-}$ ovaries exhibited a broad distribution, ranging from 9 to 40 nuclei/EC, which was restored to normal in *spo*11$^{-/-}$*rad*54$^{AA/RU}$*p*53$^{-/-}$ animals (blue group). Scale bars, 10μm.

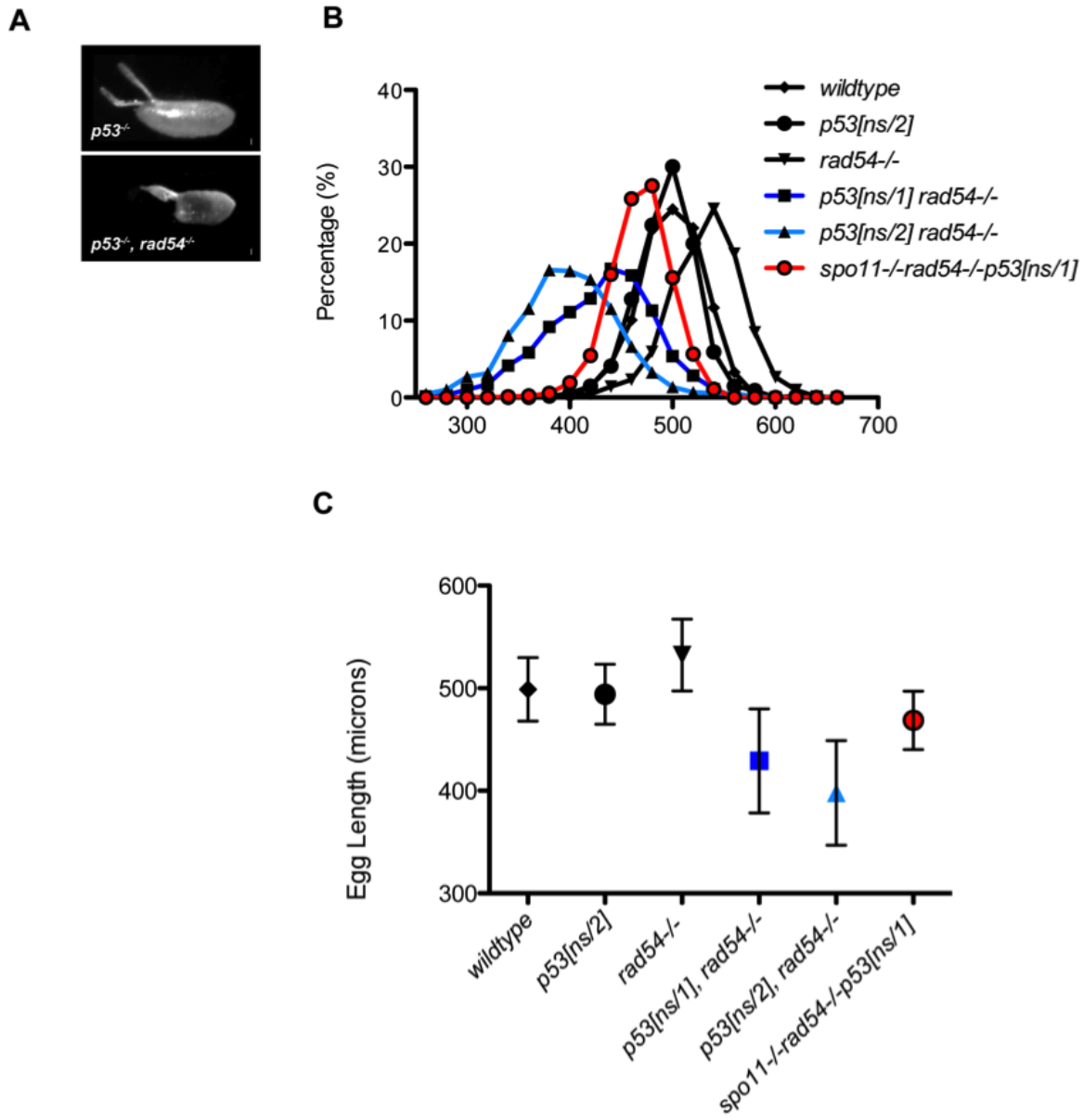

Figure 3-9. Egg length measurements for genetic interactions of *p53* with *rad54*

(A) Image of the eggs laid by $p53^{-/-}$ or $p53^{-/-}$,$rad54^{AA/RU}$ females. **(B)** Frequency distribution of the measured egg length. Scale bar, 10 microns. **(C)** Average egg length ± S.D. from at least three independent trials. The reduction in egg length, shown by the left-shift of distribution in (B, blue lines) and lower average in (C, blue symbols), was largely rescued in eggs laid by $spo11^{-/-}p53^{-/-}rad54^{AA/RU}$ females (red symbol).

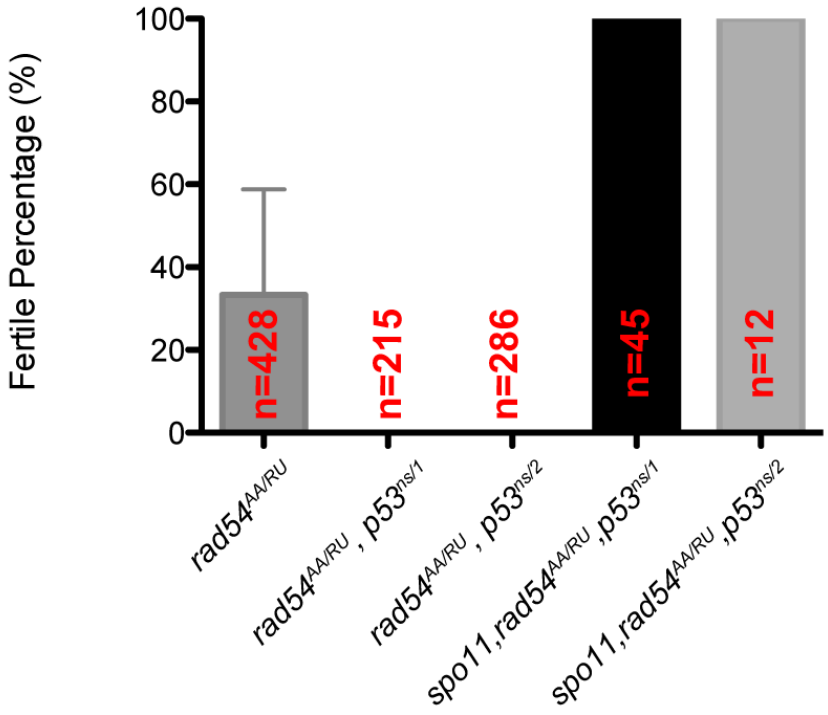

Figure 3-10. Fertility in *rad54$^{AA/RU}$ p53* double mutants

Females of indicated genotypes were assayed for their fertility. The numbers of females assayed were denoted and averages of three independent trials were plotted.

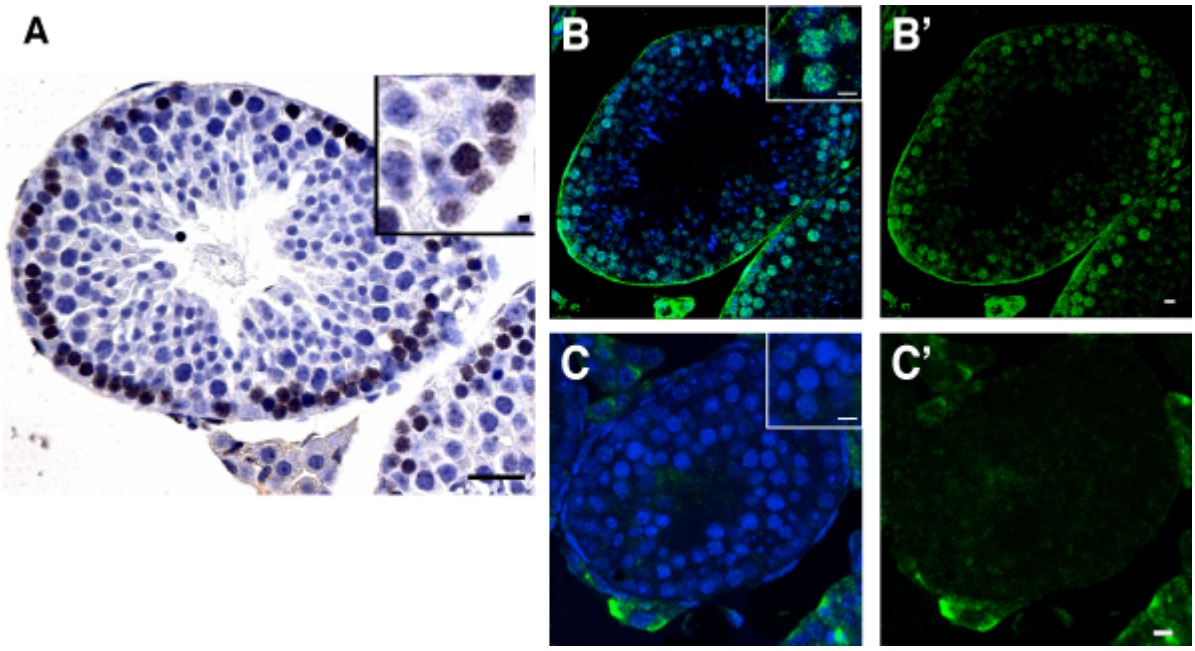

Figure 3-11. Spo11 dependent p53 activation in mouse testes

(A-C) Immunostainings for phospho-Ser15 p53 in paraffin sections from *wild type* (A, B) and Spo11 knockout (C) mouse testes. DAB chromogen (A, brown) and fluorescent (B,C, green) detection methods showed transient activations of p53 in meiotic cells were absent in Spo11-deficient testes. DNA staining (hematoxylin or Hoechst) in blue. B' and C' showed signal without Hoechst counterstain. Insets in (B) and (C) showed nuclear localized staining of Ser15-p53 under comparable magnifications. Scale bar, 100 µm (A); 10µm (B-C, insets in A).

A

Maternal Genotype	No. of eggs			Fertilization rate (%)	n
	Complete sperm entry	Incomplete sperm entry	No sperm entry	Fertilized by sperm entry	
Wildtype	1186	6	14	98.84%	1206
p53[ALL]	1396	29	214	87.05%	1637
p53[NS]/[1]	295	5	26	92.02%	326
p53[NS]/[2]	287	3	47	86.05%	337
p53[1]/[2]	814	21	141	85.55%	976

B

Maternal Genotype	Fertilization rate (%)	Hatch rate (%)	Inferred abortion rate (%)
Wildtype	98.84%	93.52%	5.32%
p53[ALL]	87.05%	76.64%	10.41%
p53[NS]/[1]	92.02%	77.56%	14.46%
p53[NS]/[2]	86.05%	74.89%	11.16%
p53[1]/[2]	85.55%	77.56%	7.99%

Table 3-1. Break down of dominant lethality contributed by maternal p53

(A) Fertilization rate of embryos laid by maternal genotypes as indicated. Complete sperm tail entry was used as indicator for fully fertilized eggs. **(B)** Aborted embryogenesis (dominant lethality) was estimated by the difference between fertilized and hatched embryos.

Meiotic recombination frequency in p53 mutants

Interval	Genotype		Frequency	95% CI (low, high)	Relative Difference (%)	p value†
c-px	WT-Average		0.245			
		CS	0.211	(0.1866, 0.2368)		
		yw	0.279	(0.2496, 0.3097)		
	p53	*ns/1*	0.174	(0.1486, 0.2036)	-28.7	0.00001 ***
		ns/2	0.206	(0.1810, 0.2341)	-15.7	0.00766 **
		1/2	0.185	(0.1419, 0.2365)	-24.5	0.02431 *
px-sp	WT-Average		0.098			
		CS	0.095	(0.0772, 0.1168)		
		yw	0.101	(0.0807, 0.1260)		
	p53	*ns/1*	0.046	(0.0319, 0.0646)	-53.5	0.00001 ***
		ns/2	0.066	(0.0504, 0.0854)	-32.9	0.00226 **
		1/2	0.060	(0.0352, 0.0987)	-39.0	0.04884 *
c-sp	WT-Average		0.319			
		CS	0.287	(0.2604, 0.3160)		
		yw	0.351	(0.3200, 0.3839)		
	p53	*ns/1*	0.207	(0.1793, 0.2379)	-35.2	0.00000 ***
		ns/2	0.265	(0.2367, 0.2945)	-17.2	0.00045 ***
		1/2	0.238	(0.1906, 0.2940)	-25.3	0.00515 **

† Significance degrees were denoted with ***, p<0.001; **, p=0.001 to 0.01; *, p=0.01 to 0.05

Table 3-2. Statistics analysis of meiotic recombination frequency

Symmetrical confidence interval at 95% CI was used to analyze recombination frequency from Figure 3-6. Difference is denoted with negative value, calculated from each *p53* strain to the averaged *wild-type* strains (WT-average). Significance of p value are denoted with ***, p<0.001; **, p=0.001 to 0.01; *, p=0.01 to 0.05; ns, p>0.05.

Meiotic nondisjunction rate in p53 mutants

Maternal genotype	N	XO	X non-disjunction rate (%)
Canton S/yw	2,323	1	0.086
p53[ns]/[1]	2,270	1	0.088

Chromosome segregation defects were scored from a cross of yvf/Y males to wild type (CS/yw) or w/yw; p53[ns]/[1] females from 0~2weeks old. Normal disjunction of the X chromosome in females gives rise to +/Y (XY) males; nondisjunction gives rise to exceptional yvf/O (XO) males that can be distinguished from their wild-type siblings. Male progeny were counted, and the number of XO males was multiplied by 2, to account for the YO products. Nondisjunction was calculated as (2 × [XO males]/N) × 100.

Table 3-3. Meiotic X chromosome non-disjunction rate in p53 mutants

Special thanks to:

Arfaa Ali and Ashley Olivo (STARS program, 2007) for assisting genetic analysis described in this chapter.

Dr. Kent Hamra, Alethia Villasenor /Cleaver lab, John Shelton/ Molecular Pathology Core, Brie Thaden/Cell biology, Victor Stastny/Gazdar lab and Tomoyuki Mashimo/Bachoo lab for helping immunohistochemistry studies in mice.

Chapter Four.

Functional p53 activation in germ line stem cells by genotoxic stress and oncogenic stress

SUMMARY

Using p53 reporters we discovered physiological functions of p53 in germ line stem cells (GSCs) associated with DNA damage and retrotransposon silencing defects. Functions related to this specific activation are needed for regeneration of fertility after IR induced temporary sterility. Part of the tumor suppressor functions of p53 in human is associated with its activation by oncogenic stress. However, whether this regulatory axis is evolutionary conserved remains unknown. In this chapter I describe p53 activation by overexpression of RasV12 in the germ line and in *bam*$^{-/-}$ GSCs that fail to differentiate. My results suggest an ancient link between p53 and oncogenic stress in the germ line without the involvement of ARF or Mdm2. This result established a foundation to identify ancient pathways linking inappropriate growth to p53 in the *Drosophila* model system. Data presented in this chapter is part of a soon to be submitted manuscript.

INTRODUCTION

p53 and stem cells

Distinct physiological functions of p53 and its relatives (p63 and p73) in stem cells emerges from recent studies that showed their roles in quiescent, tissue progenitor cells for homeostasis/regeneration after tissue injury or chemotherapy (Liu et al 2009a, Meletis et al 2006b, Senoo et al 2007). For example, during self-renewal of hematopoietic stem cells (HSCs), p53 mediates DNA damage response pathways that is distinct from somatic cells and also independent of apoptosis (Milyavsky et al). Furthermore, during reprogramming of somatic cells into induced pluripotent stem cells (iPSCs), p53 acts as a "barrier" since inactivation of the p53 pathway facilitated the efficiency of reprogramming (summarized in (Krizhanovsky & Lowe 2009)).

p53 and stem cell competition

During development, aging and tumorgenesis, competition among cells results in the active elimination of "less fit" cells. This phenomenon was originally identified in *Drosophila* tissue, when compensatory proliferation occurs to reconstitute injured organ (Huh et al 2004, Kondo et al 2006, Wells et al 2006). When proto-oncogenes such as dmyc, a human c-myc homolog, was overexpressed to create fast growing, advantageous "winner" cells, they outcompeted "loser" cells in wing disc by inducing apoptosis of the "loser" cells (de la Cova et al 2004, Moreno & Basler 2004). Competition among stem cells was also found in both male and female germ line; germ line stem cells (GSCs) competed for niche position for their maintenance by regulating cell adhesion expression levels without affecting proliferation rate (Issigonis et al 2009, Jin et al 2008, Rhiner et al 2009, Wu & Johnston 2009). In mammals, p53 mediates cell competition behavior in hematopoietic stem cells (HSCs); irradiated *p53+/-* or *p53-/-* HSCs outcompeted irradiated wild type cells after transplantation for bone marrow reconstitution (Bondar & Medzhitov , Marusyk et al). After tissue injury or chemotherapy,

quiescent stem cells will produce transit-amplifying cells, and knowledge on how p53 funcions by specifying their growth rate and survival will be informative to prevent cancer development.

Drosophila female germ line stem cell (GSCs)

Drosophila oogenesis has been used as a model system to understand basic mechanisms controlling stem cell maintenance and differentiation. In the *Drosophila* female ovary, all the eggs are derived from GSCs located at the very tip of germarium in each ovariole (Figure 3-1), which can be easily identified by its stereotyped positioning and cytoskeleton organization using immunohistochemical staining for a structure calle the fusome. In the adult stage, GSCs are maintained by both extrinsic signals and intrinsic factors (reviewed in (Wong et al 2005, Xie et al 2005)). A member of the Bone Morphogenetic Protein (BMP) ligand family, Decapentaplegic (Dpp), suppresses differentiation of GSCs and maintains female adult GSCs, which acts non-autonomously from somatic cells in short range to GSCs through its receptor, *thickvein (Tkv)*. One of the downstream outputs in GSCs is to repress the transcription of *bag of marbles (bam)*, which is a key determinant for differentiation of cystoblast (CB). Loss of *bam* or expansion of *dpp* signaling blocks the differentiation of GSCs and causes ovaries to be filled up by over-proliferating GSC-like cells (Gonczy et al 1997, Lavoie et al 1999, McKearin & Ohlstein 1995, McKearin & Spradling 1990, Ohlstein et al 2000, Ohlstein & McKearin 1997).

p53 activation by oncogenic stress

Many distinct pathways converge on p53 including DNA damage and oncogene activation. It is possible that DNA damage generated in replicating cells leads to p53 activation, however, genetic data from ARF-deficient mice have showed that animals developed tumor while DNA damage response remained normal (Efeyan et al 2006,

Lowe 1999), suggesting that ARF is dedicated for oncogene-induced p53 mediated tumor suppressor functions.

Dependence of ARF in tumor suppression

Known sources of oncogenic stimuli include: mutations in protooncogenes, NRAS and KRAS, MYC, PIK3CA, cyclin E, E2f and viral protein E1A (Bartkova et al 2006, Bos 1989, Di Micco et al 2006, Kim et al 2007, Lowe 1999, Meek 2009). Oncogenic RAS induces cell senescence that is associated with accumulation of p53 and p16/INK4a (Ferbeyre et al 2002, Pantoja & Serrano 1999, Pearson et al 2000, Serrano et al 1997).

Mice models have provided evidence that ARF pathway is required for cancer-protection function of p53 independent of DNA damage response (Christophorou et al 2006, Efeyan et al 2006). However, the existence of selective pressure for accumulation of mutations at ARF locus remains unclear in humans. No mutations were found in human ARF(p14) in most of the human cancer cell lines, except in certain tumor types such as such as sporadic melanoma and glioblastoma, where the entire INK4a/ARF locus was lost due to chromosome 9p21 deletion (Sharpless 2005). Therefore, while ARF does prevent tumors in mice, it remains unclear whether ARF constitutes a major barrier to prevent tumorgenesis in humans.

Mechanism of p53 activation by oncogenic stress: MDM2

The expression level of ARF is normally low in cells and only increases under oncogenic stimuli. Molecularly, ARF protein inhibits MDM2 by blocking its E3 ubiquitin ligase activity, releasing p53 from MDM2 (Honda & Yasuda 1999, Pomerantz et al 1998). Additionally, ARF localizes to nucleolus with MDM2, preventing it from interacting with p53 (Bothner et al 2001, Weber et al 2000). Inhibition of MDM2 by ARF therefore stabilizes p53 protein, promoting its downstream functions such as senescence or apoptosis.

Homologues of *mdm2* and *p19ARF* (or *p14ARF*) are apparently absent in the *Drosophila* genome (Fortini et al 2000). Therefore *Drosophila* offers an attractive model to test whether the activation of p53 can occur via an alternative p19ARF-like pathway in response to oncogenic stress.

MATERIALS AND METHODS

Fly stocks and genetics

All fly stocks were maintained at 22-25°C on standard food media. I-SceI endonuclease cut site transgenic line was generated by K. Galindo (Abrams lab, unpublished). STI150; HS-(70Flp)(70 I- Sce I)/TM6 was used for heat-inducible I-SceI endonuclease expression. The adults were fattened for 2-3 days after eclosion, prior to heat shocks which were performed in a circulating water bath at 38°C for 90 min and repeated for 3 consecutive days. We obtained *aubergine* and *cutoff* mutants: aub^{HN}, aub^{QC}, $cuff^{WM}$, and $cuff^{QQ}$ from T. Schupbach (Princeton University, Princeton, NJ, USA). All other stocks were from Bloomington Stock Center (Indiana University, Bloomington, IN, USA). In fertility assay, two p53 null alleles, 238H (ns) and 5A-1-4 (1) were used in trans-combination to reduce genetic background influences. Two *wild type* strains, *yw* and w^{1118} were used for comparison. Homozygous viable allele of $bam^{delta86\ hv}$ (McKearin & Ohlstein 1995, McKearin & Spradling 1990) and UASp-tkvCA (Chen & McKearin 2003), were obtained from D. McKearin.

Immunostaining of fly tissue

3-5 days old well-fed females were dissected in PBS and fixed in 4% EM-grade formaldehyde (Polysciences) diluted in PBS-0.1% tween-20, with three times volume of heptane. After washing, tissues are blocked in 1.5% BSA, then incubated with mouse anti-dmp53 clone c7a4 (Hybridoma Bank), 1:250; anti-dmp53 clone H2 (provided by M. Ollmann, Exelixis, Inc.), 1:250; rabbit α-H2Av, 1:500 (provided by K. McKim with specific staining protocols) and mouse α-HTS clone 1B1, 1:500-1000 (D. McKearin) at 4°C overnight. Alex-488, 568, 1:250-500 (Invitrogen) were used for fluorescence visualization. 0.1µg/ml of DAPI (Invitrogen) was used for DNA staining. Ovaries were further hand dissected and mounted in VECTASHIELD (Vector Laboratories) for microscopy imaging.

Lysotracker staining

3-5 days old well-fed females were dissected in PBS. Staining of Lysotracker Red (Invitrogen) at final concentration of 0.8μM as described here (Hou et al 2008). Ovaries were then washed three times with PBS and mounted in Glycerol/PBS for microscopy imaging.

RT-PCR of retrotransposon activities from fly ovaries

Ovaries were dissected in cold PBS and divided in triplicates such that each sample consisted of 10–12 pairs of ovaries. Total RNA was extracted with TRIzol Reagent (Invitrogen) according to manufacturer's instructions. Single-strand cDNA synthesis was performed on 1 μg of total RNA from each sample using the Superscript II cDNA Synthesis Kit (Invitrogen). Primer pairs used for RT-PCR as following: Flamenco (220bp), CAG ATT ACC ATT TGG CTA TGA GGA TCA GAC and TGG TGA AAT ACC AAA GTC TTG GGT CAA C; Gypsy (213bp), CTT CAC GTT CTG CGA GCG GTC T and CGC TCG AAG GTT ACC AGG TAG GTT C (Brennecke et al 2007); Het-A (105bp), CGC AAA GAC ATC TGG AGG ACT ACC and TGC CGA CCT GCT TGG TAT TG; Copia (219bp), GCA TGA GAG GTT TGG CCA TAT AAG C and GGC CCA CAG ACA TCT GAG TGT ACT ACA; I element (127bp), TGA AAT ACG GCA TAC TGC CCC CA and GCT GAT AGG GAG TCG GAG CAG ATA (Klenov et al 2007); Het-A (100bp), ATC CTT CAC CGT CAT CAC CTT CCT and GGT GCG TTT AGG TGA GTG TGT GTT; Tart (100bp), AGA GAG GGA AAG AAG GGA AAG GGA and ATT TCC TGC CTG GTT AGA TCG CCA; rp49 (272bp as internal control), ATG ACC ATC CGC CCA GCA TAC and CTG CAT GAG CAG GAC CTC CAG (Pane et al 2007).

Fertility assay

Three to five days old females were irradiated at 11k Rads and crossed to wild-typed canton-S males. In grouped trials, 10 females were assayed for fertility at

indicated time points. In single-female trials, about 0.1% of females remained fertile and did not show radiation induced sterility. This outlier effect was found in all genotypes at the same frequency and was considered as “super-radiation resistant outliers” and excluded. For morphology analysis, ovaries were dissected in PBS and fixed in 4% EM-grade formaldehyde (Polysciences) diluted in PBS-0.1% tween-20, with three times volume of heptane. After washing, ovaries were further hand dissected and mounted in VECTASHIELD with DAPI (Vector Laboratories) for microscopy imaging. Criteria for egg chamber staging were based on the descriptions in (Spradling 1993).

Germ line mosaic analysis

Two *Drosophila* alleles of p53, 238H (NS) and 5A1-4 (k1) alleles were recombined onto FRT82B chromosomes. Recombinants were validated using G418 selection and genomic PCR analysis. Primer sets for NS: left arm (6kb), natA (AAC ATT GGC TAC GGC GAT TGT TCG CGC) and w-hsA2 (GAC GCT CCG TCG ACG AAG CGC CTC TAT T); right arm (5kb), w-hsB (GTG ACC TGT TCG GAG TGA TTA GCG TTA C) and natB (GGC ATT GGC GTA CAC CAC GAG GAT ATG); native p53 locus (4kb), natA and natB. For K1 allele (4kb, 5A1-4 specific): p53-C1 (TCG ATA AAC ATT GGC TAC GGC GAT TGT) and p53-C2 (AGC TAA TGT GAC TTC GCA TTG AAC AAA). Clonal analyses were conducted by crossing yw,hsFLP; p53-FRT82B animals to yw,hsFLP; FRT82B, ubi-GFP/TM3, Sb. F1 females were collected, fed on wet yeast overnight, transferred to empty vials and subjected to heat shock in a 37°C water bath for 1hr three times per day for three consecutive days. Heat-shocked animals were kept on wet yeast and aged for the appropriate number of days prior to dissection and immunostaining. GSC maintenance was determined as the percentage of germaria with negatively marked GSCs at 4, 6, 10, 14, and 21 days after heat shock (n>100 germaria per genotype per time point).

RESULTS

Selective p53 activation in germ line stem cell compartment by DNA damage

A genetic reporter indicating the status of the p53 regulatory network has been previously described (see Chapter two). To test if DNA damage can activate p53 in germ line stem cells (GSCs), we exposed transgenic animals carrying p53 reporters to ionizing radiation (IR). We found that GFP activation was specifically induced in GSCs and cystoblasts (CBs) but strikingly no activation was seen in other cell type including later stages of egg chambers and somatic cells (Figure 4-1, Figure 4-2 panel B). The percentage of germaria with radiation-induced p53R-GFP was close to 100% and did not require *spo11* (Figure 4-2 panel D; Table 4-1).

Next I tested whether GSCs were sensitive to a single DSB generated by a sequence specific endonuclease, I-SceI. After heat-shock to induce I-SceI expression, p53R-GFP was observed in GSCs after one day and the frequency of activation was comparable to IR (Figure 4-2 panel C and D; Table 4-2). Although DNA breaks were generated ubiquitously in all cells, only GSCs and their immediate progeny CBs showed stimulus dependent p53 activation after DNA damage. In $p53^{-/-}$ and $chk2^{-/-}$ mutants, p53R-GFP expression was not detected in germarium after IR, indicating a requirement for chk2-p53 signaling to induce this activation (Figure 4-3). To exclude the observation was not due to the absence of p53, I tested DNA repair defective *ATR* mutants for its selective response in GSCs. I found that p53R-GFP expression was observed in later stages of egg chambers and follicle cells in ATR^{D3} mutants (Figure 4-4), suggesting that the somatic cells were still able to activate p53 in response to DNA damage, but with higher resistance than GSCs.

Survey of factors for selective p53 activation in germ line stem cell

DNA repair defects

Mutations in various pathways were surveyed to see to what stimuli GSCs were sensitive to using p53R-GFP. In non-irradiated *wild type* animals, the percentage of germarium with p53R-GFP expression was low (~7%); in comparison, a modest increase in percentage of p53 activation was seen in $rad54^{AA/RU}$ and $ATR/mei\text{-}41^{D3}$ (Figure 4-8 and Table 4-3), and significantly increased in $spo11^{-/-}mei\text{-}41^{D3}$ and $rad50^{ep1/d5.1}$ (a component for MRN complex) mutants (Figure 4-6, Table 4-3).

Retrotransposon silencing defects

The piwi-associated RNA (piRNA) pathways are important for maintaining germ line genome stability by repressing retrotransposon activity (Aravin et al 2007, Brennecke et al 2007, Klattenhoff et al 2007, Klenov et al 2007, Malone et al 2009, Pane et al 2007, Tushir et al 2009, Vagin et al 2006, Zamore 2007). In order to test other stimuli that could activate p53 in GSCs, I tested if p53R-GFP responds to defects in piRNA pathway, where the activities of retrotransposons are de-repressed. I used two mutations in this pathway, *aubergine* and *cutoff* (Chen et al 2007) to examine p53R-GFP expression in GSCs under the condition of defective retrotransposon silencing. The result showed in increase in percentage of germaria with p53 activation in GSCs (Figure 4-7, Figure 4-8). Interestingly, *aubergine* mutants showed increased p53 activation in both GSCs and beyond region 3, whereas *cutoff* mutants showed an increase only in the GSCs (Figure 4-9, Figure 4-10). Next I tested whether p53 can supress transposition in the germ line, activities of several retrotransposon: Het-A, I element, Copia, and Flamenco loci, were examined by RT-PCR. I did not find increase in transcripts of the retrotransposons from $p53^{-/-}$ ovaries (data not shown, see materials and methods). The results excluded direct role of p53 in this pathway, and future experiments are needed to further understand p53 function downstream of defective retrotransposon silencing (see discussion).

Environmental factors and autophagy

Many environmental factors such as diet and hypoxia are known to impact the p53 regulatory network (Vousden & Prives 2009). To test if those responses were also present in GSCs, p53Rps animals were exposed to short periods of hypoxia or caloric restriction by a protein-deprived diet. Percentages of p53R-GFP in germarium region 1 were quantified and no difference was found (Table 4-4).

In mammals and worms, one of the p53 downstream functions is to regulate constitutive autophagy levels in response to stress or during development (Crighton et al 2006, Crighton et al 2007, Maiuri et al 2009, Tavernarakis et al 2008). Under well-fed nutrient conditions, Lysotracker Red was used as an autophagy marker, and I found that puncta were present in *wild type* germaria but not in *p53*$^{-/-}$ ovaries. However, *spo11*$^{-/-}$ ovaries showed similar pattern as in *wild type*, indicating the decrease of staining in *p53*$^{-/-}$ was not due to meiotic activation of p53 (Figure 4-11). Additional autophagy markers, *Drosophila* LC3 (datg8)-GFP and datg8-mcherry (Neufeld 2008), were used to confirm the lysotracker observation, but no consistent results were found (data not shown). Therefore, whether p53 regulates autophagy in germ line tissue remains inconclusive.

Recovery of fertility after IR requires p53

Despite the fact that all cells in an irradiated ovary are stressed, p53 activation occurs selectively in GSCs, why? What are the associated functions downstream of this activation? I focused on whether radiation induced p53 activity was functionally important by searching for phenotypes associated with *p53*$^{-/-}$ mutants after IR.

At 4k Rads (the dose at which IR induced p53R-GFP was observed), *p53*$^{-/-}$ mutants did not show obvious defects. When the radiation dose was raised to 11k Rads, *p53*$^{-/-}$ mutants became permanently sterile, while *wild-typed* females recovered their fertility in 10 days after IR (Figure 4-12). This resultssuggested that IR-induced p53 function is necessary for the recovery after temporary ablation of fertility, and further

experiments are needed to narrow down specific mechanism of p53 action in regeneration.

Oncogenic stimulus activates p53

In *Drosophila*, a defined niche signaling from somatic cells maintains two to three GSCs throughout the adult lifespan. GSCs undergo asymmetric division and push out daughter cells from the niche, which subsequently differentiate. In this system, increased niche signaling or mutations in differentiation factors is sufficient to induce over-proliferation of GSCs and lead to the devlopment of germ line tumors in adult ovary. To answer whether p53 activation could occur in GSCs when they adapted tumor-like cell fate, p53R-GFP was examined in the “over-proliferation” condition.

In *bag of marble (bam)* mutants, ovaries are filled with GSC-like germ cells because their differentiation process is blocked (McKearin and Ohlstein, 1995). In such tumor-like context, p53R-GFP expression was observed in $bam^{\Delta 86}$ ovaries (Figure 4-13), and was absent in $chk2^{-/-}bam^{\Delta 86}$, showing this activation of p53 in over-proliferating cells also required *chk2* (Figure 4-14).

In addition to blocking differentiation, the expansion of niche by upregulating dpp signaling also causes GSCs to overproliferate (Chen & McKearin 2003). To test if p53 responds to increased DPP signaling, p53R-GFP was examined when DPP secreation from somatic cells was increased, and by overexpressing constitutively active receptor UAS-Tkv^{CA} in germ cells. Both causes can effectively stimulate GSC hyperplasia, however, I did not find a robust p53R-GFP expression in 3-5 day old females, but detectable in a few number or cells when animals were raised in higher temperature to increase GAL4 expression (Figure 4-15). When the number of GFP-expressing cells are compared to overproliferating $bam^{-/-}$ cells in Figure 4-13, incrased DPP signaling seems to be less effective in activating p53.

My observation of p53 activation in overproliferating GSCs raised the possibility that oncogenic activation of p53 could occur in *Drosophila* as in mammalian systems.

To specifically test whether oncogenic stress could activate p53 network in the female germ line, I overexpressed a mutated oncogene, RasV12 using a germline specific driver, nanos-Gal4:VP16 and then examined p53R-GFP activity in the ovary. Although UASt-RasV12 can not be efficiently induced by Gal4 in the germ line (Rorth 1998), shifting temperature to 29 degree allowed more effective GAL4/UAS (Duffy 2002). I found RasV12 overexpression caused lethality if higher temperatures were used during embryonic development, but not after adult stage. I found about 10% of the ovaries showed tumor-like features after 3 days in higher temperature, and expressed p53R-GFP at high level where egg chambers were filled with overproliferating cells (Figure 4-16). Other oncogenic proteins (dmyc and dE2f) were also examined, no effect was found, probably due to the combination of nanos-Gal4 driver and somatic UASt used here are less effective than nanos-Gal4:VP16 (Figure 4-17).

Oncogenic activation of p53 does not engage excessive DNA damage response

In mammalian systems, p53 activation by oncogenic stress often leads to either senescence or apoptosis, and is associated with excessive DNA damage responses (Halazonetis et al 2008, Negrini et al). To detect if p53 activation by oncogenic stress was due to excessive DNA damage, phospho-gamma H2Ax antibody staining was performed. To our surprise, gamma-H2Ax staining was mostly absent in *bam* and *bamp53* mutants (Figure 4-18), suggesting that DNA damage was not the major stimuli for p53 activation associated with “overgrowth” phenotypes. To investigate functions of p53 activation in overproliferating GSCs in the fly germ line, molecular markers for cell death (cleaved caspase-3), cell cycle progression (BrdU incooperation, phospho-histone H3, cyclin E), were examined in *bam* and *bamp53* germ cell tumors. However no p53 dependent activation of apoptosis (Figure 4-19) or accelerated cell division rate was found (data not shown).

DISCUSSION

In this chapter, I have described the selective activation of p53 in germ line stem cells (GSCs) in response to various stimuli such as DNA damage and retrotransposon hyper-activity. Two lines of evidence suggested that this “stemness” feature was not due to the lack of p53 expression in other cell types. First, a monoclonal antibody against dmp53 detected p53 expression in all stages of oogenesis (Figure 4-20). Second, ATR mutants were able to show p53R-GFP expression in follicle cells in later egg chamber stages (Figure 4-4). I proposed that the thresholds for p53 activation are cell type specific; GSCs are most sensitive to genomic instability and their propensity for engaging the p53 network is higher than the surrounding somatic cells. Further studies are underway to discover the factors required for this selective activation, as well as its downstream effects; these are outlined below:

Supression of P element transposition by p53

The P-M system of hybrid dysgenesis can be used to assay P element transposon mobility. To examine whether p53 mutations can cause higher transposition in dysgenic animals compared to wild-type (Margulies et al 1986), sterility, X-linked dominant and recessive lethality will be measured in G2 hybrid dysgenic *p53*$^{-/-}$ and *wild type* females whose X chromosomes will be derivied from M x P crosses.

Regulation of the steady-state or damage induced GSCs competition

To test if dmp53 can mediate GSCs survival or their self-maintaining abilities, I am generating mosaic clones using FLP/FRT mediated recombination and will analyze whether competition occurs between p53+/+ and p53-/- GSCs. Both physiological and irradiated conditions will be tested.

Morphological characterization of fertility recovery after IR

In irradiated females, fertility ceased at 3-5 days after exposure to 11k Rads of IR, and ~30% of the females recovered their fertility on 7-10 days after IR. The genetic requirement of p53 in this phenotype (Figure 4-12) raises the following questions: how does p53 function to promote this regneration phenotype? Does this actually reflect p53Rps activation in the GSCs? Future characterization of the morphological changes induced by IR may offer clues on the downstream functions of p53. A review article by McCall et al. described that the degeneration of egg chambers in mid-oogenesis stages can be induced by various conditions such as nutrient deprivation or treatment with chemicals (Peterson et al 2003). The number of mid-stage egg chambers will be quantified in irradiated animals on different days post-IR to test whether the regeneration of fertility is due to the recovery of stage 8-10 egg chambers.

Phenotypic consequence of p53 hyperactivation

In *bam*$^{\Delta 86}$ animals, GSCs failed to differentiate and showed hyperactivation of p53R-GFP expression (Figure 4-13). The functional consequence of this p53 activity remains unclear because no evidence of direct regulation in cell death or cell division by p53 was found (Figure 4-19 and data not shown). I proposed to use heat-shock inducible bam transgene to restore differentiation after tumor is formed in adult females. This would allow mature egg to form, which could then be examined for visible defects and thus could provide information on the function of p53 in overproliferative GSCs.

Mechanisms of p53 action in stem cells

The selectivity of IR induced p53 activation in GSCs (Figure 4-1) indicates distinct regulation of this network exists in different cell types. In order to analyze downstream targets and to what protein p53 can interact with, it would be technical challenging to obtain homogeneous single cell type from dissected ovaries in large quantity that would allow chromatin immunoprecipitation and microarray analysis. For this purpose, tissue culture system may be needed. However, cultured S2 cells did not

capitulate IR inducible p53R-GFP response (Abrams lab, unpublished results), possibly due to the upstream components for p53 activation are lost when cell lines were being adapted. It will be essential to have the correct cell type, and in particular an ovarian stem cell culture sytem (Niki et al 2006) may be suitable for our purpose. If this fails, then dissected tissue from animals with $bam^{\Delta 86}$ mutations or overexpressing oncogenic protein may be considered as an alternative approach.

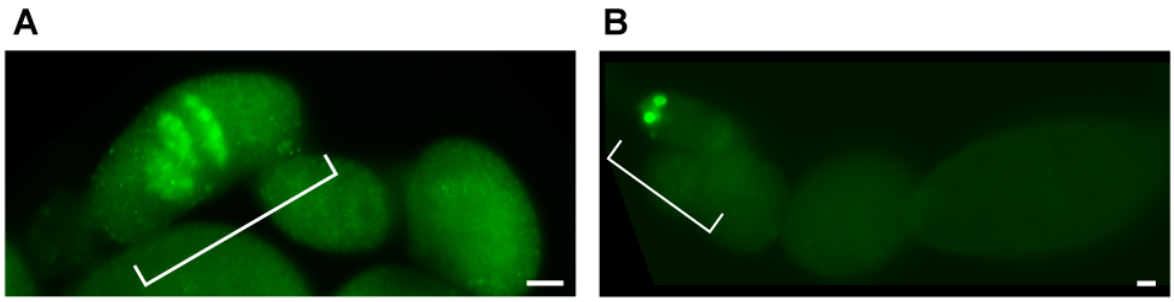

Figure 4-1. Selective p53 activation in stem cell compartment by IR

Epifluoresent images showing immunostaining of p53R-GFPnls in wild-type ovaries that were unirradiated (A) and irradiated (B). Note that in non-irradiated animals, GFP was expressed in region 2a and 2b. After IR, selective GFP expression was observed in region 1. Bracket denotes germarium region. Scale bars, 10μm.

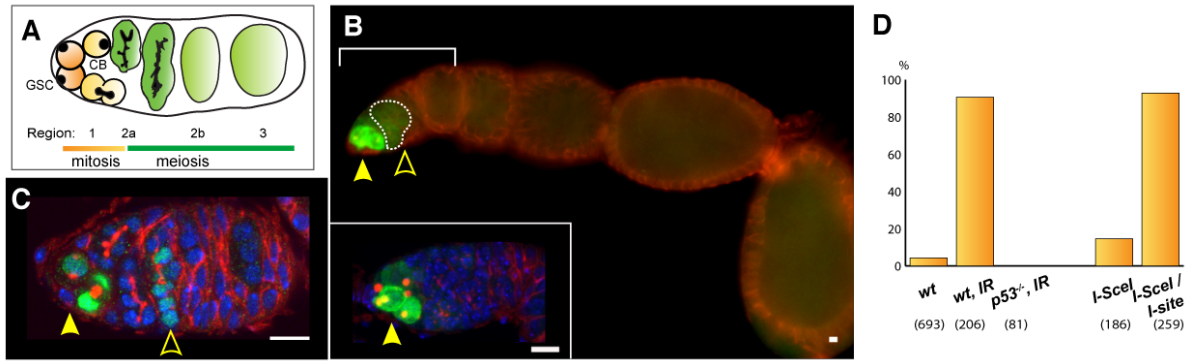

Figure 4-2. Selective p53 activation in stem cell compartment by DNA Double-strand breaks

(A) Illustration of general morphology of *Drosophila* female germarium. Germ line stem cell (GSC), cystoblast (CB) and germarium regions are annotated. **(B-C)** Immunofluorescence staining of GFP (green) and a membrane protein hu li tai shao (HTS, in red) in ovaries. Animals in (B) carried p53R-GFPcyt transgene and were irradiated. Bracket indicates the germarium. Inset in (B) shows GFP expression in GSC in a different germarium that is magnified forclarity. DAPI staining is in blue. Animals in (C) carried p53R-GFPnls. I-SceI cut site transgenes and expression of I-SceI endonuclease was induced by heat-shock. Solid arrowheads indicate GFP expression induced in region 1. Open arrowheads indicate stimulus independent, meiotic activation of p53 in regions 2a and 2b. **(D)** Quantification of reporter activation in region 1. Sample sizes are denoted within parentheses. Scale bars, 10μm.

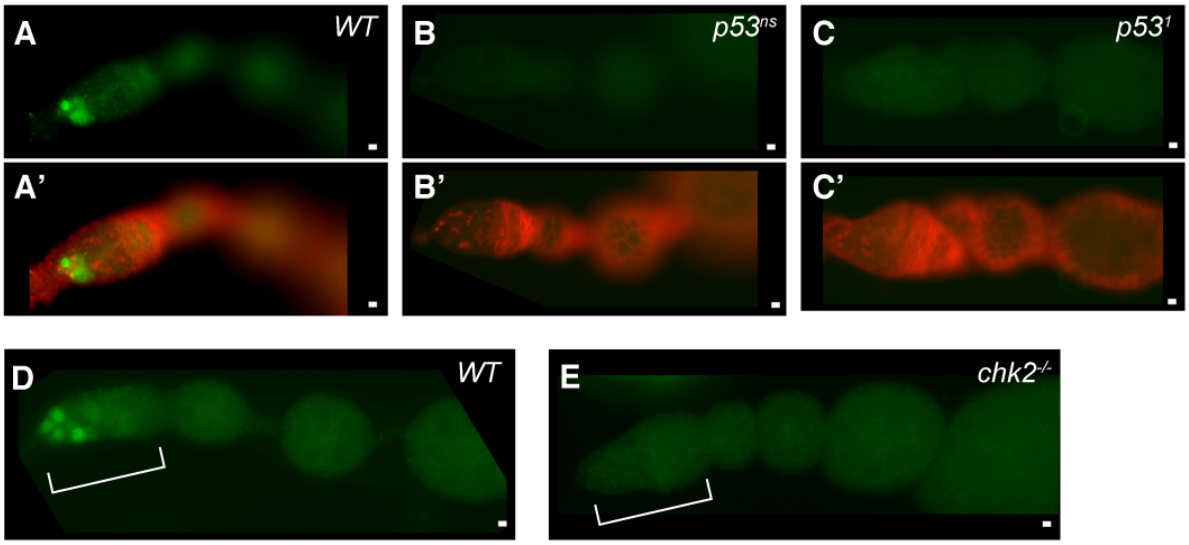

Figure 4-3. Genetic requirement of p53 and chk2 for radiation induced p53 activation in stem cell compartment

Immunofluorescent staining of GFP (green) and a membrane protein hu li tai shao (HTS, in red) in ovaries. **(A-C)** *wild-type (WT)*, $p53^{ns}$ and $p53^{1}$ (carrying p53R-GFPnls transgene) were irradiated. **(D-E)** *wild-type (WT)* and $chk2^{-/-}$ (carrying p53R-GFPcyt transgene) were irradiated. Bracket indicates the location of germarium. Scale bars, 10μm.

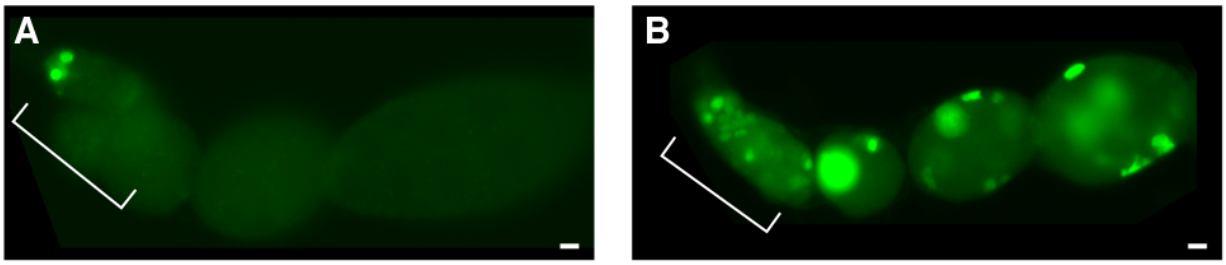

Figure 4-4. Radiation induced activation of p53 in ATR mutants is unconstrained

Epifluorescent images showing immunostaining of p53R-GFPnls in *wild-type* (A) and *ATR*$^{[RT]}$ (B) ovaries both irradiated at 4k Rads. Bracket denotes germarium region. Scale bars, 10µm.

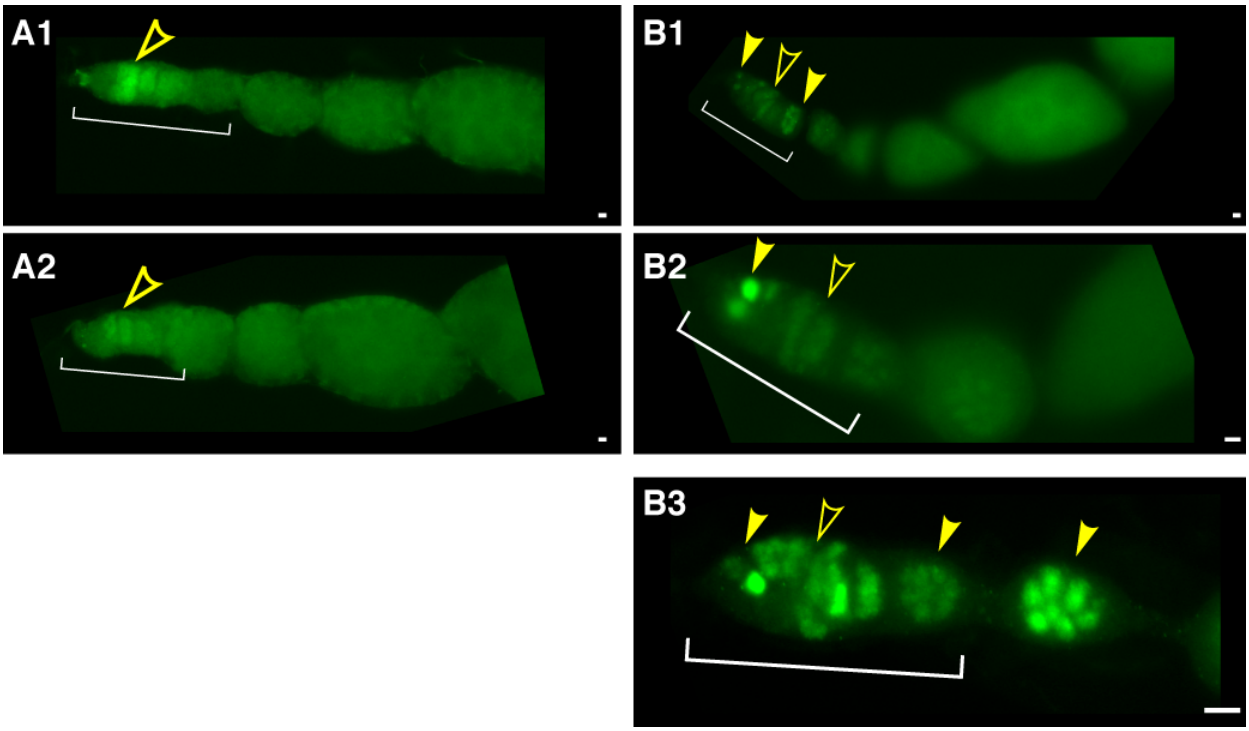

Figure 4-5. Spontaneous activation of p53 in *ATR* mutants without IR

(A-B) Epifluorescent images showing immunostaining of GFP (green) in *wild type* (A1, A2) and $ATR^{[D3]}$ (B1) and $ATR^{[RT]}$ (B2-B3) ovaries. Open arrows denote meiotic activation of p53 and solid arrows denote ectoptic activities. Bracket denotes germarium region. Scale bars, 10µm.

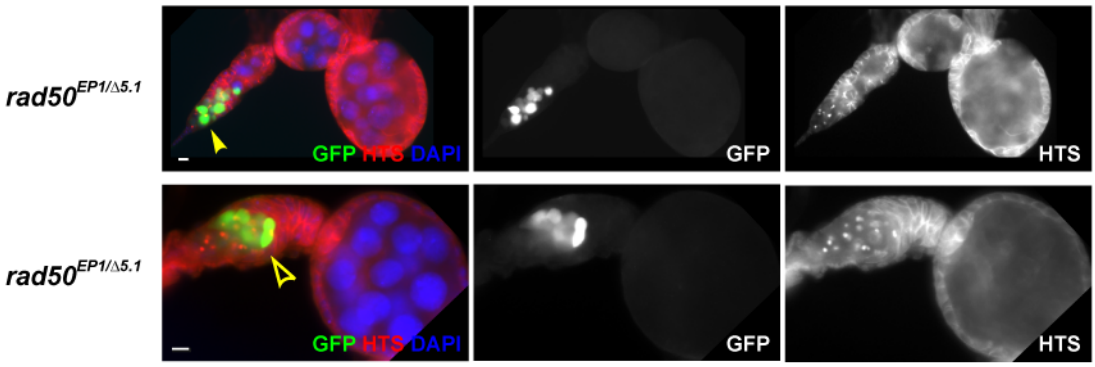

Figure 4-6. Spontaneous activation of p53 in *rad50* mutants

Epifluorescent images showing immunostaining of p53R-GFPcyt (green), HTS (red) and DAPI (blue) in *rad50*$^{EP1/d5.1}$ mutants. Activation in region 1 is denoted by solid arrow and cells located at resembling region 2a are marked with open arrow. Scale bars, 10µm.

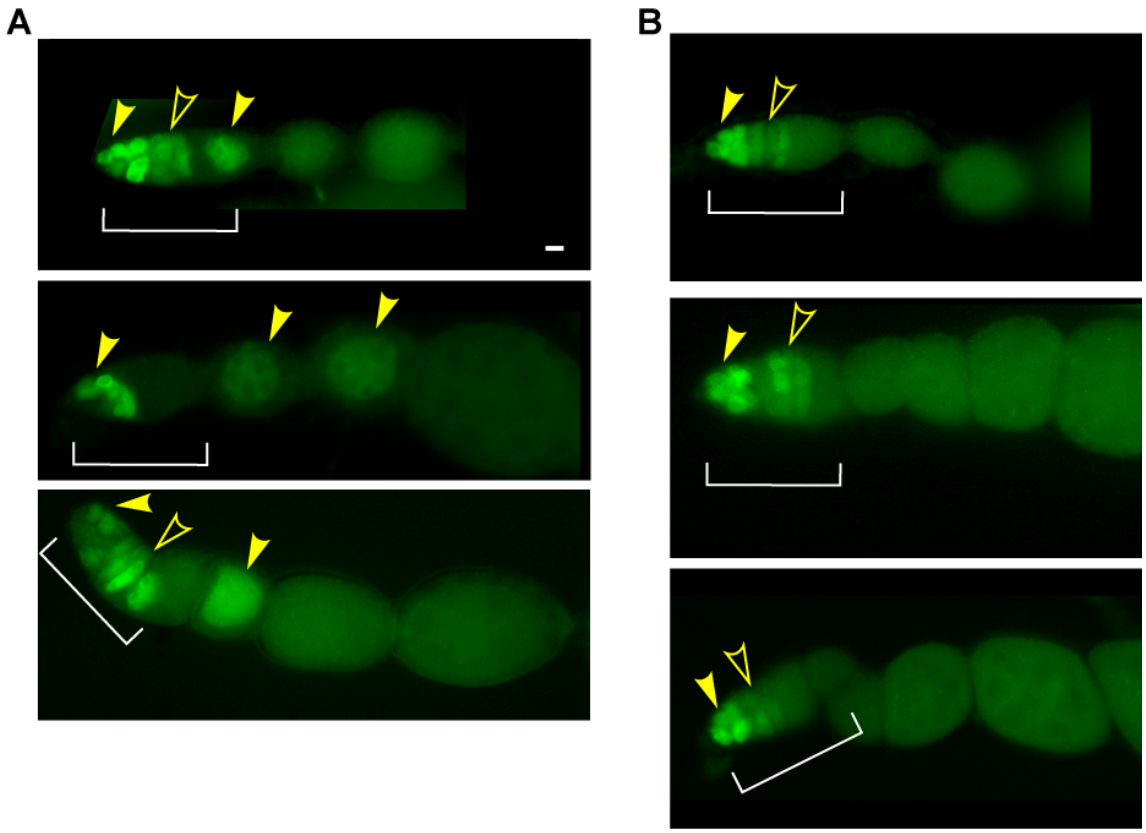

Figure 4-7. Spontaneous activation of p53 in piRNA pathway mutants, *aubergine* and *cutoff*

(A-B) Epifluorescent images showing immunostaining of GFP (green) in $aub^{HN/QC}$ (A) and $cuff^{QQ/WM}$ (B) ovaries. Three examples of each genotype are shown. Bracket denotes germarium region. Scale bars, 10µm.

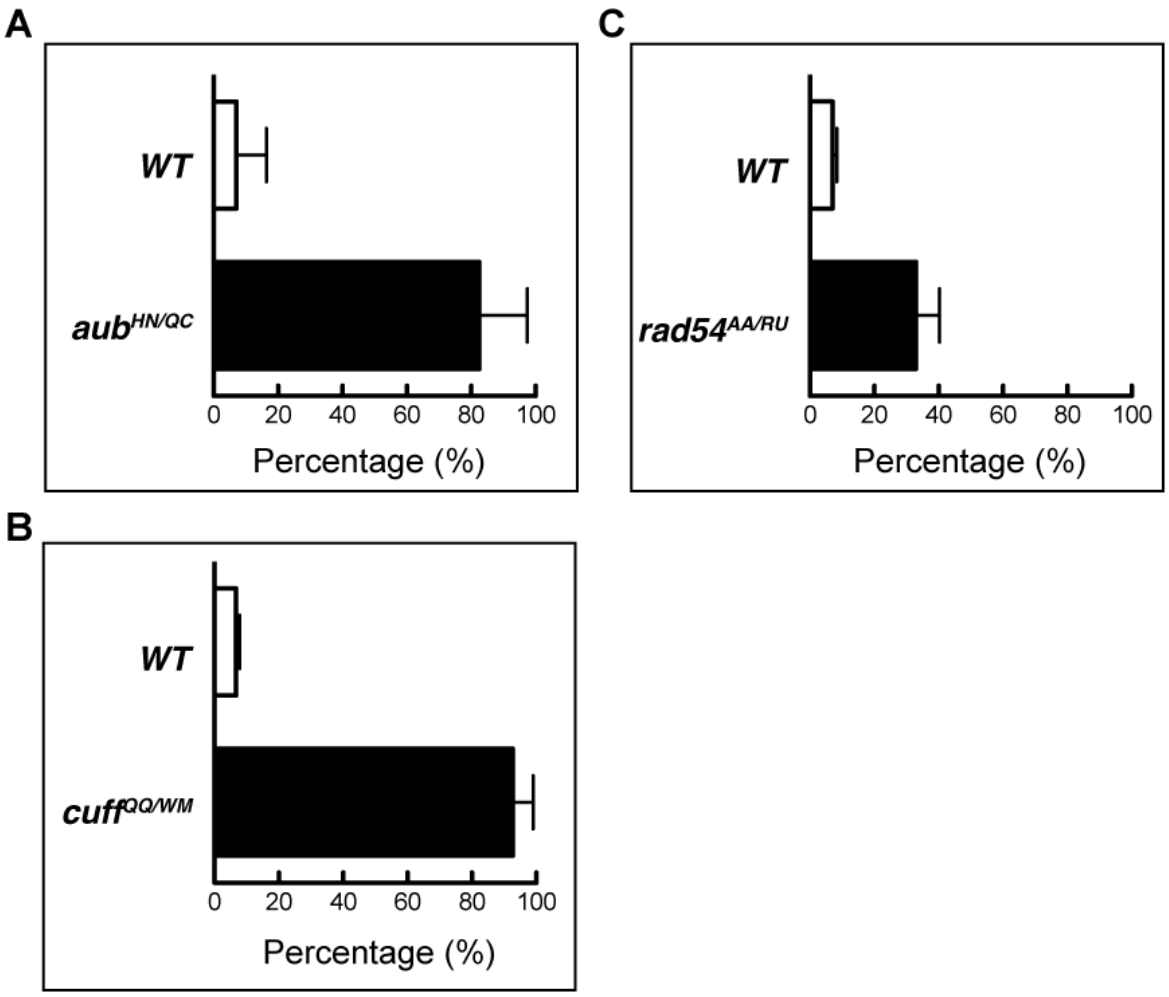

Figure 4-8. Induced p53 activation in region 1 by defective retrotransposon silencing and meiotic DNA repair

Percentage of GFP expression in germarium region 1 was quantified in (**A)** *aub*$^{HN/QC}$, (**B)** *cuff*$^{QQ/WM}$ and (**C)** *rad54*$^{AA/RU}$ mutants. p53R-GFPcyt was used in all three genotypes. Means of at least three independent trials ± standard deviation are plotted.

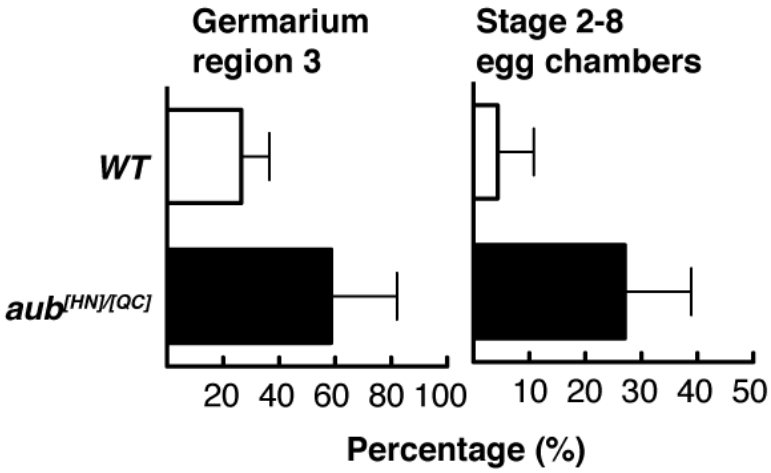

Figure 4-9. Persisting p53 activation in *aubergine* mutants

Persisting GFP expression beyond region 2a/2b is observed in $aub^{HN/QC}$ mutants carrying p53R-GFPcyt transgenic constructs. The incidence of p53Rps expression in region 3 and in stage 2-8 egg chambers is quantified. Means of at least three independent trials ± standard deviation are plotted.

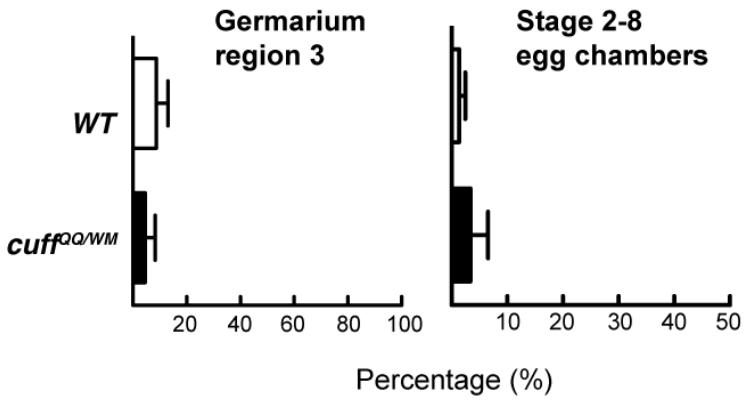

Figure 4-10. p53 activation in retrotransposon silencing defective mutants, *cutoff*

The incidence of p53R-GFPcyt expression in region 3 and in stage 2-8 egg chambers is quantified in *cuff*$^{QQ/WM}$ females. Means of at least three independent trials ± standard deviation are plotted.

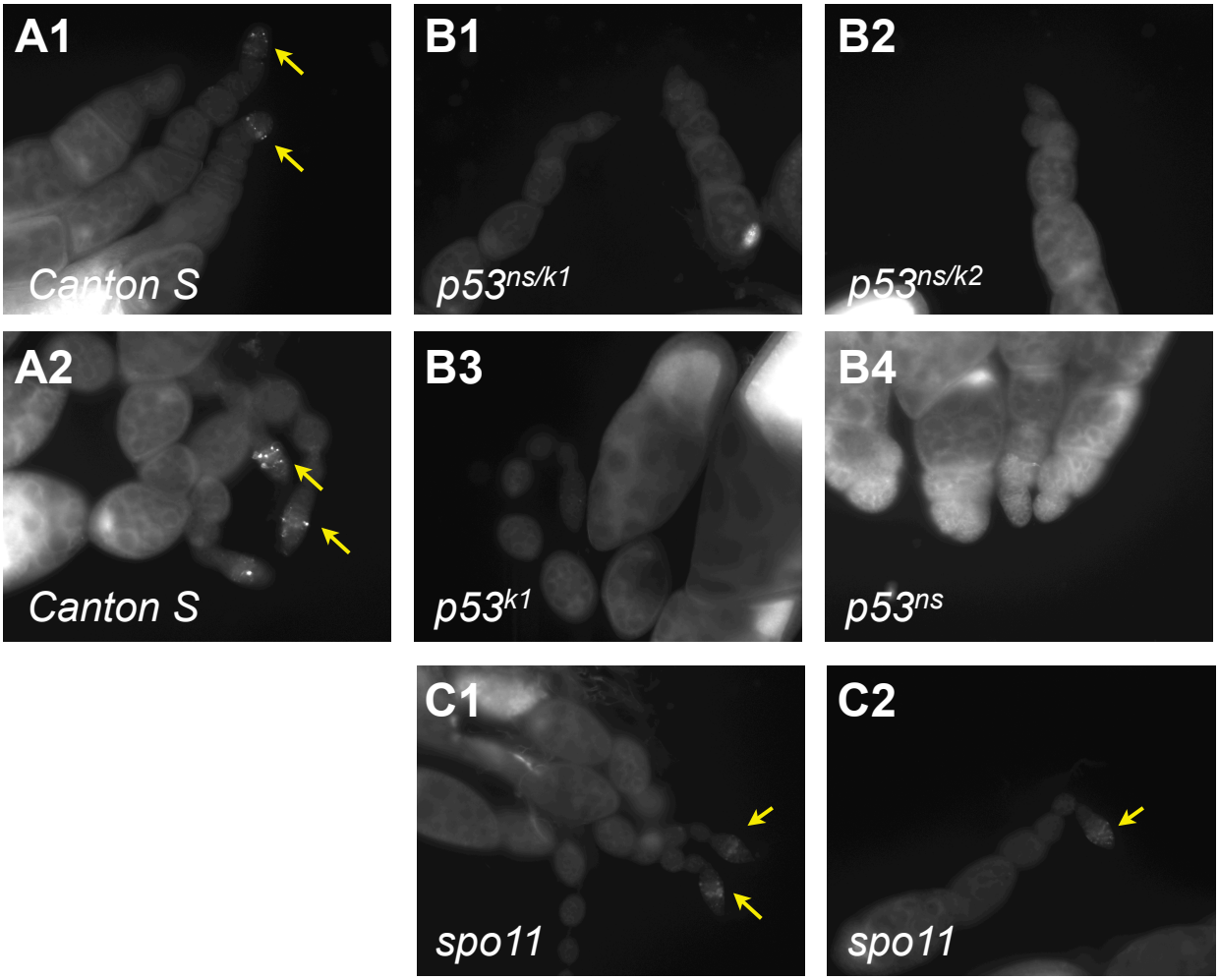

Figure 4-11. Lysotracker Red staining of p53 and spo11 mutants

Epifluorescent images of live Lysotracker Red staining from ovaries that are **(A1-A2)** *wild type (Canton S)*, **(B1-B4)** *p53*$^{-/-}$ mutants and **(C1-C2)** *spo11* mutants. Note that the strong lysotracker stinings seen in *wild type* and *spo11* (denoted with arrows) are not observed in *p53*$^{-/-}$ mutants.

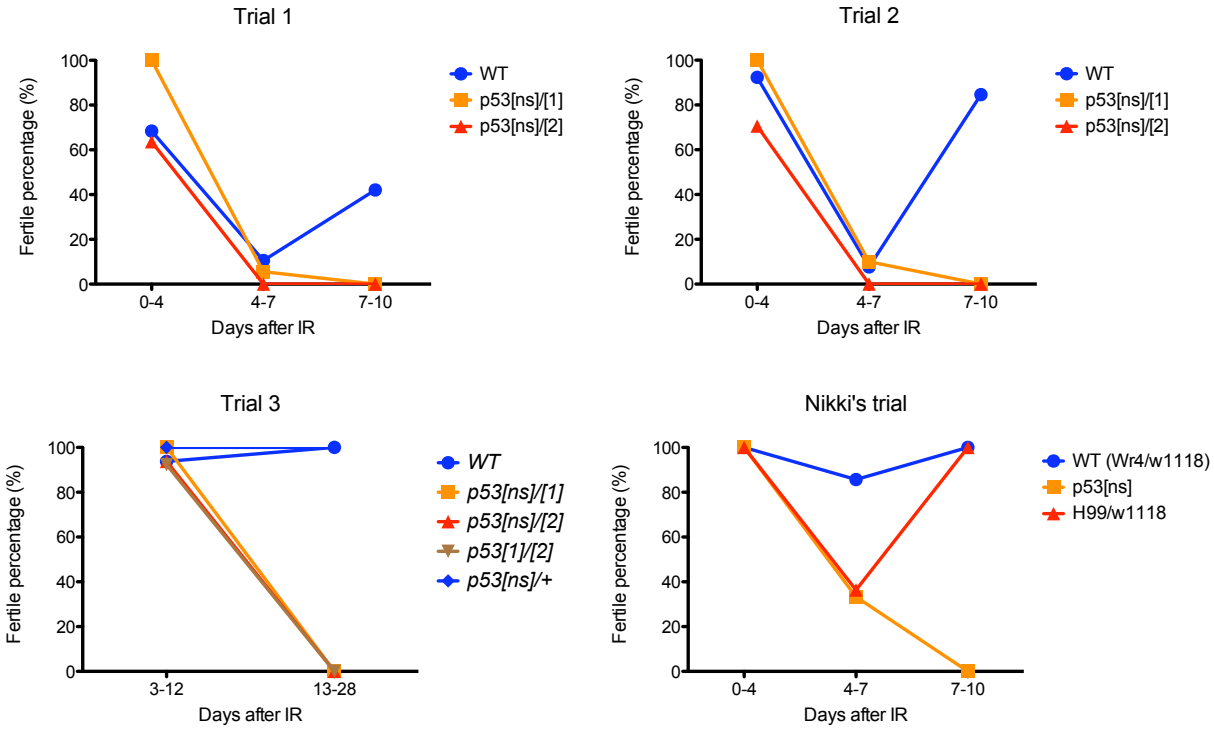

Figure 4-12. Comparative female fertility measures after radiation indicates a p53 phenotype

Females in groups of ten were followed for fertility at indicated time points after 11k Rads of IR. Four individual trials were plotted separately.

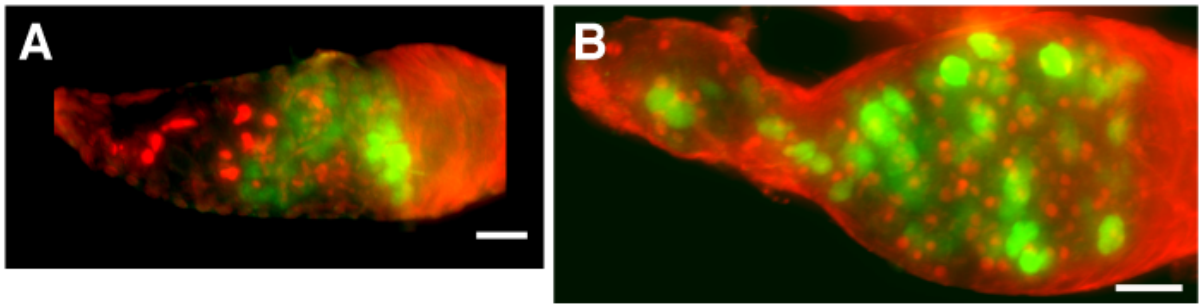

Figure 4-13. Hyper-activation of p53 in *bag of marbles (bam)* mutants

(**A-B)** Epifluorescent images showing immunostaining of GFP (green) and HTS (red) in (A) *wild type* and (B) $bam^{\Delta 86}$ mutant ovaries. p53R-GFPnls transgene was used. Scale bars, 10µm.

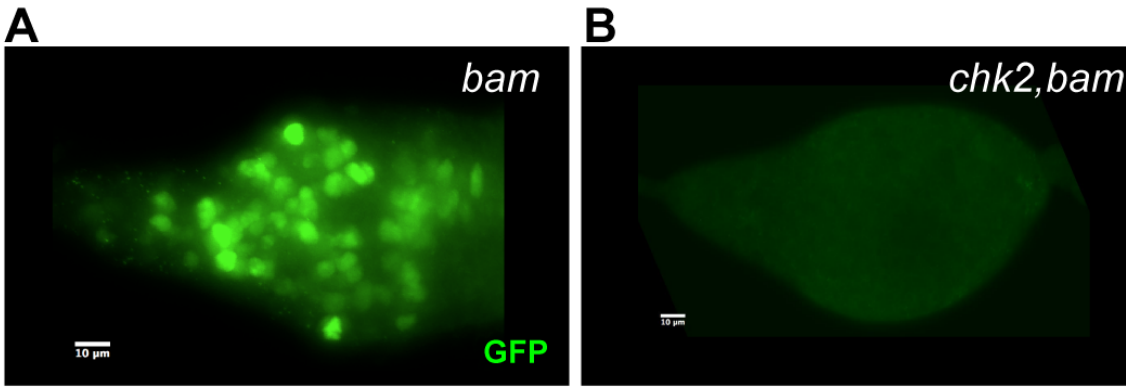

Figure 4-14. Activation of p53 in *bam* tumor requires *chk2*

Epifluorescent images showing immunostaining of p53R-GFPnls (green) in bam (A) and chk2,bam (B) ovaries. Scale bars, 10µm.

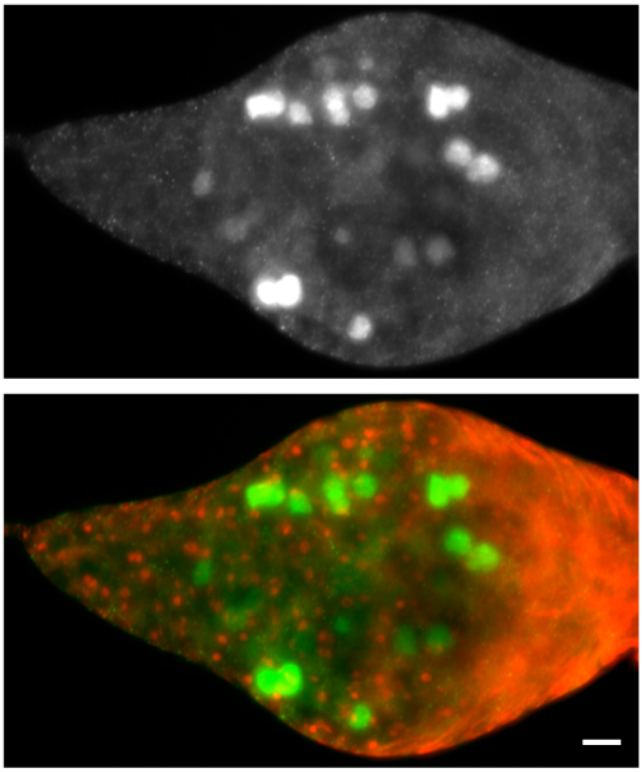

Figure 4-15. Activation of p53 in germ line tumor caused by increased niche signaling

Epifluorescent images showing immunostaining of GFP (green) and HTS (red) in germ line overexpressing a constitutively active receptor for decapentaplegic morphogen, Thickveins (UASp-Tkv-CA) by nanos-Gal4vp16. Increased DPP signaling expands the niche for GSC and causes overgrowth phenotype. p53R-GFPnls transgene was used to detect p53 activation. Scale bars, 10μm.

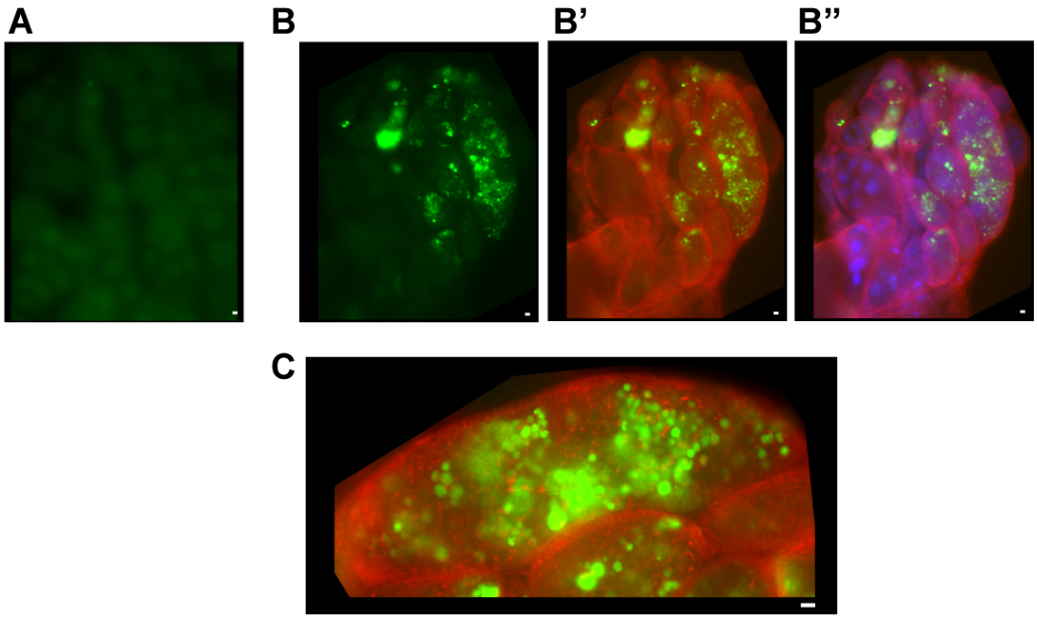

Figure 4-16. Activation of p53 by oncogenic RasV12 overexpression

Epifluorescent images showing immunostaining of GFP (green) and HTS (red) in germ line overexpressing oncogenic RasV12 transgene. **(A)** Background staining at low magnification in the presence of nanos-Gal4 driver alone. **(B, B', B'')** p53 activation in ovaries overexpressing RasV12. **(C)** Higher magnification view of ovaries showing hyperactivation of p53 in germ cells. p53R-GFPnls transgene was used in (A-C). Scale bars, 10µm.

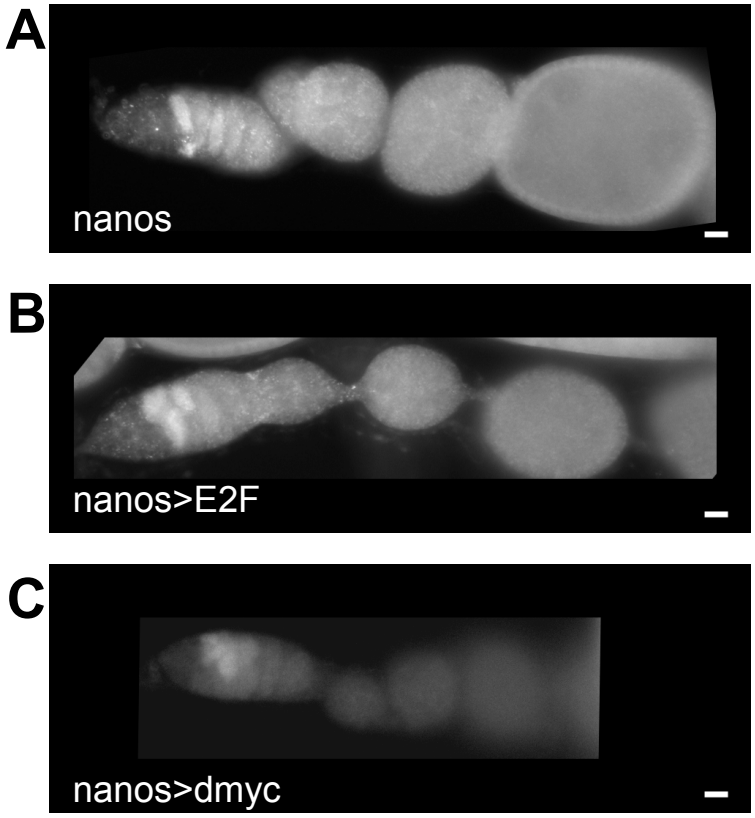

Figure 4-17. Overexpression of E2F and dmyc does not lead to ectopic p53R-GFP expression

Epifluorescent images of GFP from animals expressing **(A)** nanos-Gal4 driver alone, **(B)** driver with UAS-E2f and **(C)** driver with UAS-dmyc. Note that meiotic activation of p53R-GFP activation in region 2a and 2b remains unaffected irrespective of the genotype, however it is not known if expression of UASt-transgene was succesful. All animals are homozygous of p53R-GFPcyt transgene. Scale bars, 10μm.

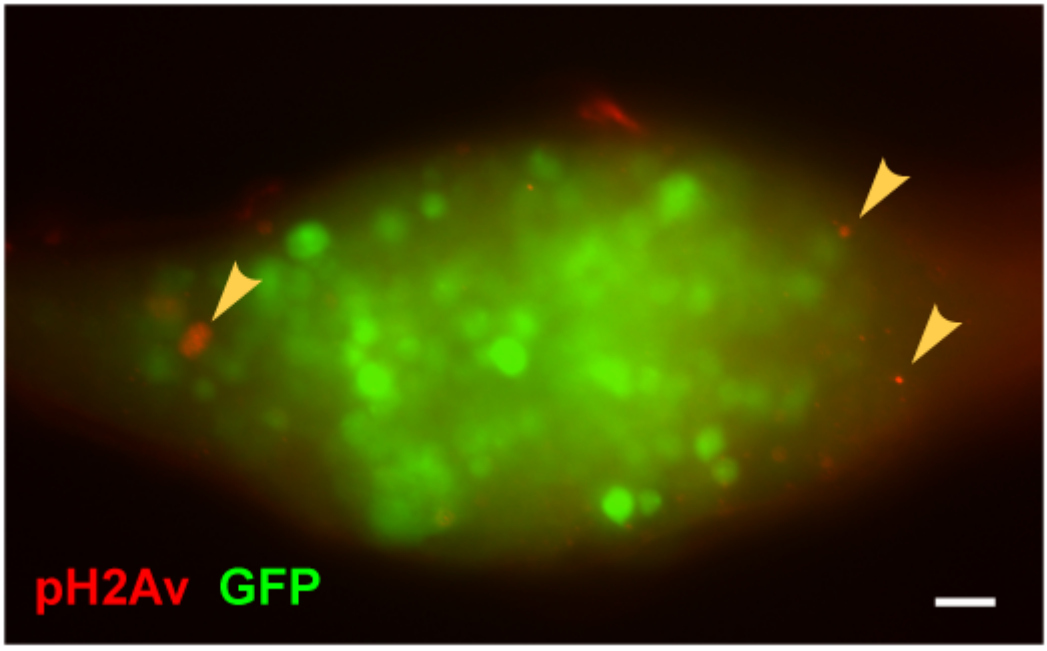

Figure 4-18. Phospho-gamma H2Av (H2Ax) staining in bam mutants

Epifluorescent images showing immunostaining of phospho-H2Av (red) and p53R-GFPnls (green) in *bam*$^{\Delta 86}$ ovaries. Note that the incidence of H2Av (arrows) is rare and does not co-localize with p53R-GFP. Scale bars, 10µm.

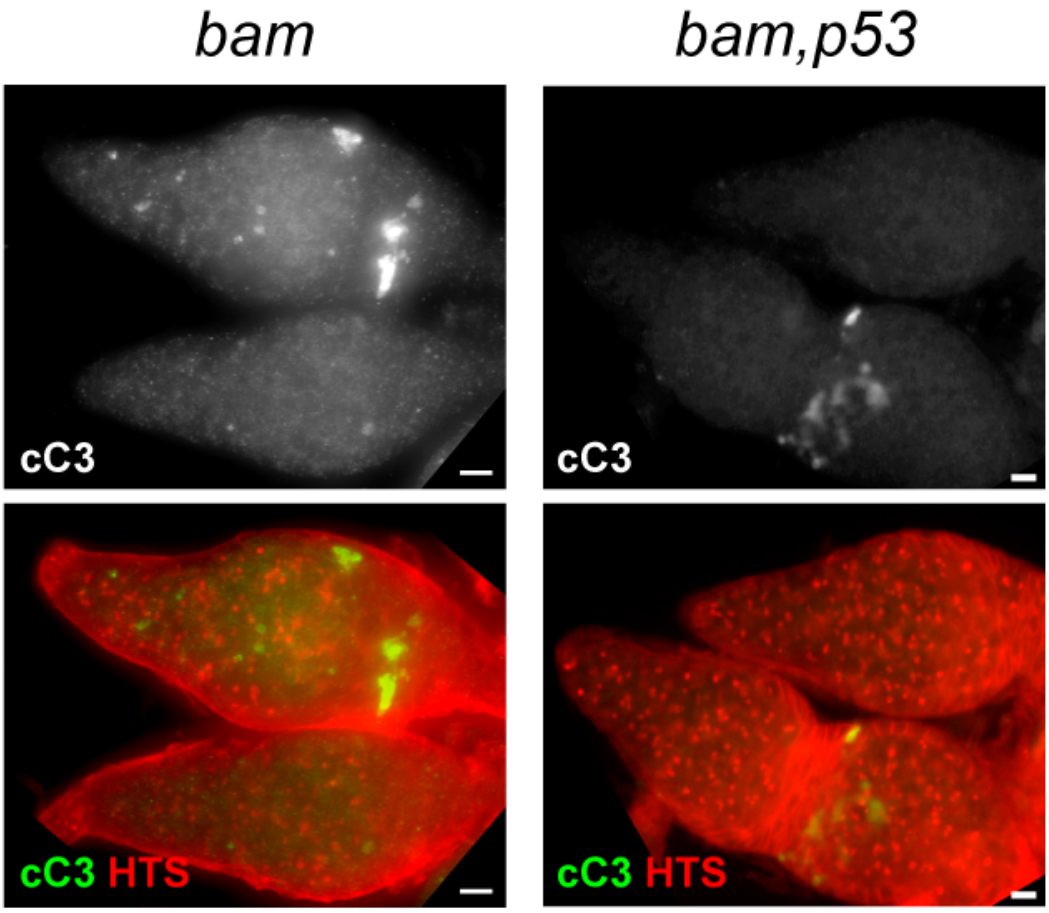

Figure 4-19. Cleaved caspase-3 staining

Epifluorescent images showing immunostaining of cleaved caspase-3 (cC3, green) and HTS (red) in *bam* or *bamp53* background. Scale bars, 10μm.

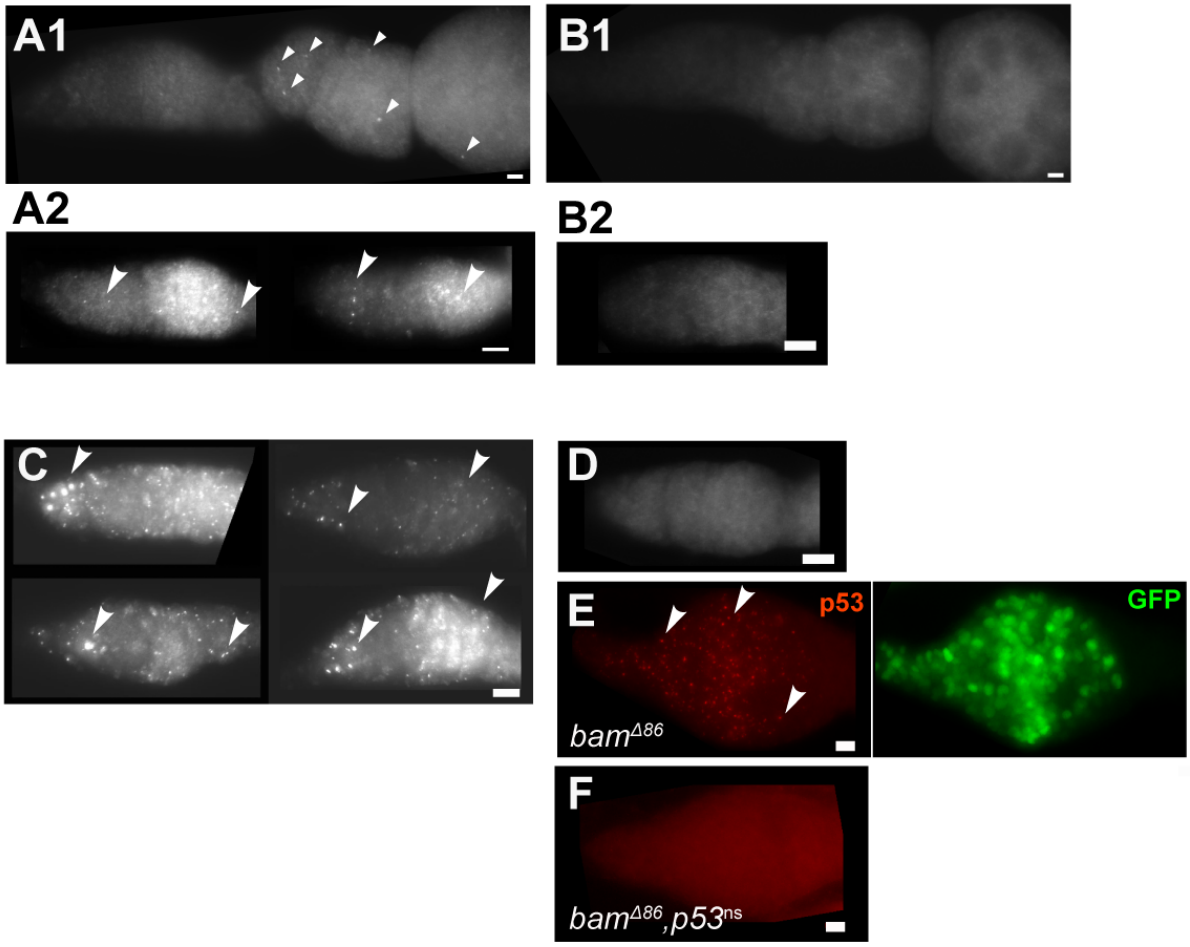

Figure 4-20. p53 antibody staining in the ovary

Epifluorescent images showing immunostaining of dmp53 (clone c7a4) in unirradiated wild-type (A), *p53*$^{-/-}$ (B) or irradiated *wild-type* (C), *p53*$^{-/-}$ (D) *animals*. (E) show p53 protein (red) and p53R-GFP (green) in *bam*$^{\Delta 86}$ became absent in *bam* $^{\Delta 86}$*p53*$^{-/-}$ (F). Note that the punctate quality of stainings (indicated by arrows) suggest subcellular localization of dmp53 in this tissue. Scale bars, 10µm.

Radiation induced p53R-GFP activation

(A)	region 1	SD	2a/2b	SD	3	SD	stage 2	SD	n
Wild-type	**5.0%**	**0.0342**	**96.2%**	**0.0559**	**n/a**		**n/a**		**892**
spo11	**12.2%**	**0.0192**	**0.0%**	**0**					**348**
(B)									
Wild-type, IR	**90.6%**	**0.0926**	**100.0%**	**0**	**n/a**		**n/a**		**206**
spo11, IR	**90.3%**	**0.056**	**92.8%**	**0.0774**	**n/a**		**n/a**		**239**

All genotype with p53R-cyt-GFP
4hr after 3.5kR

Table 4-1. Radiation induced p53 activation in germarium region 1

(A) Unirradiated and **(B)** irradiated p53R-GFPcyt animals that were either *wild-type* or *spo11*$^{-/-}$ were quantified for percentage of GFP expression in regions of germaria (based on HTS staining). Note that the radiation induced p53 activation is not affected in *spo11*$^{-/-}$ animals. Means of at least three independent trials with total sample number are shown (n). SD, standard deviation.

p53R-GFP activation is elevated after I-SceI induced DSB

	region 1		2a/2b	3	stage 2	
	All	GSC				n
I-SceI only	14.6%		4.7%			186
20081220	16.2%	3.4%	5.1%	n/a	n/a	117
20081230	13.0%		4.3%	n/a	n/a	69
I-SceI/cutsite	92.8%		64.0%			259
20081230	86.9%	41.0%	66.1%	n/a	n/a	183
20081124	98.7%		61.8%	n/a	n/a	76

All genotype with p53R-nls-GFP, 24hr after heatshock

Table 4-2. p53 activation by single DNA break using I-SceI endonuclase and specific cutsite

p53R-GFP activation at germarium in DNA repair mutants

(A)	region 1		2a/2b		3		stage 2		n
		SD		SD		SD		SD	
Wild-type	**7.1%**	**0.0132**	**100.0%**	**0**	**21.3%**	**0.0156**	**3.1%**	**0.0099**	**1564**
rad54[AA]/[RU]	**32.9%**	**0.0739**	**100.0%**	**0**	**68.2%**	**0.2002**	**68.2%**	**0.2002**	**1754**
rad50[ep1]/[d5.1]	**97.4%**	**0.0183**	**n/a**		**n/a**		**n/a**		**211**
mei-41[D3]	**24.6%**		**n/a**						**118**
mei-41[D3], spo11	**90.9%**		**n/a**						**99**
(B)									
mei-41[RT]	**32.7%**		**n/a**						**110**
mei-41[D3]	**33.3%**		**n/a**						**81**

Table 4-3. p53 reporter activation in DNA repair mutants

(A) p53R-GFPcyt **(B)** p53R-GFPnls were quantified as percentage of activation in regions of germaria based on HTS staining. Means of at least three independent trials with total sample number are shown (n). SD, standard deviation.

Condition		Age (days)	Percentage of p53 activation in region 1	n
Normal oxygen	Control	5	**6.9%**	275
Hypoxic	Hypoxia-1hr	5	**5.4%**	56
	Hypoxia-1hr + 4hr recovery	5	**5.3%**	57
	Hypoxia-4hr	5	**4.0%**	50
	Hypoxia-4h + 4hr recovery	5	**5.5%**	55
Diet	Control	3	**6.8%**	220
	Control	10	**9.2%**	401
	Starved	3	**11.6%**	346
	Starved	10	**7.8%**	586
Aged		60	**6.6%**	287

Table 4-4. p53R-GFP activation in response to hypoxia, protein starvation and aging

Special thanks to:

Bart Morris (2010 SURF program), Cara Spanel-Weber (2009 SURF) and Meagan Olsen (2009 Green fellow) for assisting genetic analysis described in this chapter.

Chapter Five.

Genetic analysis of a p53 target gene, CUL-2 and programmed cell death in adult wing

Part of this chapter is included in:

A collective form of cell death requires homeodomain interacting protein kinase.

Journal of Cell Biology 178: 567-574. (2007)

Nichole Link, Po Chen, Wan-Jin Lu, Kristi Pogue, Amy Chuong,

Miguel Mata, Joshua Checketts, and John M. Abrams

p53 directs focused genomic responses in *Drosophila.*

Oncogene 26: 5184-5193. (2007)

Fatih Akdemir, Anna Christich, Naoko Sogame, Joseph Chapo, and John M. Abrams

INTRODUCTION

Expression profiling identifies a set of radiation-Induced Dp53 dependent genes

To achieve a more complete picture of ancestral functions governed by p53, our lab produced a genomic profile of Dp53-mediated genotoxic stress responses using Affymetrix microarrays (Akdemir et al 2007). The rationale of the study was a comparative analysis of radiation responsive genes in wild type and Dp53 mutants. From this work, several unexpected observations and important conclusions were derived. First, measured on a genomic scale, radiation-responsive genes governed by Dp53 were limited in scope. Second, the physical distribution of responsive genes was non-uniform; there were at least eight 'territories' implicating large-scale chromosomal organization features could contribute to Dp53 target regulation. Third, the overwhelming majority of stress responders (more than 90%) were Dp53 dependent. Among these, we described a 'core set' of 29 genes that were strictly Dp53 dependent and consistently induced, regardless of genetic background. Notably, more than half of the genes in this core set have human counterparts and only five are specific to insect genomes.

Expression profiling has been used in numerous studies to search for p53 targets genes, but the vast majority of these examine the dominant consequences of ectopic p53, typically driven by forced overexpression in unstressed 'transformed' cultured cells. Consequently, the interpretation of these studies must be made with caution, since they reflect gain-of-function effects that include 'off-target' outcomes absent from the larger context of the stressed state. In fact, from a survey totaling 12 studies of this kind, at least eight profiled the impact of forced wild type or dominant negative variants in cultured lines and, surprisingly, we found only one instance where loss-of-p53 function was profiled in stressed primary cells (Burns & El-Deiry 2003). Hence, I combined loss-of-function genetics in the *Drosophila* model, together with genome wide profiling tools, to examine stimulus-dependent consequences that require p53 function. The strategy was to understand effectors that contribute to genomic instability in Dp53 mutants. An

advantage of this approach derives from functional determinations in whole animal studies, allowing the opportunity to examine gene action in native, physiologic contexts. As outlined in result section, I prioritized the relevance of each candidate to determine the highest priority gene, and cul-2, was selected for study.

Programmed cell death during wing development

During development, cells are eliminated by programmed cell death (PCD) by a well-conserved machinery called apoptosome. Components of *Drosophila* apoptosome including mammlian apaf-1 homolog (dark) and CED-3/caspase-9 homolog (dronc) are required for the execution of PCD. Previously, our lab showed that genetic elimination of *dark* or *dronc* caused a unique, age-dependent late onset phenotype on adult wing (Chew et al 2004). Later studies showed that this progressive, melanized blemishes with age phenotype was a characteristic shared among mutants in canonical PCD pathways. Moreover, the phenotype is caused by defective death in newly eclosed wing epithelium cells. Persisting epithelial cells can be detected post eclosion by UAS-DsRed transgene and imaged in real-time (Link et al 2007).

Genetic screens using preexisting transposon collections were performed to identify novel components of PCD pathway. As part of a collaborative effort, I analyzed the strains on second chromosome and only this part of the results is described in this chapter. Full description of this genetic screen can be found here (Link et al 2007).

MATERIALS AND METHODS

Fly stocks and genetics:

Deletions were generated using the Exelixis collection of P elements as described previously (Parks et al 2004, Thibault et al 2004). To delete the *cul-2* locus, insertion strains f2046 and f0147 were crossed to place P elements in trans, followed by the iinduction of FLP recombinase by heat shock to generate FRT-mediated deletion. PCR primers were used to identify deletion alleles: left arm (1000bp mutant specific product) TAA CCA CCG ACG TCT CAC AAC ACT (cul-2 5' check Fwd, "1" in Figure 5-1) and CCT CGA TAT ACA GAC CGA TAA AAC (WH3'plus fwd, "a"); right arm (800bp mutant specific product), TCC AAG CGG CGA CTG AGA TG (WH5' outward, "b") and GTA TGG CCA TGG ATT CAG AAG CGT (cul-2 3' check Rev, "2"). Native *cul-2* locus was identified as a 6.2kb product using "1" and "2", and as a 13kb product from mutation locus. Genomic DNA was extracted from homozygous L1 larvae of two isolated lines, A06 and B06, and PCR products of primer set "1+2" were sequenced to confirm breakpoints at 2L:21658408.. 21663427.

MS1096-Gal4, UAS-FLP flies were provided by J. Jiang (UT Southwestern Medical Center, Dallas, TX). The l(3)Sxxxxxx (Bellotto et al 2002) and l(2)SHxxxx (Oh et al 2003) FRT stocks were obtained from Szeged Stock Center.

Genetic screen for blemished wing phenotypes

For phenotypic screens for late onset of wing blemishes, MS1096-Gal4:UAS-FLP; FRT42B was used for mutations on 2R. Briefly, 4 males of the genotype l(2)SHxxxx were crossed to 3 virgin females of MS1096-Gal4:UAS-FLP; FRT42B. F1 flies were examined at eclosion and at 1, 2 wk of age for melanized wing blemish.

Genetic screen for persisting cells in living wing epithelium

The FLP/FRT system was used to generate mutant wing clones, and persisting cells were visualized using UAS-DsRed transgene. After eclosion, wings were removed, mounted on glass slides, and imaged on a fluorescent DLM (Axioplan; Carl Zeiss).

Radiation response assay in larval imaginal discs:

See MATERIALS AND METHODS in Chapter Two.

RESULTS

Determination of cul-2 gene as the subject of study

Through genome scale analyses, a set of radiation-responsive genes governed by Dp53 was discovered. Among these are a 'core set' of 14 genes that are strictly Dp53 dependent and consistently induced in two independent studies (Brodsky et al 2004, Lee et al 2003a): Cyp307, Ku80, CG15479, CG15480, Rad50, CG6272, RnrL, eIF6, CG12171, CG18596, CG12194, GstD5, CG5664 and cul-2 (Table 5-1). Based on genome-wide profiling data, I sought to generate a loss-of-function mutation to examine stimulus-dependent consequences of p53 function. With the currently available genetic tools in *Drosophila*, relevant information for the mutational representation is compiled in Table 5-2. The table shows that the 11 radiation-induced and p53 dependent (RIPD) genes sharing definitive homologs in humans are potentially covered by multiple alleles. Among these genes, *cul-2* gene has a predicted human ortholog based on sequence homology to Cullin protein family, and therefore it is likely to be involved in proteolysis and regulation of cell cycle (Table 5-3). In addition, this gene is the only contender that a complete loss of function locus can be generated through FLP/FRT genetic recombination method using two pre-existing P element strains. Therefore I decided to generate loss of function *cul-2* mutants.

Generation of cul-2 loss-of function mutants

By a customized deletion strategy, illustrated in Figure 5-1, two FRT-containing P element insertions flanking the coding region of *cul-2* were used to generate a loss-of-function mutation. PCR was used to verify recombination between P elements (in Figure 5-1), and two deletion strains, $cul\text{-}2^{D}$ were recovered. These validated alleles eliminate all coding sequence in the open reading frame. Deletions at the *cul-2* locus were uniformly lethal before the 3rd instar stage. In addition, in zygotic $cul\text{-}2^{D}$ embryos, no

programmed cell death defects such as head involution defects were found. Further clonal analysis was hindered by failure to obtain recombinants of *cul-2*^{D} with FRT40; which failed due to the proximity in chromosome location (cul-2 locus: 39E3-E6, flybase).

Cul-2 overexpression had normal IR induced cell death response

So far there is no evidence to show that Dp53 stabilization occurs during execution of cell death. If cul-2 is functionally related to p53 degradation, we would expect overexpression of cul-2 would lead to failure of IR-induced cell death in wing imaginal discs, which mimics the phenotype of p53 mutants. To test this hypothesis, the protein trap line (Bloomington #19883), which contains a UAS sequence at its 5'UTR, was used to over-express cul-2 in larval imaginal discs using two Gal4 drivers, Vg-Gal4 and Engrailed-Ga4. When late L3 wandering larvae were assayed for radiation induced cell death, no effect was found in cul-2 over-expressed animals.

Genetic screens to uncover new PCD components

Using the wing blemish phenotype to uncover novel components in PCD pathways, we analyzed a collection of preexisting transposon mutants to identify genetic leisions that exhibit normal wing at eclosion but develop melanized wing blemishes with age. By using FLP/FRT system with wing specific drivers, genotypes of mosaic clones could be examined without causing lethality.

13 mutations on second chromosme (2R) were analyzed for both melanized wing blemish and persisting DsRed epithelial cells. Table 5-4 summarizes the transposon strains that showed phenotypes. I also analyzed additional strains on 3R (data not shown), and all the possible candidates were PCR verified and their functions annotated on Flybase are listed (Table 5-5). From this genetic screen, we uncovered several new candidates for PCD pathway, as well as pre-existing PCD components, such as *dark*

and *thread*. The degree of blemish in *dark* is more minor when compared to a previously characterized allele, $dark^{CD4}$ (Chew et al 2004); therefore it was likely a hypomorphic allele. This observation reassured our strategy and increased our confidence in identified components. One of the signaling kinase, homeodomain interacting protein kinase (HIPK) was selected, and Link et al. showed that there was a generalized requirement for HIPK in the regulation of cell death and cell numbers (Link et al 2007).

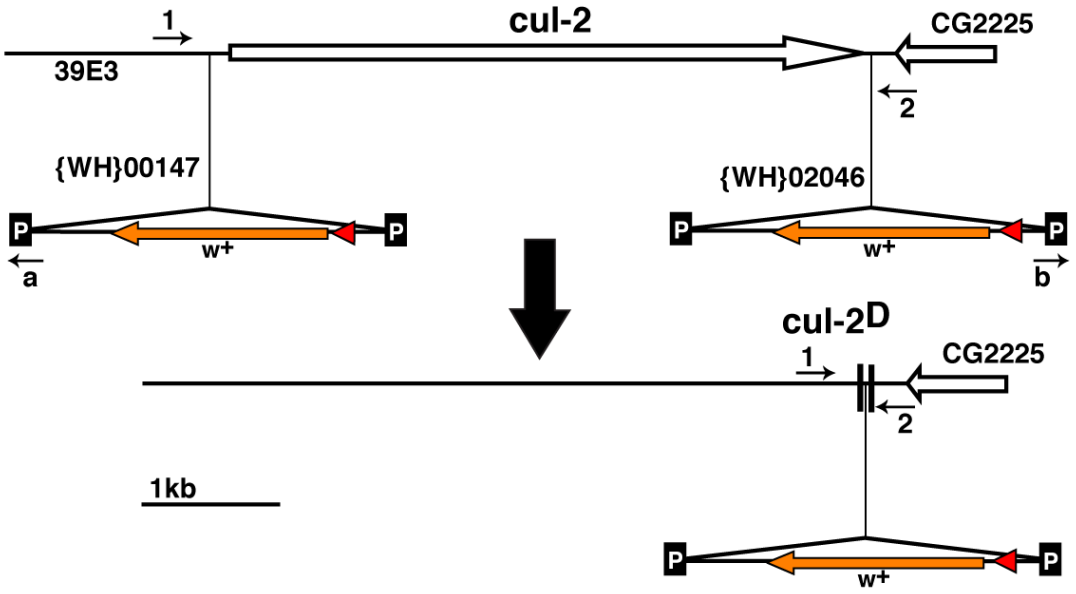

Figure 5-1. Illustration of cul-2 deletion scheme

The CUL-2 locus is illustrated with the two transposon insertions, {WH}00147 and {WH}02046, which were used to generate a deletion cul-2^{D} (bottom), which replaced all of the CUL-2 coding sequences with white+ (w+) marker gene. Primer sets 1-a, b-2, and 1-2 were used to identify recombination events by genomic PCR. Deletions were verified by picking homozygous mutant DNA from L1 larvae and only one deletion-specific PCR product was obtained using primer set 1-2. P, Pelement, red triangle, FRT site.

Hits	Gene	CG#	Our array	Brodsky's array	Q-PCR confirmed by Brodsky	Eric's array, IR induced (Steroid)	Function	Note
3	XRP1	CG17836	7.4-11.2	4.9-6.2	9.8	24.3		
3	Eiger**	CG12919	2.4-4.4	1.6-2.3	4.5	9.1		
3	corp	CG10965	3.8-4.6	2.0-2.1	-	4.4 (15.7)		
3	esc1**	CG5202	2.2-3.0	2.1-2.4	-	3.9		
3	Mre11**	CG16928	2.0-5.6	2.0-3.1	3.1	2.8		
2	Cyp307a1/Spo	CG10594	1.6-4.4	1.2-5.5	5.5		cyt p450	
2		CG15479	1.8-5.4	1.8-2.6	-			
1.9	Ku80	CG18801	?	1.9-2.5	4.1			Not strictly p53 dependent in our array
1.9	Rad50	CG6339	?	2.5	-			Not strictly p53 dependent in our array
1.7		CG6272	3.0-4.8			4.2		
1.7	eIF6	CG17611	1.6-2.0			2		
1.7		CG12194**	3.4-5.4			4.5		
1.7	GstD5	CG12242	2.2-3.0			6.6		
1.7	cul-2**	CG1512	1.6-2.6			2.7		
1.6	RnrL**	CG5371	1.6-2.2			2 [0.048]		
1.6		CG12171**	2.2-8.6			11.4 [0.05]		basal expression affected by p53 status
1.6		CG18596	2.0-4.0			4.8 [0.04]		
1.6		CG5664	2			2.1 [0.02]		
1.5		CG15480	-	1.6-3.4	-	2.1 [0.03]		
1		CG13714	-	1.5-2.7	-			
1	Ku70		-	2.2-3.7	-			
1		CG15658	-	1.5-2.0	-			
1		CG16815	-	1.5-1.7	-			
1		CG11897	2.2-4.0					basal expression affected by p53 status
1		CG6171**	1.8-2.6					
1	Pka-c3**	CG6117	3.6-7.8					
1	mus205**	CG1925	2.2-3.8					
1		CG9836**	2.2-4.4					
1		CG15479	1.8-5.4					
1		CG13204	1.6-4.6					
1		CG1718**	1.6-2.2					basal expression affected by p53 status
1	halo	CG7428	1.6-2.2					
1	pyd**	CG31349	1.6-2.2					
1	mus210**	CG8153	1.6-2.0					basal expression affected by p53 status
	** putative human orthlog, based on sequence homology							

Table 5-1. Comparisons of RIPD genes with two other genome-wide microarray studies

Arrays used for comparison:

Brodsky et al. 2004. *Mol Cell Biol* 24: 1219--31

Lee et al. 2003. *Curr Biol* 13: 350-7

Gene	Allele/strain name
CG11897	RB e00291, WH f02598, WH f03489, XP d10266
CG12171	WH f03156, WH f04657, XP d06231, CG12171^{f04657}
CG13204	XP d7476, XP d1004, XP d03909, XP d00129, P{EP}EP2427, CG13204^{KG04554}, CG13204^{EY11838}
CG17836	XP d06938, XP d04790, CG17836^{142}, CG17836^{J3}, CG17836^{J3E1}, CG17836^{rev}
CG18596	WH f07273, XP d10065
CG5664	WH f06146
CG6171	RB e02686, XP d07444, CG6171^{d07444}
CG6272	WH f05006, XP d07141
Corp	WH f03996, WH f06123, WH f07305, XP d00300, XP d05362, P{EP}EP1167
cul-2	WH f00147, WH f02046, WH f05122, cul-2^{02074}, cul-2^{05230}
eIF6	eIF6^{k13214}, eIF6^{5E24}
eiger	RB e02904, RB e02940, XP d07461, XP d1757, XP d3029, XP d5660, eiger^{1}, eiger^{3}
GstD5	RB e01161, GstD5^{1}
mus205	mus205^{A1}, mus205^{A034}, mus205^{B1}, mus205^{P}, mus205$^{ZII-1713}$, mus205$^{ZII-2129}$, mus205$^{ZII-4981}$, mus205$^{ZII-5692}$
mus210	mus210^{B1}, mus210^{C2}, mus210^{G1}, mus210^{C1}
Pka-C3	WH f00695, WH f06761, Pka-C3^{EY02687}, Pka-C3^{EY03065}, Pka-C3^{KG00222}
pyd	WH f00349, pyd^{BG00007}, pyd^{BG02735}, pyd^{EY04259}, pyd^{EP787}, pyd^{PL00355}, pyd^{C5}, pyd^{L85C}, pyd^{tam}, pyd^{G1}, pyd^{G7}, pyd^{G18}, pyd^{J2}, pyd^{J4}, pyd^{J14}, pyd^{J17}, pyd^{unspecified}
RnrL	WH f06649, RnrL^{k06709}, RnrL^{k13717a}
spo/Cyp307a1	RB e02785, spo^{e02785}, spo^{1}, spo^{2}, spo^{D3-110}, spo^{D4-25}, spo^{E2-13}, spo^{E2-68}, spo^{unspecified}

Table 5-2. Genetic material accessible for RIPD genes

For purposes considered here, our definition of ‘accessibility’ includes pre-existing single gene alleles and any transposon insertions mapping inside, or within 1kb of the query locus.

Hits	Gene	CG#	Function	Human orthlog (based on seq)	Conserved protein domain	GO:Biological process	GO:Molecular function
3	XRP1	CG17836		none	HMG-I and HMG-Y, DNA-binding	cellular physiological process, regulation of transcription, DNA-dependent	DNA binding; protein dimerization activity | inferred from sequence similarity; protein dimerization activity; DNA binding | inferred from electronic annotation
3	Eiger**	CG12919	JNK cascade	none	Tumor necrosis factor (NCBI cd00184)	JNK cascade apoptosis immune response induction of apoptosis response to pathogenic bacteria	tumor necrosis factor receptor binding protein binding | inferred from physical interaction with FLYBASE:wgn; FB:FBgn0030941
3	corp	CG10965	Companion of reaper	none		DNA damage response, signal transduction resulting in induction of apoptosis	
3	esc1**	CG5202	protein binding; Tc reg	EED (embryonic ectoderm development) HomoloGene:2814	Regulator of chromosome condensation, RCC1 WD-40 repeat WD40-like (NCBI cd00200)	cell surface receptor linked signal transduction nucleobase, nucleoside, nucleotide and nucleic acid metabolism regulation of transcription from RNA polymerase II promoter signal transduction transcription from RNA polymerase II promoter	transcription regulator activity protein binding
3	Mre11**	CG16928	meiotic recombination 11	hMre11 (HomoloGene:4083)	Metallophosphoesterase (pfam00149) Mre11 (pfam04152), DNA repair exonuclease (COG0420)	chromosome organization and biogenesis (sensu Eukaryota); double-strand break repair; meiosis; nucleotide-excision repair; telomere maintenance	nucleic acid binding; endonuclease activity; exonuclease activity; endodeoxyribonuclease activity; exodeoxyribonuclease activity; manganese ion binding;
2	Cyp307a1/Spo	CG10594	electron transport	(HomoloGene:89145. Gene conserved in Diptera)	p450 (pfam00067) CypX: Secondary metabolites biosynthesis, transport, and catabolism][COG2124]	central nervous system development; cholesterol metabolism; dorsal closure; electron transport; head involution; midgut development	electron transporter activity; oxidoreductase activity; monooxygenase activity
2		CG15479	unknown	no obvious	CCAAT/enhancer-binding protein delta; C/EBP delta at C ter (low score)	unknown	unknown
2	Ku80	CG18801	DNA binding, ATP-dependent helicase	Ku80	vWFA (cd00198); KU (cd00594/); Ku80 (cd00873)	DNA recombination; DNA repair; double-strand break repair via nonhomologous end-joining; telomere maintenance	DNA binding; nucleic acid binding; ATP-dependent DNA helicase activity; single-stranded DNA-dependent ATP-dependent DNA helicase activity
2	Rad50	CG6339	ATP-exodeoxyribonuclease	Rad50 (HomoloGene:38092. Gene conserved in Eukaryota)	ABC_sbcCD (cd03279); ABC_SMC_barmotin (cd03278); ABC_PstB_phosphate_transporter (cd3260)	DNA recombination; DNA repair; chromosome organization and biogenesis (sensu Eukaryota); larval development (sensu Insecta); telomere maintenance	ATP binding; damaged DNA binding; endodeoxyribonuclease activity; exodeoxyribonuclease activity; lyase activity; ATPase activity;
2		CG6272	DNA-dependent Tc regulation	no obvious	Basic-leucine zipper (bZIP) transcription factor; CCAAT/enhancer binding protein (C/EBP), gamma	regulation of transcription, DNA-dependent	DNA binding; protein heterodimerization activity
2	eIF6	CG17611	DNA binding, regulate Tc	eIF6 (p27BBP)	Ribosome anti-association factor IF6 domain (cd0527)	protein biosynthesis; translational initiation	translation initiation factor activity
2		CG12194*	?	MFSD1(HomoloGene:11228. Gene conserved in Coelomata) major facilitator superfamily domain containing 1	Sugar_tr (pfam00083), NarK (Nitrate/nitrite transporter (cog2223); PTR2: Dipeptide/tripeptide permease (cog3104)	transport, metabolism	transporter activity
2	GstD5	CG12242	Glutathione S transferase	no obvious	GST_Nter	?	glutathione transferase activity
2	cul-2**	CG1512	Proteolysis, cell cycle reg	CUL2 (HomoloGene:2662. Gene conserved in Bilateria)	Cullin family (pfam00888)	proteolysis; regulation of progression through cell cycle	
2	RnrL**	CG5371	Ribonucleotide reductase subunit-large	ribonucleotide reductase M1 subunit RRM1 (HomoloGene:806. Gene conserved in Eukaryota)	Ribonuc_reductase	DNA replication; purine base metabolism; pyrimidine base metabolism	ribonucleoside-diphosphate reductase activity
2		CG12171*	?	no obvious (HomoloGene:80280. Gene conserved in Eukaryota)	short chain dehydrogenase, Glucose/ribitol dehydrogenase,	lipid metabolism	oxidoreductase activity, acting on CH-OH group of donors
2		CG18596	?	no obvious (TAR RNA binding protein 1)	SpoU rRNA Methylase (Cter)		
2		CG5664	?	no obvious	No (insecta)		
2		CG15480	?	No obvious	No (insecta)		
1		CG13714					
1	Ku70						
1		CG15658					
1		CG16815					
1		CG11897	basal expression affected by p53 status				
1		CG6171**					
1	Pka-c3**	CG6117					
1	mus205**	CG1925					
1		CG9836**					
1		CG15479					
1		CG13204					
1		CG1718**	basal expression affected by p53 status				
1	halo	CG7428					
1	pyd**	CG31349					
1	mus210**	CG8153	basal expression affected by p53 status				
** putative human orthlog, based on sequence homology							
	CCAAT/enhancer-binding protein: CG15479, CG6272						

Table 5-3. Human ortholog and functions of RIPD genes

Strain		Blemish		RFP PC		Mapped	
		Severity	Pen (%)	Severity	Pen (%)	Gene	Function
13	SH0173	good	94.1	ex /g/m	30	dark (5'UTR)	apoptosis
14	SH0201	mild-2	61.1	m/g	63	vps32 (5'UTR)	intracellular protein transport
12	SH0070	mild-2	34.4	m/g	19	cg2765	-
8	SH2342	mild-1	38.9	good	50	Prosα6	proteolysis
7	SH2275	mild-2	65.1	mild	10	intronic	2kb upstream mir-14 / downstream of cg1888 (unknown)
5	SH2106	mild-2	41.2	mild		vps32	-
11	SH0971	mild-1	2.3	funky	5	ranbp11 (CDS)	Ran GTPase binding
2	SH0742	mild-1	2.3	mild	11	fkbp13 (IntA)	Fk506 binding activity
6	SH2214	mild-1	8.0	mild	13	-	-
9	SH0676	-	-	mild	13	cg1845/incenp	
10	SH0636	-	-	mild	16.7	skf (5'UTR)	guanylate kinase activity/protein binding
1	SH0497	-	-	-	0		
4	SH1453	mild-1	5.6	-	0	-	-

Table 5-4. Wing cell death screen using Ms1096-Gal4 wing-specific driver

l(2)SHxxxx strains were tested for wing blemish phenotype and persisting RFP cells (RFP C) and the degree of phenotype severity are indicated as mild or good with the penetrance of phenotype. The insertion site of the transposons were mapped by inverse PCR. The gene associated with lesions and its annotated function are also listed.

Candidate gene	Allele	Persisting cells	Putative molecular function	Insertion location
dark	l(2)SH0173-FRT40	+	protein binding, caspase activator	flybase
thread (th)	l(3)S048915-FRT80	+	inhibitor of apoptosis (dIAP)	flybase
mir-14	l(2)SH2275-FRT42	+	gene regulation	flybase
homothorax (hth)	l(3)S132307-FRT82		transcription factor	flybase
	l(3)S142204-FRT82			
Sequence-specific single-stranded DNA-binding protein (Ssdp)	l(3)S018222-FRT82*		DNA binding, transcription factor	
grunge (gug)	l(3)S146907-FRT80*		Transcription corepressor	
bicoid stability factor (bsf)	l(2)SH1181-FRT40		mRNA binding	flybase
held out wings (how)	l(3)S097074-FRT82*	+	mRNA binding	3R:17878295
	l(3)S090417-FRT82*			3R:17868472
	l(3)S053606-FRT82*			
homeodomain interacting protein kinase (HIPK)	l(3)S134313-FRT80*	+	signaling kinase	3L:527728
misshapen (msn)	l(3)S55409-FRT80*		signaling kinase	3L:2569755
furry (fry)	l(3)S126608-FRT80*		signaling molecule	3L: 9649518
BRWD3	l(3)S070701-FRT82*	+	signaling molecule	3R:20146062

casein kinase IIα (CKIIα)	l(3)S012815-FRT80*		signaling kinase	3L:23037572
	l(3)S130012-FRT-80*			3L:23037587
	l(3)S095808-FRT80*			3L:23037528
cyclin A (CycA)	l(3)S003302-FRT80		kinase activator	flybase
CG9924	l(3)S086909-FRT82*		protein binding	3R:9802015
vps32	l(2)SH2106-FRT42	+	carrier activity	flybase
CG8177	l(3)S11505-FRT80*		anion exchanger	3L:9737695
CG17646	l(2)SH0142-FRT40		anion transporter	flybase
CG5919	l(3)S119515-FRT82*		isopentenyl-diphosphate delta-isomerase	3R:17096238
Proteasome α6 subunit (prosα6)	l(2)SH2342-FRT42	+	endopeptidase activity	flybase
grappa (gpp)	l(3)S073214-FRT82*		methyltransferase	3R:2232379
belle (bel)	l(3)S097074-FRT82*		ATP binding	3R:4484608
CG2765	l(2)SH0070-FRT42*	+		2R: 20471915

Lethal insertions on the second or third chromosome causing late-onset blemishes in wing clones are represented along with candidate gene and function. Insertions marked with * were mapped using inverse PCR. Insertion sites were estimated using sequencing information (*Drosophila* genome release 4) and confirmed using genomic PCR.

All other insertion sites were identified using www.flybase.org. Notice that known players in the apoptotic pathway (*dark* and *thread*) as well novel candidate genes were isolated. PCD mutants testing positive for the persisting cell phenotype using *vg: DsRed* are marked with +.

Table 5-5. Loci implicated in coordinated death in the wing epithelium

Excerted from Table S2 (Link et al 2007)
http://jcb.rupress.org/content/suppl/2007/08/06/jcb.200702125.DC1/3.html

Special thanks to:

Alex D'Brot for assisting genetic analysis of cul-2^{D} described in this chapter.

Chapter Six.

Perspective

The general aim of my dissertation work was to explore physiological functions associated with the p53 regulatory network. Several lessons were learned using genetic reporters to observe functional output from this network. First, I found a transient activation of p53 during germ line development instigated by meiotic recombination and extended this observation from flies to mice. The functional relevance of the p53 activities discussed in Chapter Three suggested an “alarm” system used for germ line quality control. Second, I found a selective preference of p53 activation by stress in the germ line stem cells (GSCs), described in Chapter Four. These studies suggest that the “stemness” factor that distinguishes stem cells from differentiated cells may be closely related to regulation on the p53 network. A third related discovery was inappropriate proliferation of GSCs and oncogenic RasV12 are sufficient to activate p53 in the germ cells. Based on these results, I proposed the ancient p53 regulatory network is originally invented for a dilemma: need for proliferation under stress. This is a major challenge in the process of gametogenesis and regeneration after tissue injury, which will be discussed in detail below.

It seems unlikely that the p53 gene was originally selected to prevent cancer because p53-like and p63/p73-like genes are both present in unicellular protists (discussed in Chapter One), then what is the selective pressure that preserved p53 regulatory network during evolution? Incidentally, most unicellular protists do not use meiosis for reproduction unless environmental stress occurs. In addition, duplication of the chromosomes and generation of DNA breaks are required for initiating meiotic

recombination. This process is critical for exchange of the genetic materials and increase fitness for evolutionary adaptation. From this scenerio, how can cells be ensure it's safe to undergo meiosis while the environment is suboptimal? Proliferation under stress was a challenge to overcome, and p53 is probably needed for ensure the quality control of the outcome. Consistent with my hypothesis, the meiotic protein that is responsible for initiating meiotic recombination and p53 activation, Spo11, has wider degree of conservation and homologs are found in fungi, animals and plants (Malik et al 2007). It would be interesting to see if p53-like genes in unicellular organisms possess roles as "gatekeepers" between the transitions from mitosis to meiosis under stressful conditions.

In multi-cellular organisms, some of the somatic cells are kept under a quiescent state and considered as "stem cells" because of their ability to reconstitute multiple lineages of cells when needed. For example, when tissue injury occurs, stem cells can undergo a transit-amplifying stage for regeneration process, where proliferation has to coexist with stressful environment that origically caused the injury. Therefore, it is possible that the p53 network to adapted oncogenic stress as a stimulus for its activation during this process. Two major components linking stress to p53, ARF and MDM2 are absent from the fly genome (Fortini et al 2000). Therefore, it is a surprising discovery that our p53 reporter is responsive to RasV12 in *Drosophila*, suggesting a primordial axis of oncogenic regulation of p53 is also co-opted from other ancestral functions. I propose alternative p19ARF-like pathway is responsible for p53 activation

described here in the germ line, which provides a great opportunity for uncovering new components using genetic tools available in this model system.

Can knowledge of primordial p53 functions and conserved topologies in the p53 network illuminate new insights regarding cancer-related functions? I believe that the use of model organisms will continue to offer new insights to illuminate this ancient regulatory network.

BIBLIOGRAPHY

Abdu U, Brodsky M, Schupbach T. 2002. Activation of a meiotic checkpoint during Drosophila oogenesis regulates the translation of Gurken through Chk2/Mnk. *Curr Biol* 12: 1645-51

Ahmed EA, de Rooij DG. 2009. Staging of mouse seminiferous tubule cross-sections. *Methods Mol Biol* 558: 263-77

Akdemir F, Christich A, Sogame N, Chapo J, Abrams JM. 2007. p53 directs focused genomic responses in Drosophila. *Oncogene* 26: 5184--93

Almon E, Goldfinger N, Kapon A, Schwartz D, Levine AJ, Rotter V. 1993. Testicular tissue-specific expression of the p53 suppressor gene. *Dev Biol* 156: 107-16

Aranda-Anzaldo A, Dent MAR. 2007. Reassessing the role of p53 in cancer and ageing from an evolutionary perspective. *Mech Ageing Dev* 128: 293--302

Aravin AA, Hannon GJ, Brennecke J. 2007. The Piwi-piRNA pathway provides an adaptive defense in the transposon arms race. *Science* 318: 761-4

Bae B-I, Xu H, Igarashi S, Fujimuro M, Agrawal N, et al. 2005. p53 mediates cellular dysfunction and behavioral abnormalities in Huntington's disease. *Neuron* 47: 29-41

Baker NE. 2001. Master regulatory genes; telling them what to do. *Bioessays* 23: 763--6

Barker CM, Calvert RJ, Walker CW, Reinisch CL. 1997. Detection of mutant p53 in clam leukemia cells. *Exp Cell Res* 232: 240-5

Barolo S, Castro B, Posakony JW. 2004. New Drosophila transgenic reporters: insulated P-element vectors expressing fast-maturing RFP. *Biotechniques* 36: 436--40

Bartkova J, Rezaei N, Liontos M, Karakaidos P, Kletsas D, et al. 2006. Oncogene-induced senescence is part of the tumorigenesis barrier imposed by DNA damage checkpoints. *Nature* 444: 633-7

Baudat F, Manova K, Yuen JP, Jasin M, Keeney S. 2000. Chromosome synapsis defects and sexually dimorphic meiotic progression in mice lacking Spo11. *Mol Cell* 6: 989--98

Bauer JH, Poon PC, Glatt-Deeley H, Abrams JM, Helfand SL. 2005. Neuronal expression of p53 dominant-negative proteins in adult Drosophila melanogaster extends life span. *Curr Biol* 15: 2063-8

Bellotto M, Bopp D, Senti KA, Burke R, Deak P, et al. 2002. Maternal-effect loci involved in Drosophila oogenesis and embryogenesis: P element-induced mutations on the third chromosome. *Int J Dev Biol* 46: 149-57

Bergamaschi D, Samuels Y, O'Neil NJ, Trigiante G, Crook T, et al. 2003. iASPP oncoprotein is a key inhibitor of p53 conserved from worm to human. *Nat Genet* 33: 162-7

Berghmans S, Murphey RD, Wienholds E, Neuberg D, Kutok JL, et al. 2005. tp53 mutant zebrafish develop malignant peripheral nerve sheath tumors. *Proc Natl Acad Sci U S A* 102: 407-12

Bi X, Gong M, Srikanta D, Rong YS. 2005a. Drosophila ATM and Mre11 are essential for the G2/M checkpoint induced by low-dose irradiation. *Genetics* 171: 845-7

Bi X, Srikanta D, Fanti L, Pimpinelli S, Badugu R, et al. 2005b. Drosophila ATM and ATR checkpoint kinases control partially redundant pathways for telomere maintenance. *Proc Natl Acad Sci U S A* 102: 15167-72

Bondar T, Medzhitov R. p53-mediated hematopoietic stem and progenitor cell competition. *Cell Stem Cell* 6: 309-22

Bos JL. 1989. ras oncogenes in human cancer: a review. *Cancer Res* 49: 4682-9

Bothner B, Lewis WS, DiGiammarino EL, Weber JD, Bothner SJ, Kriwacki RW. 2001. Defining the molecular basis of Arf and Hdm2 interactions. *J Mol Biol* 314: 263-77

Bourdon J-C, Fernandes K, Murray-Zmijewski F, Liu G, Diot A, et al. 2005. p53 isoforms can regulate p53 transcriptional activity. *Genes Dev* 19: 2122-37

Brennecke J, Aravin AA, Stark A, Dus M, Kellis M, et al. 2007. Discrete small RNA-generating loci as master regulators of transposon activity in Drosophila. *Cell* 128: 1089-103

Briat A, Vassaux G. 2008. A new transgenic mouse line to image chemically induced p53 activation in vivo. *Cancer Sci* 99: 683-8

Brodsky MH, Nordstrom W, Tsang G, Kwan E, Rubin GM, Abrams JM. 2000. Drosophila p53 binds a damage response element at the reaper locus. *Cell* 101: 103--13

Brodsky MH, Weinert BT, Tsang G, Rong YS, McGinnis NM, et al. 2004. Drosophila melanogaster MNK/Chk2 and p53 regulate multiple DNA repair and apoptotic pathways following DNA damage. *Mol Cell Biol* 24: 1219--31

Burns TF, El-Deiry WS. 2003. Microarray analysis of p53 target gene expression patterns in the spleen and thymus in response to ionizing radiation. *Cancer Biol Ther* 2: 431-43

Chen C, Shimizu S, Tsujimoto Y, Motoyama N. 2005. Chk2 regulates transcription-independent p53-mediated apoptosis in response to DNA damage. *Biochem Biophys Res Commun* 333: 427-31

Chen D, McKearin D. 2003. Dpp signaling silences bam transcription directly to establish asymmetric divisions of germline stem cells. *Curr Biol* 13: 1786-91

Chen Y, Pane A, Schupbach T. 2007. Cutoff and aubergine mutations result in retrotransposon upregulation and checkpoint activation in Drosophila. *Curr Biol* 17: 637-42

Cheng R, Ford BL, O'Neal PE, Mathews CZ, Bradford CS, et al. 1997. Zebrafish (Danio rerio) p53 tumor suppressor gene: cDNA sequence and expression during embryogenesis. *Mol Mar Biol Biotechnol* 6: 88-97

Chew SK, Akdemir F, Chen P, Lu WJ, Mills K, et al. 2004. The apical caspase dronc governs programmed and unprogrammed cell death in Drosophila. *Dev Cell* 7: 897-907

Christich A, Kauppila S, Chen P, Sogame N, Ho SI, Abrams JM. 2002. The damage-responsive Drosophila gene sickle encodes a novel IAP binding protein similar to but distinct from reaper, grim, and hid. *Curr Biol* 12: 137-40

Christophorou MA, Ringshausen I, Finch AJ, Swigart LB, Evan GI. 2006. The pathological response to DNA damage does not contribute to p53-mediated tumour suppression. *Nature* 443: 214-7

Ciapponi L, Cenci G, Ducau J, Flores C, Johnson-Schlitz D, et al. 2004. The Drosophila Mre11/Rad50 complex is required to prevent both telomeric fusion and chromosome breakage. *Curr Biol* 14: 1360-6

Clem RJ, Fechheimer M, Miller LK. 1991. Prevention of apoptosis by a baculovirus gene during infection of insect cells. *Science* 254: 1388-90

Clevers H. 2006. Wnt/beta-catenin signaling in development and disease. *Cell* 127: 469--80

Crighton D, Wilkinson S, O'Prey J, Syed N, Smith P, et al. 2006. DRAM, a p53-induced modulator of autophagy, is critical for apoptosis. *Cell* 126: 121--34

Crighton D, Wilkinson S, Ryan KM. 2007. DRAM links autophagy to p53 and programmed cell death. *Autophagy* 3: 72-4

Danilova N, Sakamoto KM, Lin S. 2008. p53 family in development. *Mech Dev* 125: 919--31

de la Cova C, Abril M, Bellosta P, Gallant P, Johnston LA. 2004. Drosophila myc regulates organ size by inducing cell competition. *Cell* 117: 107-16

Dehal P, Satou Y, Campbell RK, Chapman J, Degnan B, et al. 2002. The draft genome of Ciona intestinalis: insights into chordate and vertebrate origins. *Science* 298: 2157--67

Derry WB, Bierings R, van Iersel M, Satkunendran T, Reinke V, Rothman JH. 2007. Regulation of developmental rate and germ cell proliferation in Caenorhabditis elegans by the p53 gene network. *Cell Death Differ* 14: 662--70

Derry WB, Putzke AP, Rothman JH. 2001. Caenorhabditis elegans p53: role in apoptosis, meiosis, and stress resistance. *Science* 294: 591-5

Di Micco R, Fumagalli M, Cicalese A, Piccinin S, Gasparini P, et al. 2006. Oncogene-induced senescence is a DNA damage response triggered by DNA hyper-replication. *Nature* 444: 638-42

Donehower LA, Harvey M, Slagle BL, McArthur MJ, Montgomery CA, et al. 1992. Mice deficient for p53 are developmentally normal but susceptible to spontaneous tumours. *Nature* 356: 215--21

Drummond-Barbosa D, Spradling AC. 2001. Stem cells and their progeny respond to nutritional changes during Drosophila oogenesis. *Dev Biol* 231: 265-78

Du C, Fang M, Li Y, Li L, Wang X. 2000. Smac, a mitochondrial protein that promotes cytochrome c-dependent caspase activation by eliminating IAP inhibition. *Cell* 102: 33-42

Duffy JB. 2002. GAL4 system in Drosophila: a fly geneticist's Swiss army knife. *Genesis* 34: 1-15

Efeyan A, Garcia-Cao I, Herranz D, Velasco-Miguel S, Serrano M. 2006. Tumour biology: Policing of oncogene activity by p53. *Nature* 443: 159

Ellis HM, Horvitz HR. 1986. Genetic control of programmed cell death in the nematode C. elegans. *Cell* 44: 817-29

Ferbeyre G, de Stanchina E, Lin AW, Querido E, McCurrach ME, et al. 2002. Oncogenic ras and p53 cooperate to induce cellular senescence. *Mol Cell Biol* 22: 3497-508

Fernald RD. 2006. Casting a genetic light on the evolution of eyes. *Science* 313: 1914-8

Fernandes AD, Atchley WR. 2008. Biochemical and functional evidence of p53 homology is inconsistent with molecular phylogenetics for distant sequences. *J Mol Evol* 67: 51--67

Fortini ME, Skupski MP, Boguski MS, Hariharan IK. 2000. A survey of human disease gene counterparts in the Drosophila genome. *J Cell Biol* 150: F23-30

Garcia-Muse T, Boulton SJ. 2005. Distinct modes of ATR activation after replication stress and DNA double-strand breaks in Caenorhabditis elegans. *EMBO J* 24: 4345-55

Gartner A, Milstein S, Ahmed S, Hodgkin J, Hengartner MO. 2000. A conserved checkpoint pathway mediates DNA damage--induced apoptosis and cell cycle arrest in C. elegans. *Mol Cell* 5: 435-43

Gatz SA, Wiesmüller L. 2006. p53 in recombination and repair. *Cell Death Differ* 13: 1003--16

Ghabrial A, Ray RP, Schüpbach T. 1998. okra and spindle-B encode components of the RAD52 DNA repair pathway and affect meiosis and patterning in Drosophila oogenesis. *Genes Dev* 12: 2711--23

Ghafari F, Pelengaris S, Walters E, Hartshorne G. 2009. Influence of p53 and genetic background on prenatal oogenesis and oocyte attrition in mice. *Hum Reprod*

Gilley J, Fried M. 2001. One INK4 gene and no ARF at the Fugu equivalent of the human INK4A/ARF/INK4B tumour suppressor locus. *Oncogene* 20: 7447-52

Gonczy P, Matunis E, DiNardo S. 1997. bag-of-marbles and benign gonial cell neoplasm act in the germline to restrict proliferation during Drosophila spermatogenesis. *Development* 124: 4361-71

Gottlieb E, Haffner R, King A, Asher G, Gruss P, et al. 1997. Transgenic mouse model for studying the transcriptional activity of the p53 protein: age- and tissue-dependent changes in radiation-induced activation during embryogenesis. *EMBO J* 16: 1381-90

Greenblatt MS, Bennett WP, Hollstein M, Harris CC. 1994. Mutations in the p53 tumor suppressor gene: clues to cancer etiology and molecular pathogenesis. *Cancer Res* 54: 4855-78

Halazonetis TD, Gorgoulis VG, Bartek J. 2008. An oncogene-induced DNA damage model for cancer development. *Science* 319: 1352-5

Hays R, Wickline L, Cagan R. 2002. Morgue mediates apoptosis in the Drosophila melanogaster retina by promoting degradation of DIAP1. *Nat Cell Biol* 4: 425-31

Hill R, Song Y, Cardiff RD, Van Dyke T. 2005. Selective evolution of stromal mesenchyme with p53 loss in response to epithelial tumorigenesis. *Cell* 123: 1001-11

Hirao A, Kong YY, Matsuoka S, Wakeham A, Ruland J, et al. 2000. DNA damage-induced activation of p53 by the checkpoint kinase Chk2. *Science* 287: 1824--7

Holley CL, Olson MR, Colon-Ramos DA, Kornbluth S. 2002. Reaper eliminates IAP proteins through stimulated IAP degradation and generalized translational inhibition. *Nat Cell Biol* 4: 439-44

Honda R, Yasuda H. 1999. Association of p19(ARF) with Mdm2 inhibits ubiquitin ligase activity of Mdm2 for tumor suppressor p53. *EMBO J* 18: 22-7

Hou YC, Chittaranjan S, Barbosa SG, McCall K, Gorski SM. 2008. Effector caspase Dcp-1 and IAP protein Bruce regulate starvation-induced autophagy during Drosophila melanogaster oogenesis. *J Cell Biol* 182: 1127-39

Hu W, Feng Z, Teresky AK, Levine AJ. 2007. p53 regulates maternal reproduction through LIF. *Nature* 450: 721--4

Huh JR, Guo M, Hay BA. 2004. Compensatory proliferation induced by cell death in the Drosophila wing disc requires activity of the apical cell death caspase Dronc in a nonapoptotic role. *Curr Biol* 14: 1262-6

Ishioka C, Englert C, Winge P, Yan YX, Engelstein M, Friend SH. 1995. Mutational analysis of the carboxy-terminal portion of p53 using both yeast and mammalian cell assays in vivo. *Oncogene* 10: 1485-92

Issigonis M, Tulina N, de Cuevas M, Brawley C, Sandler L, Matunis E. 2009. JAK-STAT signal inhibition regulates competition in the Drosophila testis stem cell niche. *Science* 326: 153-6

Jackson GR, Salecker I, Dong X, Yao X, Arnheim N, et al. 1998. Polyglutamine-expanded human huntingtin transgenes induce degeneration of Drosophila photoreceptor neurons. *Neuron* 21: 633-42

Jang JK, Sherizen DE, Bhagat R, Manheim EA, McKim KS. 2003. Relationship of DNA double-strand breaks to synapsis in Drosophila. *J Cell Sci* 116: 3069-77

Jiang J, Hui C-C. 2008. Hedgehog signaling in development and cancer. *Dev Cell* 15: 801--12

Jin S, Martinek S, Joo WS, Wortman JR, Mirkovic N, et al. 2000. Identification and characterization of a p53 homologue in Drosophila melanogaster. *Proc Natl Acad Sci USA* 97: 7301--6

Jin Z, Kirilly D, Weng C, Kawase E, Song X, et al. 2008. Differentiation-defective stem cells outcompete normal stem cells for niche occupancy in the Drosophila ovary. *Cell Stem Cell* 2: 39-49

Jones SN, Roe AE, Donehower LA, Bradley A. 1995. Rescue of embryonic lethality in Mdm2-deficient mice by absence of p53. *Nature* 378: 206--8

Karr TL. 1991. Intracellular sperm/egg interactions in Drosophila: a three-dimensional structural analysis of a paternal product in the developing egg. *Mech Dev* 34: 101-11

Kerr JF, Wyllie AH, Currie AR. 1972. Apoptosis: a basic biological phenomenon with wide-ranging implications in tissue kinetics. *Br J Cancer* 26: 239-57

Kim JS, Lee C, Bonifant CL, Ressom H, Waldman T. 2007. Activation of p53-dependent growth suppression in human cells by mutations in PTEN or PIK3CA. *Mol Cell Biol* 27: 662-77

King N, Westbrook MJ, Young SL, Kuo A, Abedin M, et al. 2008. The genome of the choanoflagellate Monosiga brevicollis and the origin of metazoans. *Nature* 451: 783--8

Klattenhoff C, Bratu DP, McGinnis-Schultz N, Koppetsch BS, Cook HA, Theurkauf WE. 2007. Drosophila rasiRNA pathway mutations disrupt embryonic axis specification through activation of an ATR/Chk2 DNA damage response. *Dev Cell* 12: 45--55

Klenov MS, Lavrov SA, Stolyarenko AD, Ryazansky SS, Aravin AA, et al. 2007. Repeat-associated siRNAs cause chromatin silencing of retrotransposons in the Drosophila melanogaster germline. *Nucleic Acids Res* 35: 5430-8

Ko LJ, Prives C. 1996. p53: puzzle and paradigm. *Genes Dev* 10: 1054-72

Komarova EA, Chernov MV, Franks R, Wang K, Armin G, et al. 1997. Transgenic mice with p53-responsive lacZ: p53 activity varies dramatically during normal development and determines radiation and drug sensitivity in vivo. *EMBO J* 16: 1391-400

Kondo S, Senoo-Matsuda N, Hiromi Y, Miura M. 2006. DRONC coordinates cell death and compensatory proliferation. *Mol Cell Biol* 26: 7258-68

Kooistra R, Vreeken K, Zonneveld JB, de Jong A, Eeken JC, et al. 1997. The Drosophila melanogaster RAD54 homolog, DmRAD54, is involved in the repair of radiation damage and recombination. *Mol Cell Biol* 17: 6097--104

Krizhanovsky V, Lowe SW. 2009. Stem cells: The promises and perils of p53. *Nature* 460: 1085-6

Kruse J-P, Gu W. 2009. Modes of p53 regulation. *Cell* 137: 609--22

La Spada AR, Morrison RS. 2005. The power of the dark side: Huntington's disease protein and p53 form a deadly alliance. *Neuron* 47: 1-3

Langheinrich U, Hennen E, Stott G, Vacun G. 2002. Zebrafish as a model organism for the identification and characterization of drugs and genes affecting p53 signaling. *Curr Biol* 12: 2023-8

Laurencon A, Purdy A, Sekelsky J, Hawley RS, Su TT. 2003. Phenotypic analysis of separation-of-function alleles of MEI-41, Drosophila ATM/ATR. *Genetics* 164: 589-601

Lavoie CA, Ohlstein B, McKearin DM. 1999. Localization and function of Bam protein require the benign gonial cell neoplasm gene product. *Dev Biol* 212: 405-13

Lee C-Y, Clough EA, Yellon P, Teslovich TM, Stephan DA, Baehrecke EH. 2003a. Genome-wide analyses of steroid- and radiation-triggered programmed cell death in Drosophila. *Curr Biol* 13: 350-7

Lee JH, Lee E, Park J, Kim E, Kim J, Chung J. 2003b. In vivo p53 function is indispensable for DNA damage-induced apoptotic signaling in Drosophila. *FEBS Lett* 550: 5--10

Levine AJ. 1997. p53, the cellular gatekeeper for growth and division. *Cell* 88: 323-31

Lin H, Spradling AC. 1993. Germline stem cell division and egg chamber development in transplanted Drosophila germaria. *Dev Biol* 159: 140-52

Link N, Chen P, Lu WJ, Pogue K, Chuong A, et al. 2007. A collective form of cell death requires homeodomain interacting protein kinase. *J Cell Biol* 178: 567-74

Liston P, Fong WG, Korneluk RG. 2003. The inhibitors of apoptosis: there is more to life than Bcl2. *Oncogene* 22: 8568-80

Liu Y, Elf SE, Miyata Y, Sashida G, Huang G, et al. 2009a. p53 regulates hematopoietic stem cell quiescence. *Cell Stem Cell* 4: 37-48

Liu Y, Elf SE, Miyata Y, Sashida G, Liu Y, et al. 2009b. p53 regulates hematopoietic stem cell quiescence. *Cell Stem Cell* 4: 37--48

Lowe SW. 1999. Activation of p53 by oncogenes. *Endocr Relat Cancer* 6: 45-8

MacQueen AJ, Villeneuve AM. 2001. Nuclear reorganization and homologous chromosome pairing during meiotic prophase require C. elegans chk-2. *Genes Dev* 15: 1674--87

Mahadevaiah SK, Turner JM, Baudat F, Rogakou EP, de Boer P, et al. 2001. Recombinational DNA double-strand breaks in mice precede synapsis. *Nat Genet* 27: 271-6

Maisse C, Guerrieri P, Melino G. 2003. p73 and p63 protein stability: the way to regulate function? *Biochem Pharmacol* 66: 1555-61

Maiuri MC, Malik SA, Morselli E, Kepp O, Criollo A, et al. 2009. Stimulation of autophagy by the p53 target gene Sestrin2. *Cell Cycle* 8: 1571--6

Malik SB, Ramesh MA, Hulstrand AM, Logsdon JM, Jr. 2007. Protist homologs of the meiotic Spo11 gene and topoisomerase VI reveal an evolutionary history of gene duplication and lineage-specific loss. *Mol Biol Evol* 24: 2827-41

Malone CD, Brennecke J, Dus M, Stark A, McCombie WR, et al. 2009. Specialized piRNA pathways act in germline and somatic tissues of the Drosophila ovary. *Cell* 137: 522-35

Mandal S, Guptan P, Owusu-Ansah E, Banerjee U. 2005. Mitochondrial regulation of cell cycle progression during development as revealed by the tenured mutation in Drosophila. *Dev Cell* 9: 843-54

Margulies L, Briscoe DI, Wallace SS. 1986. The relationship between radiation-induced and transposon-induced genetic damage during Drosophila oogenesis. *Mutat Res* 162: 55-68

Martins CP, Brown-Swigart L, Evan GI. 2006. Modeling the therapeutic efficacy of p53 restoration in tumors. *Cell* 127: 1323--34

Martins LM, Iaccarino I, Tenev T, Gschmeissner S, Totty NF, et al. 2002. The serine protease Omi/HtrA2 regulates apoptosis by binding XIAP through a reaper-like motif. *J Biol Chem* 277: 439-44

Marusyk A, Porter CC, Zaberezhnyy V, DeGregori J. Irradiation selects for p53-deficient hematopoietic progenitors. *PLoS Biol* 8: e1000324

McKearin D, Ohlstein B. 1995. A role for the Drosophila bag-of-marbles protein in the differentiation of cystoblasts from germline stem cells. *Development* 121: 2937-47

McKearin DM, Spradling AC. 1990. bag-of-marbles: a Drosophila gene required to initiate both male and female gametogenesis. *Genes Dev* 4: 2242-51

McKim KS, Hayashi-Hagihara A. 1998. mei-W68 in Drosophila melanogaster encodes a Spo11 homolog: evidence that the mechanism for initiating meiotic recombination is conserved. *Genes Dev* 12: 2932--42

Meek DW. 2009. Tumour suppression by p53: a role for the DNA damage response? *Nat Rev Cancer* 9: 714-23

Meletis K, Wirta V, Hede S-M, Nister M, Lundeberg J, Frisen J. 2006a. p53 suppresses the self-renewal of adult neural stem cells. *Development* 133: 363--9

Meletis K, Wirta V, Hede SM, Nister M, Lundeberg J, Frisen J. 2006b. p53 suppresses the self-renewal of adult neural stem cells. *Development* 133: 363-9

Mendoza L, Orozco E, Rodriguez MA, Garcia-Rivera G, Sanchez T, et al. 2003. Ehp53, an Entamoeba histolytica protein, ancestor of the mammalian tumour suppressor p53. *Microbiology* 149: 885--93

Mills AA, Zheng B, Wang XJ, Vogel H, Roop DR, Bradley A. 1999. p63 is a p53 homologue required for limb and epidermal morphogenesis. *Nature* 398: 708--13

Milyavsky M, Gan OI, Trottier M, Komosa M, Tabach O, et al. A distinctive DNA damage response in human hematopoietic stem cells reveals an apoptosis-independent role for p53 in self-renewal. *Cell Stem Cell* 7: 186-97

Moreno E, Basler K. 2004. dMyc transforms cells into super-competitors. *Cell* 117: 117-29

Nedelcu AM, Tan C. 2007. Early diversification and complex evolutionary history of the p53 tumor suppressor gene family. *Dev Genes Evol* 217: 801--6

Negrini S, Gorgoulis VG, Halazonetis TD. Genomic instability--an evolving hallmark of cancer. *Nat Rev Mol Cell Biol* 11: 220-8

Neufeld TP. 2008. Genetic manipulation and monitoring of autophagy in Drosophila. *Methods Enzymol* 451: 653-67

Niki Y, Yamaguchi T, Mahowald AP. 2006. Establishment of stable cell lines of Drosophila germ-line stem cells. *Proc Natl Acad Sci U S A* 103: 16325-30

Nordstrom W, Abrams JM. 2000. Guardian ancestry: fly p53 and damage-inducible apoptosis. *Cell Death Differ* 7: 1035-8

Nordstrom W, Chen P, Steller H, Abrams JM. 1996. Activation of the reaper gene during ectopic cell killing in Drosophila. *Dev Biol* 180: 213-26

Oh SW, Kingsley T, Shin HH, Zheng Z, Chen HW, et al. 2003. A P-element insertion screen identified mutations in 455 novel essential genes in Drosophila. *Genetics* 163: 195-201

Ohlstein B, Lavoie CA, Vef O, Gateff E, McKearin DM. 2000. The Drosophila cystoblast differentiation factor, benign gonial cell neoplasm, is related to DExH-box proteins and interacts genetically with bag-of-marbles. *Genetics* 155: 1809-19

Ohlstein B, McKearin D. 1997. Ectopic expression of the Drosophila Bam protein eliminates oogenic germline stem cells. *Development* 124: 3651-62

Oikemus SR, McGinnis N, Queiroz-Machado J, Tukachinsky H, Takada S, et al. 2004. Drosophila atm/telomere fusion is required for telomeric localization of HP1 and telomere position effect. *Genes Dev* 18: 1850-61

Okada H, Suh WK, Jin J, Woo M, Du C, et al. 2002. Generation and characterization of Smac/DIABLO-deficient mice. *Mol Cell Biol* 22: 3509-17

Olivier M, Eeles R, Hollstein M, Khan MA, Harris CC, Hainaut P. 2002. The IARC TP53 database: new online mutation analysis and recommendations to users. *Hum Mutat* 19: 607--14

Olivier M, Petitjean A, Marcel V, Petre A, Mounawar M, et al. 2009. Recent advances in p53 research: an interdisciplinary perspective. *Cancer Gene Ther* 16: 1--12

Ollmann M, Young LM, Di Como CJ, Karim F, Belvin M, et al. 2000. Drosophila p53 is a structural and functional homolog of the tumor suppressor p53. *Cell* 101: 91-101

Olson EN. 2006. Gene regulatory networks in the evolution and development of the heart. *Science* 313: 1922-7

Pane A, Wehr K, Schupbach T. 2007. zucchini and squash encode two putative nucleases required for rasiRNA production in the Drosophila germline. *Dev Cell* 12: 851-62

Pankow S, Bamberger C. 2007. The p53 tumor suppressor-like protein nvp63 mediates selective germ cell death in the sea anemone Nematostella vectensis. *PLoS ONE* 2: e782

Pantoja C, Serrano M. 1999. Murine fibroblasts lacking p21 undergo senescence and are resistant to transformation by oncogenic Ras. *Oncogene* 18: 4974-82

Parant J, Chavez-Reyes A, Little NA, Yan W, Reinke V, et al. 2001. Rescue of embryonic lethality in Mdm4-null mice by loss of Trp53 suggests a nonoverlapping pathway with MDM2 to regulate p53. *Nat Genet* 29: 92--5

Parks AL, Cook KR, Belvin M, Dompe NA, Fawcett R, et al. 2004. Systematic generation of high-resolution deletion coverage of the Drosophila melanogaster genome. *Nat Genet* 36: 288-92

Patton EE, Widlund HR, Kutok JL, Kopani KR, Amatruda JF, et al. 2005. BRAF mutations are sufficient to promote nevi formation and cooperate with p53 in the genesis of melanoma. *Curr Biol* 15: 249-54

Pearson M, Carbone R, Sebastiani C, Cioce M, Fagioli M, et al. 2000. PML regulates p53 acetylation and premature senescence induced by oncogenic Ras. *Nature* 406: 207-10

Peters M, DeLuca C, Hirao A, Stambolic V, Potter J, et al. 2002. Chk2 regulates irradiation-induced, p53-mediated apoptosis in Drosophila. *Proc Natl Acad Sci USA* 99: 11305--10

Peterson JS, Barkett M, McCall K. 2003. Stage-specific regulation of caspase activity in drosophila oogenesis. *Dev Biol* 260: 113-23

Plaster N, Sonntag C, Busse CE, Hammerschmidt M. 2006. p53 deficiency rescues apoptosis and differentiation of multiple cell types in zebrafish flathead mutants deficient for zygotic DNA polymerase delta1. *Cell Death Differ* 13: 223-35

Pomerantz J, Schreiber-Agus N, Liegeois NJ, Silverman A, Alland L, et al. 1998. The Ink4a tumor suppressor gene product, p19Arf, interacts with MDM2 and neutralizes MDM2's inhibition of p53. *Cell* 92: 713-23

Preston CR, Flores C, Engels WR. 2006a. Age-dependent usage of double-strand-break repair pathways. *Curr Biol* 16: 2009-15

Preston CR, Flores CC, Engels WR. 2006b. Differential usage of alternative pathways of double-strand break repair in Drosophila. *Genetics* 172: 1055-68

Putnam NH, Srivastava M, Hellsten U, Dirks B, Chapman J, et al. 2007. Sea anemone genome reveals ancestral eumetazoan gene repertoire and genomic organization. *Science* 317: 86--94

Raha S, Robinson BH. 2001. Mitochondria, oxygen free radicals, and apoptosis. *Am J Med Genet* 106: 62-70

Rhiner C, Diaz B, Portela M, Poyatos JF, Fernandez-Ruiz I, et al. 2009. Persistent competition among stem cells and their daughters in the Drosophila ovary germline niche. *Development* 136: 995-1006

Rong YS, Titen SW, Xie HB, Golic MM, Bastiani M, et al. 2002. Targeted mutagenesis by homologous recombination in D. melanogaster. *Genes Dev* 16: 1568--81

Rorth P. 1998. Gal4 in the Drosophila female germline. *Mech Dev* 78: 113-8

Ryoo HD, Bergmann A, Gonen H, Ciechanover A, Steller H. 2002. Regulation of Drosophila IAP1 degradation and apoptosis by reaper and ubcD1. *Nat Cell Biol* 4: 432-8

Sablina AA, Budanov AV, Ilyinskaya GV, Agapova LS, Kravchenko JE, Chumakov PM. 2005. The antioxidant function of the p53 tumor suppressor. *Nat Med* 11: 1306-13

Schumacher B, Hanazawa M, Lee M-H, Nayak S, Volkmann K, et al. 2005a. Translational repression of C. elegans p53 by GLD-1 regulates DNA damage-induced apoptosis. *Cell* 120: 357-68

Schumacher B, Hofmann K, Boulton S, Gartner A. 2001. The C. elegans homolog of the p53 tumor suppressor is required for DNA damage-induced apoptosis. *Curr Biol* 11: 1722-7

Schumacher B, Schertel C, Wittenburg N, Tuck S, Mitani S, et al. 2005b. C. elegans ced-13 can promote apoptosis and is induced in response to DNA damage. *Cell Death Differ* 12: 153-61

Senoo M, Pinto F, Crum CP, McKeon F. 2007. p63 Is essential for the proliferative potential of stem cells in stratified epithelia. *Cell* 129: 523--36

Serrano M, Lin AW, McCurrach ME, Beach D, Lowe SW. 1997. Oncogenic ras provokes premature cell senescence associated with accumulation of p53 and p16INK4a. *Cell* 88: 593-602

Sharpless NE. 2005. INK4a/ARF: a multifunctional tumor suppressor locus. *Mutat Res* 576: 22-38

Shepard JL, Amatruda JF, Stern HM, Subramanian A, Finkelstein D, et al. 2005. A zebrafish bmyb mutation causes genome instability and increased cancer susceptibility. *Proc Natl Acad Sci U S A* 102: 13194-9

Shieh SY, Ikeda M, Taya Y, Prives C. 1997. DNA damage-induced phosphorylation of p53 alleviates inhibition by MDM2. *Cell* 91: 325-34

Sogame N, Kim M, Abrams JM. 2003. Drosophila p53 preserves genomic stability by regulating cell death. *Proc Natl Acad Sci USA* 100: 4696--701

Song Y-H. 2005. Drosophila melanogaster: a model for the study of DNA damage checkpoint response. *Mol Cells* 19: 167-79

Song Y-H, Mirey G, Betson M, Haber DA, Settleman J. 2004. The Drosophila ATM ortholog, dATM, mediates the response to ionizing radiation and to spontaneous DNA damage during development. *Curr Biol* 14: 1354-9

Soussi T. 2007. p53 alterations in human cancer: more questions than answers. *Oncogene* 26: 2145--56

Soussi T, Caron de Fromentel C, Méchali M, May P, Kress M. 1987. Cloning and characterization of a cDNA from Xenopus laevis coding for a protein homologous to human and murine p53. *Oncogene* 1: 71-8

Spradling A. 1993. Developmental genetics of oogenesis. In *Drosophila Development*, ed. M Bate, A Martinez-Arias. New York: Cold Spring Harbor Press

Srinivasula SM, Datta P, Fan XJ, Fernandes-Alnemri T, Huang Z, Alnemri ES. 2000. Molecular determinants of the caspase-promoting activity of Smac/DIABLO and its role in the death receptor pathway. *J Biol Chem* 275: 36152-7

Stergiou L, Doukoumetzidis K, Sendoel A, Hengartner MO. 2007. The nucleotide excision repair pathway is required for UV-C-induced apoptosis in Caenorhabditis elegans. *Cell Death Differ* 14: 1129--38

Suh E-K, Yang A, Kettenbach A, Bamberger C, Michaelis AH, et al. 2006. p63 protects the female germ line during meiotic arrest. *Nature* 444: 624--8

Sutcliffe JE, Brehm A. 2004. Of flies and men; p53, a tumour suppressor. *FEBS Lett* 567: 86-91

Sutcliffe JE, Korenjak M, Brehm A. 2003. Tumour suppressors--a fly's perspective. *Eur J Cancer* 39: 1355-62

Tavernarakis N, Pasparaki A, Tasdemir E, Maiuri MC, Kroemer G. 2008. The effects of p53 on whole organism longevity are mediated by autophagy. *Autophagy* 4: 870--3

Tenev T, Zachariou A, Wilson R, Paul A, Meier P. 2002. Jafrac2 is an IAP antagonist that promotes cell death by liberating Dronc from DIAP1. *EMBO J* 21: 5118-29

Thibault ST, Singer MA, Miyazaki WY, Milash B, Dompe NA, et al. 2004. A complementary transposon tool kit for Drosophila melanogaster using P and piggyBac. *Nat Genet* 36: 283-7

Tomasini R, Tsuchihara K, Wilhelm M, Fujitani M, Rufini A, et al. 2008. TAp73 knockout shows genomic instability with infertility and tumor suppressor functions. *Genes Dev* 22: 2677--91

Tushir JS, Zamore PD, Zhang Z. 2009. SnapShot: Fly piRNAs, PIWI proteins, and the ping-pong cycle. *Cell* 139: 634, e1

Vagin VV, Sigova A, Li C, Seitz H, Gvozdev V, Zamore PD. 2006. A distinct small RNA pathway silences selfish genetic elements in the germline. *Science* 313: 320-4

Van Beneden RJ, Walker CW, Laughner ES. 1997. Characterization of gene expression of a p53 homologue in the soft-shell clam (Mya arenaria). *Mol Mar Biol Biotechnol* 6: 116-22

Vousden KH, Prives C. 2009. Blinded by the Light: The Growing Complexity of p53. *Cell* 137: 413--31

Wang SL, Hawkins CJ, Yoo SJ, Muller HA, Hay BA. 1999. The Drosophila caspase inhibitor DIAP1 is essential for cell survival and is negatively regulated by HID. *Cell* 98: 453-63

Warrick JM, Paulson HL, Gray-Board GL, Bui QT, Fischbeck KH, et al. 1998. Expanded polyglutamine protein forms nuclear inclusions and causes neural degeneration in Drosophila. *Cell* 93: 939-49

Weber JD, Kuo ML, Bothner B, DiGiammarino EL, Kriwacki RW, et al. 2000. Cooperative signals governing ARF-mdm2 interaction and nucleolar localization of the complex. *Mol Cell Biol* 20: 2517-28

Wells BS, Yoshida E, Johnston LA. 2006. Compensatory proliferation in Drosophila imaginal discs requires Dronc-dependent p53 activity. *Curr Biol* 16: 1606-15

White K, Grether ME, Abrams JM, Young L, Farrell K, Steller H. 1994. Genetic control of programmed cell death in Drosophila. *Science* 264: 677-83

Wilson R, Goyal L, Ditzel M, Zachariou A, Baker DA, et al. 2002. The DIAP1 RING finger mediates ubiquitination of Dronc and is indispensable for regulating apoptosis. *Nat Cell Biol* 4: 445-50

Wong MD, Jin Z, Xie T. 2005. Molecular mechanisms of germline stem cell regulation. *Annu Rev Genet* 39: 173-95

Wu DC, Johnston LA. 2009. Preview. Competition among stem cells gets sticky. *Cell Stem Cell* 5: 459-60

Xie T, Kawase E, Kirilly D, Wong MD. 2005. Intimate relationships with their neighbors: tales of stem cells in Drosophila reproductive systems. *Dev Dyn* 232: 775-90

Yamada Y, Davis KD, Coffman CR. 2008. Programmed cell death of primordial germ cells in Drosophila is regulated by p53 and the Outsiders monocarboxylate transporter. *Development* 135: 207--16

Yang A, Kaghad M, Caput D, McKeon F. 2002. On the shoulders of giants: p63, p73 and the rise of p53. *Trends Genet* 18: 90-5

Yang A, McKeon F. 2000. P63 and P73: P53 mimics, menaces and more. *Nat Rev Mol Cell Biol* 1: 199-207

Yang A, Schweitzer R, Sun D, Kaghad M, Walker N, et al. 1999. p63 is essential for regenerative proliferation in limb, craniofacial and epithelial development. *Nature* 398: 714--8

Yang A, Walker N, Bronson R, Kaghad M, Oosterwegel M, et al. 2000. p73-deficient mice have neurological, pheromonal and inflammatory defects but lack spontaneous tumours. *Nature* 404: 99--103

Yoo SJ, Huh JR, Muro I, Yu H, Wang L, et al. 2002. Hid, Rpr and Grim negatively regulate DIAP1 levels through distinct mechanisms. *Nat Cell Biol* 4: 416-24

Zamore PD. 2007. RNA silencing: genomic defence with a slice of pi. *Nature* 446: 864-5

Zhang Y, Lin N, Carroll PM, Chan G, Guan B, et al. 2008. Epigenetic blocking of an enhancer region controls irradiation-induced proapoptotic gene expression in Drosophila embryos. *Dev Cell* 14: 481-93